Strain Path Partitioning During Forceful Emplacement of the Papoose Flat Pluton, Inyo Mountains, CA

by

Sven S. Morgan

Thesis submitted to the faculty of the Virginia Polytechnic Institute and State University in partial fulfillment of the requirements of the degree of

MASTER OF SCIENCE

in

GEOLOGY

APPROVED:

Richard D. Law

A. Krishna Sinha

Robert J. Tracy

September, 1992

Blacksburg, Virginia

Strain Path Partitioning During Forceful Emplacement of the Papoose Flat Pluton

by

Sven Soren Morgan
Richard D. Law (Chair)
Geological Sciences

(ABSTRACT)

Sedimentary units in the Inyo Mountains of eastern California can be traced into the aureole of the Papoose Flat pluton where, due to intense crystal-plastic deformation, they are thinned to less than 10% of their original stratigraphic thickness. This deformation is constrained by textural relationships to have occurred during contact metamorphism. The strain within the dominantly S>L tectonites is partitioned by lithology.

The deformation is in bulk, noncoaxial, but examination of individual lithologic units reveals large components of either pure shear or simple shear deformation.

C-axis fabric analysis of quartz tectonites within veins in the gneissic border of the pluton, and quartzites within the pluton aureole, indicate that quartz tectonites deformed under approximately simple shear deformation, and suggest that the pluton/wall rock contact is the zone of highest strain. C-axis fabrics measured from the quartz tectonites are distinctly different between the veins and the quartzites. Veins display a higher maximum concentration of c-axes per uniform distribution and fabrics are characterized by single girdles. Quartzites display decreasing maximum concentrations of c-axes with increasing distance from the pluton/wall rock contact and fabrics are characterized by asymmetric cross girdles.

Structural and field relationships indicate that; 1) pure shear deformation was dominant within the deformed border of the pluton, 2) flattening (chocolate tablet boudinage) occurred locally at the pluton/wall rock contact, 3) dominantly pure shear deformation produced the porphyroblast-matrix relationships within the aureole schists and, 4) pure shear plane strain (symmetrical boudinage) occurred locally within the aureole marbles. The direction of maximum extension within the boudinaged marbles is parallel to a stretching lineation which is well developed throughout the deformed

western margin of the pluton, and is associated with the simple shear deformation observed in the quartz tectonites. Both pure shear and simple shear deformation are believed to be occurring concurrently with intrusion.

Porphyroblast-matrix relationships within the aureole schists indicate that andalusite porphyroblasts have not rotated with respect to compositional layering. In sections viewed parallel to lineation and perpendicular to foliation, a constant angular relationship is observed between planar porphyroblast inclusion trails and matrix foliation traced around the western margin of the pluton. Unwrapping of the matrix foliation, from concordancy with the pluton margin into a planar reference frame, "unspins" the planar inclusion trails into a parallel and constant geographic orientation. This relationship, along with inclusion trail geometry, suggests that initial metamorphism was static, and that penetrative deformation did not occur until late in the growth history of andalusite. Deformation is recorded in the rims of andalusite porphyroblasts as a curvature of inclusion trails into parallelism with the matrix foliation. Inclusion trails begin curving at the same point in porphyroblast rims where inclusions coarsen in grain size and decrease in abundance, therefore a second 'stage' of metamorphism is believed to be synchronous with deformation.

The strong component of pure shear deformation (plane strain and flattening) observed within various lithologic units, the variation in strain around the pluton/wall rock contact, and the synchroneity of the second stage of metamorphism with deformation suggest that the Papoose Flat pluton was forcefully emplaced. The deformation is believed to be a result of a complex path of forceful inflation, where inflation is not symmetrical as a balloon, but is heterogeneously developed and possibly directed more in the orientation of the lineation. A regional deformational event may, or may not, have occurred synchronously with forceful emplacement.

ACKNOWLEDGEMENTS

I thank my mother and father for all their support, enthusiasm, and patience while I continue to pursue 'esoteric plutonic' questions. They may not know it, but I do follow their advice once in a while.

I do not always follow my advisor's advice, which has 'inflated' me into trouble at times, but I sincerely appreciate his willingness to listen, and his expert guidance, support, and friendship. I have learned so much more than just a master's degree. I also want to thank Bob Tracy and Krishna Sinha for listening to my ideas and for their support throughout the project.

My sincere thanks to the rest of the faculty and staff for all their help and guidance over the last three years. The main office has always been a pleasure to visit and is never lacking for smiles.

My comrades in the department I hope to always have as friends. I have really enjoyed my stay here, and my friends have been a big part of that.

I also want to thank Jennifer Tank, who for the last year has been a source of much happiness and support, (and rice and beans!). Her patience I appreciate so much. She has been the best part of this last year.

Funding has been provided by the Geology Department, the National Science Foundation, Sigma Xi, and The Graduate School.

TABLE OF CONTENTS

CHAPTER ONE

INTRODUCTION

1.1 *Purpose of Study*

The deformation of the metasedimentary units surrounding the Papoose Flat pluton is rare in its intensity and in its uniformity. Limestones, quartzites, and shales are thinned to as little as 10% of their original stratigraphic thickness within the narrow aureole surrounding the pluton and yet they maintain their stratigraphic identity (Nelson et al. 1971, 1977; Sylvester et al. 1978). The pluton is also strongly deformed at the contact with the aureole rocks. A gneissic foliation is best developed at the pluton/wall rock contact and decreases with intensity into the pluton. Examination of the various types of strain observed within the pluton and in the adjacent wall rocks aids in understanding the processes involved in granite emplacement, and also helps to determine whether regional deformation is associated with the emplacement of the Papoose Flat pluton.

The original work on the Papoose Flat pluton and aureole was conducted by C. Nelson who mapped the pluton and much of the White-Inyo Range in the 1950's and 60's (Nelson 1966; Nelson 1971; Nelson et al. 1977). Nelson et al. (1972) and Sylvester et al. (1978) were the first to publish on the deformation surrounding the pluton and their model of forceful expansion had been accepted until recently (Law et al. 1990; Godin and Paterson 1991; Morgan et al. 1991; Paterson et al. 1991; Law et al. 1992). Nelson et al. (1972) and Sylvester et al. (1978) attributed the intense deformation to swelling of the pluton, similar to how a 'blister' expands a layer of skin. In their model of forceful expansion, the more completely crystallized rind of the pluton expanded as more magma intruded into the core of the pluton. Expansion of the pluton caused the extreme attenuation of the surrounding aureole rocks.

Sylvester and Christie (1968) and Sylvester et al. (1978) demonstrated that, at least locally, structures within the aureole of the Papoose Flat pluton were indicative of a flattening type of strain. The principal axes of stress were interpreted to be oriented perpendicular to the pluton/wall rock contact. Ramsay (1989) demonstrated that in a ballooning model of forcable emplacement, flattening strains are expected at the pluton/wall rock contact.

Law et al. (1990) reexamined the deformation surrounding the Papoose Flat pluton and recognized that the prominent lineation observed throughout the contact and surrounding rocks was a true stretching lineation and conflicted with the flattening and ballooning model of Sylvester et al. (1978). The preliminary quartz crystallographic fabrics from the deformed rocks around the pluton indicated that a strong component of simple shear was involved in the deformation (Law et al. 1990). Further examination of the crystal plastic deformation was warranted in order to understand the possible involvement of a regional tectonic event during emplacement.

This study focuses on the processes involved in the deformation both surrounding and within the Papoose Flat pluton and includes examination of: 1) crystallographic preferred orientations within quartz veins in the granite and quartzites in the aureole, 2) field relationships within and immediately adjacent to the zone of intense deformation and, 3) microstuctures within the aureole schists. It will be argued that the overall deformation is explained by a partitioning of pure shear and simple shear by rock type. Pure shear and simple shear seem to have been accomodated in different rock types concurrently and adjacent to each other during a larger scale noncoaxial deformational event. In view of the amount of pure shear (plane strain and/or flattening) interpreted to be involved in the overall deformation, a model invoking forceful 'inflation', possibly directed more in the direction of the lineation, or possibly with a component of regional deformation, best explains the intense deformation surrounding and within the Papoose Flat pluton.

1.2 *Geologic Framework*

The Papoose Flat pluton is one of several Mesozoic granitic plutons that intrude into the White-Inyo Range of eastern California (Fig. 1) and which are believed to be related to, or are satellites of, the Sierra Nevada batholith (Bateman et al. 1963; Ross 1965; Nelson et al. 1977; Sylvester et al. 1978). The Papoose Flat pluton, along with the Birch Creek pluton located 33 km to the north (Fig. 1), are amongst the youngest dated plutons in the range, with average K-Ar ages on biotite of 78 and 78.5 m.y. respectively (Kistler et al. 1965; Mckee and Nash 1967). The White-Inyo Range is an elongate horst block that trends NNW and parallels the trend of the eastern Sierra Nevada Mountains 15-20 km to the west. Where the Papoose Flat pluton is situated, the White-Inyo range is approximately 18 km wide (of which the pluton comprises 16 km) and is bounded by high angle Cenozoic normal and right-oblique slip faults which separate Owens Valley on the west from Saline Valley on the east. Owens Valley is considered to be the most eastern basin in the Basin and Range extensional province (Nelson 1981).

The sedimentary rocks in the White-Inyo Range consist of late Precambrian through Paleozoic miogeoclinal rocks (Fig. 2) that are broadly folded and faulted (Sylvester et al. 1978). The major structural feature in the vicinity of the Papoose Flat pluton is the southeast plunging Inyo Mountain anticline. The Papoose Flat pluton has intruded into the southwest limb of the anticline (Fig. 3) (Nelson et al. 1972; Sylvester et al. 1978; Nelson 1987), locally overturning and deflecting strata around the pluton. A locally well developed axial planar cleavage related to the Inyo Mountain anticline strikes from N25°W to N45°W and dips from 55° to 80° to the SW (Dunne et al. 1978). Sylvester and Babcock (1975) suggest that the NW striking cleavage is older than early Jurassic due to the cleavage being crosscut by the Hunter Mountain pluton. The author has observed two NW

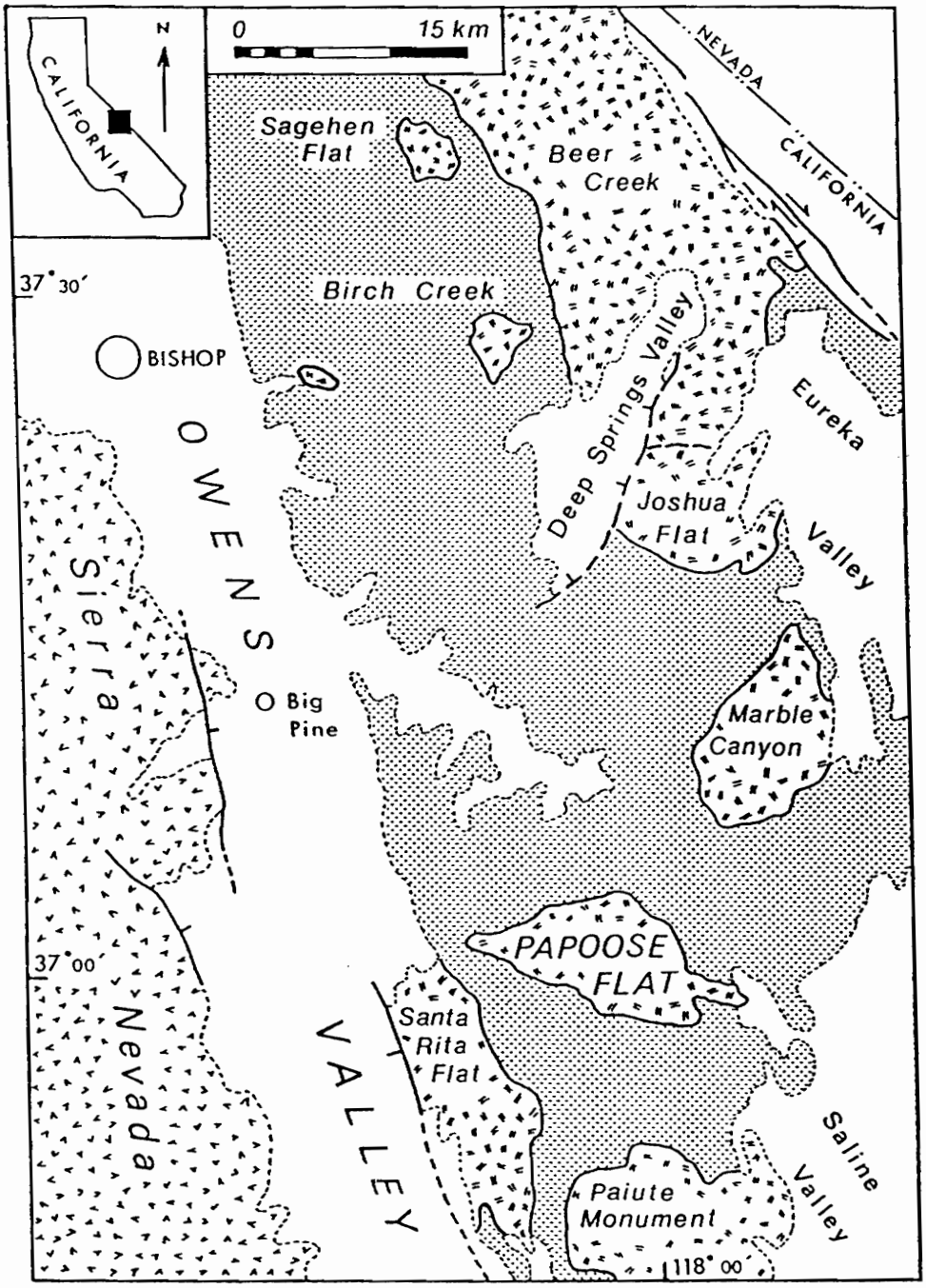

Fig. 1. Location map of Papoose Flat pluton. From Law et al. (1992).

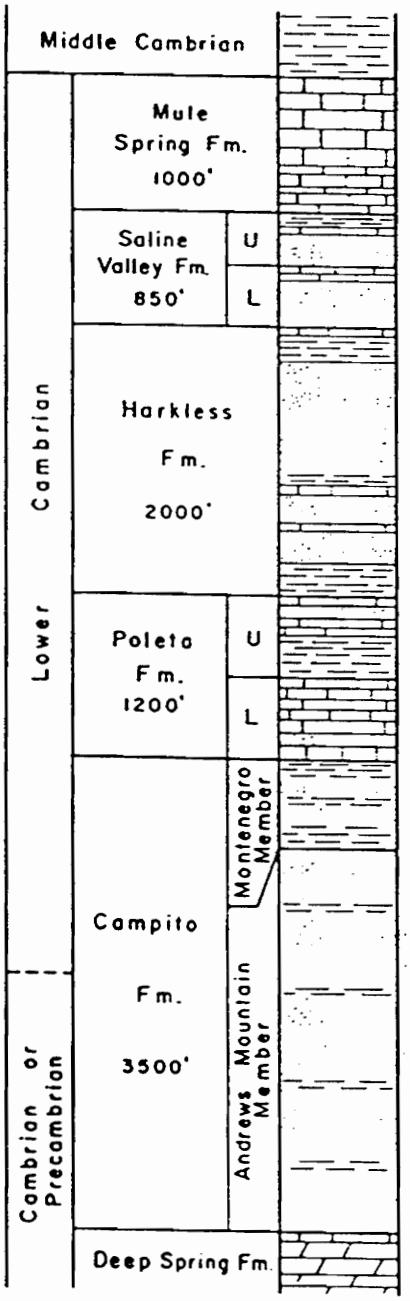

Fig. 2. Generalized stratigraphic column of the Precambrian and Cambrian rocks discussed in this paper. From Nelson (1962).

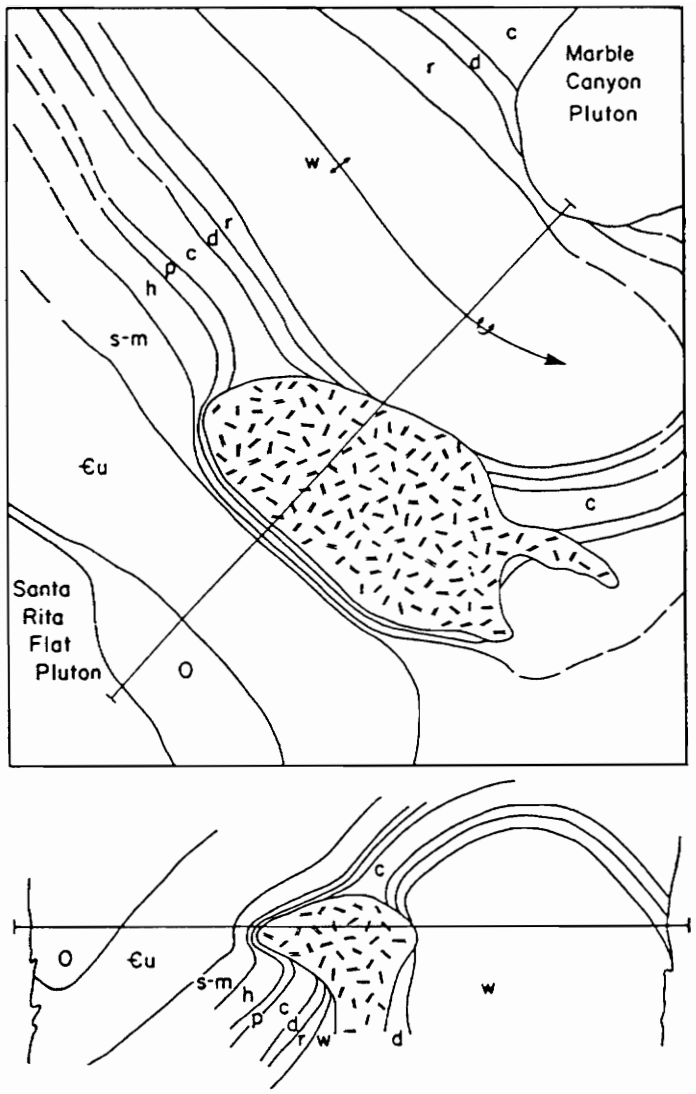

Fig. 3. Generalized palinspastic geologic map and cross section of Papoose Flat pluton. North is towards the top of the page. Present orientation of pluton is elongate to the E-W. Map units: w = Wyman Formation; r = Reed dolomite; d = Deep Spring Formation; c = Campito Formation; p = Poleta Formation; h = Harkless Formation; s-m = Saline Valley, Mule Spring, and Monola Formations; Cu = undifferentiated formations of Middle and Late Cambrian age, including Bonanza King Formation; O = undifferentiated Ordovician formations; patterned area = granite of Papoose Flat pluton. From Sylvester et al. (1978).

striking cleavages, dipping at 30° and 60° to the SSW in the Harkless Formation north of the Papoose Flat pluton.

The Papoose Flat pluton is roughly elliptical in shape, the long axis of the pluton trending WNW. A narrow 'apophysis' (Sylvester et al. 1978) of granite protrudes at the eastern end. The contact with the country rocks is characteristically very sharp, especially around the highly deformed western margin, and dips away from the pluton at about 30-40°, lending the pluton a domal shape. The pluton is in contact with the Cambrian Poleta Formation for much of the western and southern margin, and the Precambrian Wyman, Campito, and Cambrian Harkless Formations around the eastern and northern margin (Nelson et al. 1977). The metasediments are intensely deformed and concordant to the pluton around the western margin, while in contrast, they appear to be statically metamorphosed and are discordant to the pluton around the eastern margin. The Wyman formation, and therefore the Inyo Mountain anticline, is locally overturned at the northeastern margin of the pluton. The pluton is principally composed of quartz monzonite (Sylvester et al. 1978) with abundant k-feldspar megacrysts in the deformed western margin. Dikes passing outwards from the pluton into the country rocks are rare, although there are abundant aplite dikes within the margin of the pluton. There are local sills of granite at the very western margin and at the northern margin of the pluton.

1.3 *Field Relationships*

1.3.1 *High Strain Zone*

The high strain zone is broadly defined as a belt of intensely deformed metasedimentary units and granitic gneiss that lies along the Papoose Flat pluton/wall rock contact for approximately 12 km around the western margin of the pluton (Fig. 4). The metasedimentary units are locally thinned to as little as 10% of their regional stratigraphic

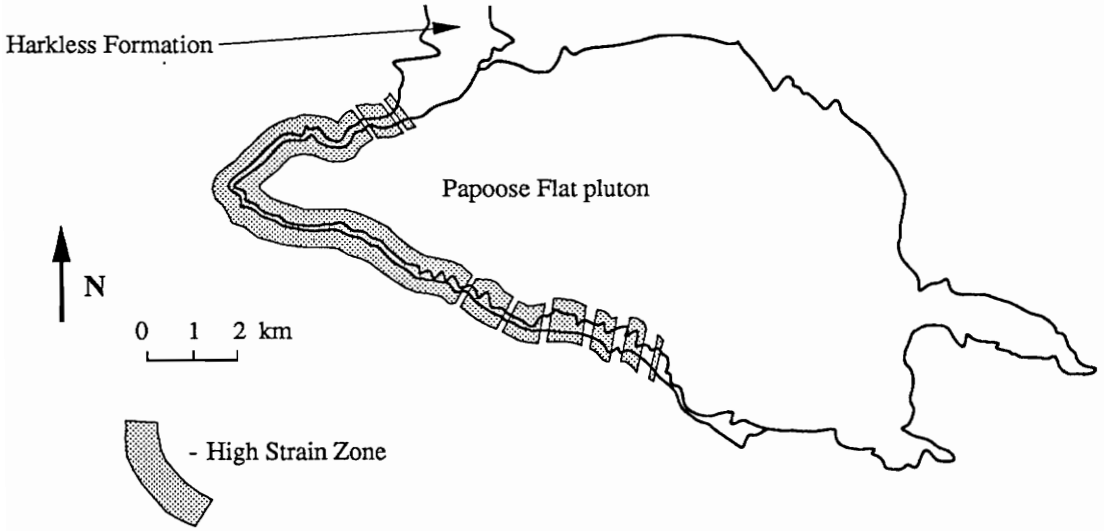

Fig. 4. Generalized outline of the high strain zone at the western margin of the Papoose Flat pluton.

thickness in the high strain zone (Nelson et al. 1972; Sylvester et al. 1978). The foliation in the gneiss and in the metasedimentary units, and the compositional layering within the metasedimentary units, are parallel to the pluton/wall rock contact. The deformation in the high strain zone rapidly decreases in intensity traced perpendicular from the pluton/wall rock contact and more gradually along the contact in the central southern and northern portions of the contact moving east. The metasedimentary units are deformed and metamorphosed Cambrian miogeoclinal rocks comprised of all or parts of the following stratigraphic succession (in order from oldest to youngest); Poleta Formation limestones, sandstones, and black shales, Harkless Formation quartzites and shales, Saline Valley Formation and Mule Spring Formation marbles. The gneiss comprises only the outermost portion of the granitic pluton (Fig. 5).

The following descriptions of the rock units that comprise the high strain zone pay particular attention to the rock types that make up the granite. Examination of the quartz veins and aplite dikes within the gneiss that have been emplaced at various stages of gneissic foliation development allow incremental strain features to be observed. Description and analysis of the deformation features within the Harkless quartzites and schists are found in chapters two and three, respectively. The Poleta, Mule Spring, and Saline Valley Formations are only briefly discussed because little work was completed on these rocks during this study.

NOTE ON STRAIN TERMINOLOGY:

In this paper, the term, "pure shear" is not restricted to plane strain ($k=1$) deformation. Pure shear deformation will be defined as any type of deformation where the incremental and finite strain axes remain parallel through the deformational event (Hobbs et al. 1976). Therefore pure shear can be used to describe flattening strain (oblate, $k=0$), prolate strain ($k=\infty$), plane strain ($k=1$), or intermediate types of strain. Pure shear and

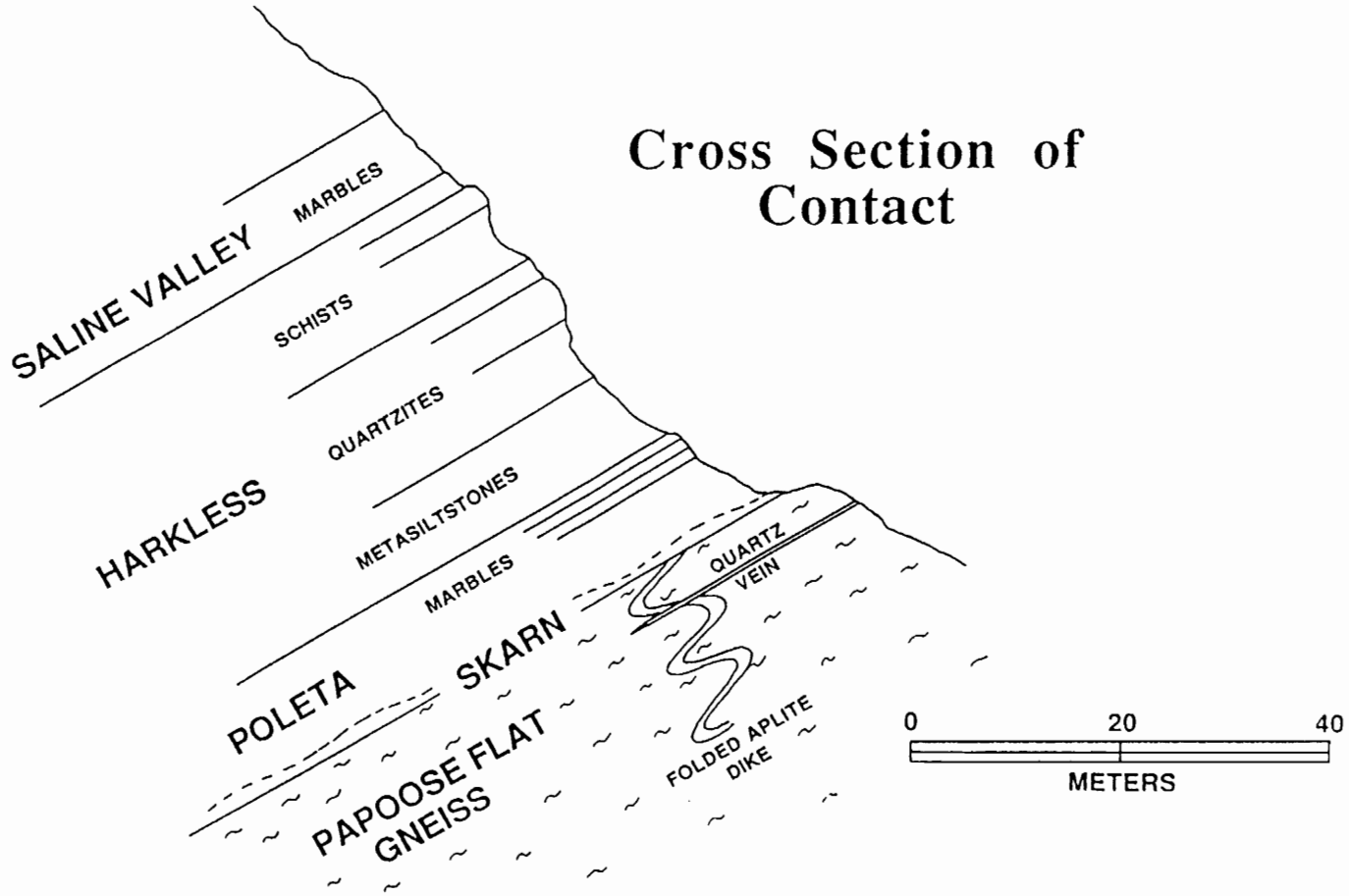

Fig. 5. Generalized cross section of the contact between Papoose Flat pluton and deformed Lower Cambrian section. Foliation and compositional layering are parallel to the pluton/wall rock contact.

simple shear are discussed in terms of their relative components in a larger scale, *noncoaxial* event.

1.3.2 *Gneissic Border Facies*

The gneissic border facies (Sylvester et al., 1978) is the portion of the high strain zone within the granite. It comprises a belt of well developed granitic gneiss that borders the pluton around the western margin. It is best developed within 20 to 30 meters of the contact and gradually decreases in intensity towards the center of the pluton. The foliation in the gneiss is parallel to the contact with the overlying metasedimentary rocks. The gneissic foliation extends over one third of the exposed pluton margin and grades into a poorly to moderately foliated granite both towards the central portion of the pluton and along the northern and southern contacts moving eastward. The intensity of the foliation in the interior of the granite varies but is mappable throughout the pluton and is concordant to roughly concordant to the contact (Nelson et al. 1977). Isolated outcrops in the interior of the pluton which are topographically high also exhibit the gneissic foliation and are probably near the inferred roof of the pluton (Sylvester et al. 1978, p. 1207). Around the western margin, the attitude of the contact and the foliation define a broad west plunging antiformal structure (Sylvester et al. 1978.)

The gneissic foliation is defined by a parallel alignment of micas, elongate plagioclase feldspar and k-feldspar crystals, elliptical shaped quartz grains and quartz ribbons, and large (up to 8 cm) tabular megacrysts of k-feldspar. The matrix constituents anastomose around the k-feldspar megacrysts which are distinctively much coarser grained and give the gneiss a porphyritic texture. A moderately well developed lineation in the gneiss parallels the lineation in the metasedimentary units and trends NNW at the western margin of the pluton. The lineation swings to the WNW approaching the southeastern end

of gneissic border facies. Lineation is best developed on faces of quartz veins that are exposed within the gneiss and locally resembles a slickenside surface. The lineation lies within the foliation plane and is defined by elongate, fine to medium grained micas and recrystallized quartz aggregates. The lineation is most commonly observed and well developed where the gneiss is well developed.

K-feldspar megacrysts within the gneissic border facies display three types of morphology depending on shape and orientation of the megacryst with respect to the foliation (Fig. 6) (descriptions are based on 2-dimensional observations): 1) equidimensional megacrysts with crystal faces at 45° to the foliation are typically euhedral and rarely have wings (sensu Hanmer and Passchier, 1991) of finer grained feldspar trailing in the foliation plane (Fig. 6a), 2) tabular megacrysts that have the long crystal face parallel to the foliation with small symmetrical wings that lie in the foliation plane and are usually euhedral (Fig. 6b) and, 3) tabular grains with the long crystal faces slightly oblique to the foliation have moderately well developed symmetrical wings of fine grained feldspar lying in the foliation plane and are usually subhedral to anhedral (Fig. 6c).

Contrary to Paterson et al. (1991, p. 324), shear sense indicators within the gneiss were rarely observed. Wings attached to the k-feldspar megacrysts are symmetrical with respect to the foliation and lineation and only one foliation plane is observable (Figs. 6 & 7a). Along the deformed western margin only two outcrops were observed, on opposite sides of the pluton, where two foliations are developed within the gneiss. These S-C structures seem to be local phenomena and the asymmetry between S and C in the two outcrops yielded opposite senses of shear.

During this study an attempt was made to quantify the strain within the gneiss. The spatial relationship between potassium feldspar megacrysts with respect to the foliation was examined using the center to center method of Fry (1979) and computer program of DePaor (1989). Two faces of rock within the gneiss, perpendicular to each other and to the

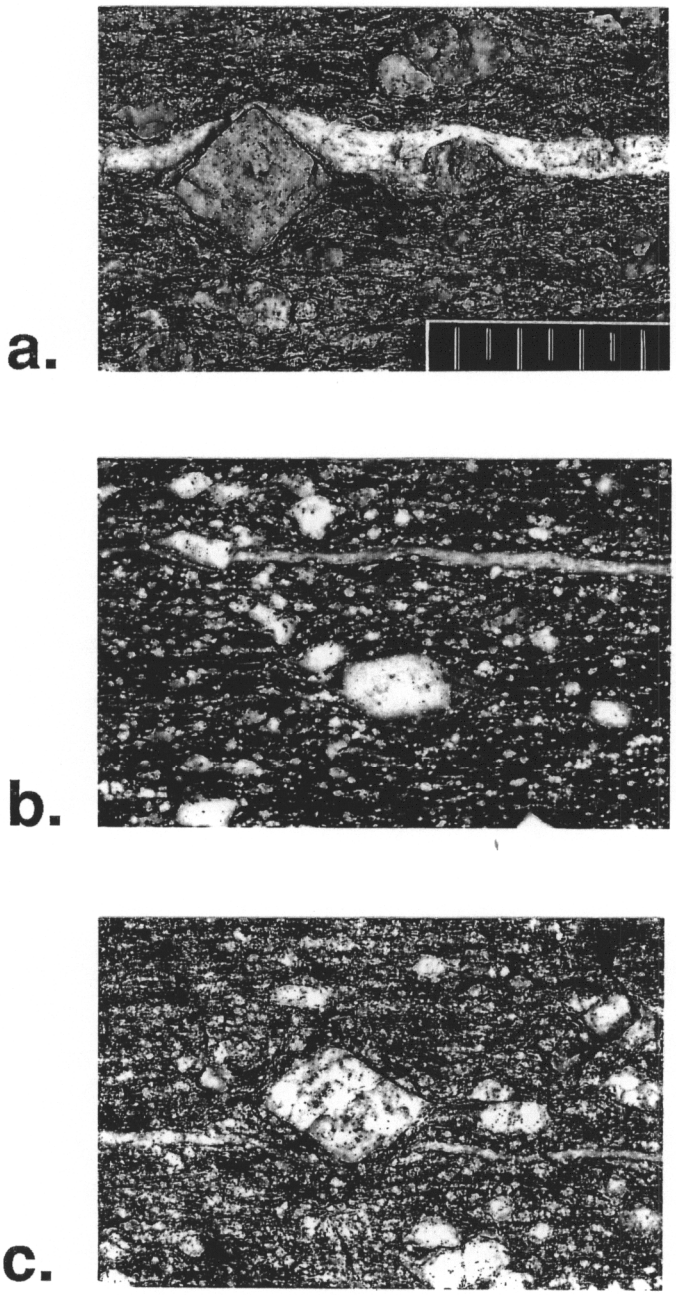

Fig. 6. Photographs of the three characteristic shapes of potassium feldspar megacrysts and their relationship to the gneissic foliation. Photographs are perpendicular to foliation and parallel to lineation. **a.** Equidimensional megacryst with crystal faces at 45° to the foliation. Each mark on scale bar equals 0.5 cm. **b.** Tabular shaped megacryst with long face of crystal parallel to the foliation. Length of rock in photo is 5.1 cm. **c.** Tabular shaped megacryst with long face of crystal slightly oblique to foliation. Length of rock in photo is 6.2 cm.

a.

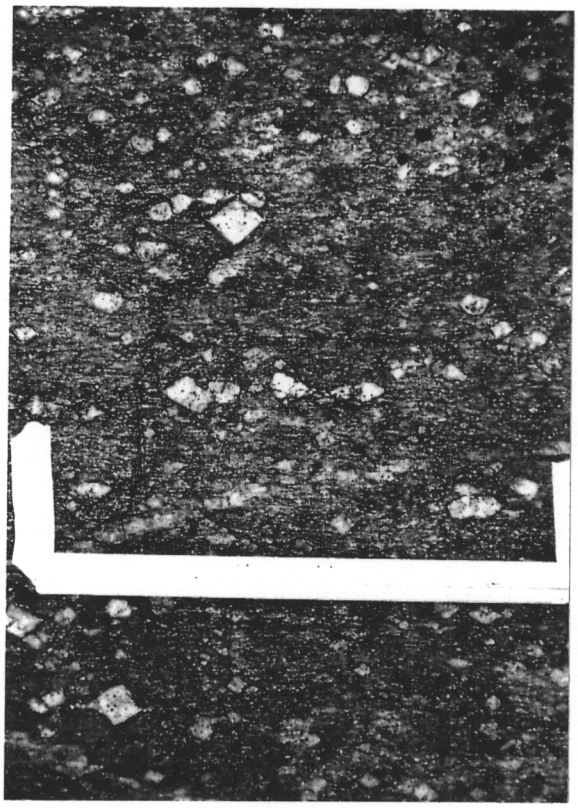

b.

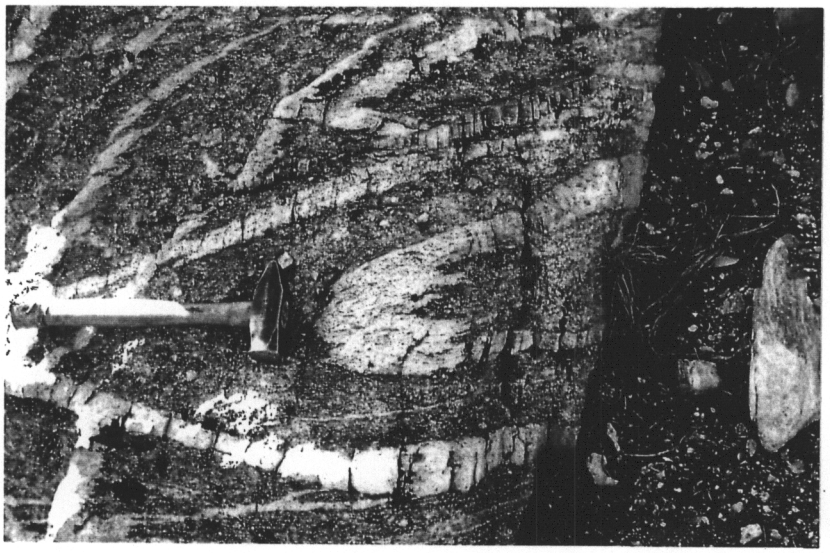

Fig. 7. Photographs of the gneissic border facies. **a**. Gneiss with potassium feldspar megacrysts. Foliation is parallel to ruler. Width of rock in photo is 34 cm. **b**. Folded aplite dike. Hammer is subparallel to foliation and is 38 cm long.

foliation, were measured at seven outcrops for positions of megacrysts with respect to each other and to the foliation. The results were ambiguous, indicating either, A) there was a pre-deformation 'clustering', or anisotropic distribution of the megacrysts, or B) there were problems with the data collection or analysis.

The last stage of deformation seems to have occurred under solid state conditions at temperatures of around 500 to 550° C (Law et al. 1991, 1992; Nyman et al. 1992) based on calcite-dolomite thermometry and on the deformation mechanisms of various mineral phases. Quartz grains locally exhibit strong undulatory extinction and are commonly recrystallized into polycrystal ribbons and flattened elliptical shapes with strong crystallographic preferred orientations. Feldspar grains (matrix and megacrysts) are commonly fractured, but there is also widespread evidence for crystal plastic deformation. Feldspar grains commonly are elliptical in shape with wings of fine grained matrix material, exhibit strong undulatory extinction, and commonly have subgrains at their margins.

A poorly developed cleavage is observed at some outcrops in the interior of the pluton and within the gneissic border facies. The orientation of the cleavage varies with position around the pluton and crosscuts the gneissic foliation.

The only macroscopic evidence for deformation by simple shear within the granite was observed at one location along the southern margin of the gneissic border facies. At three outcrops at Location 202 (Fig. 9, CHAPTER TWO), aplite dikes and quartz veins oriented at high angles to the foliation were offset parallel to the foliation with a top to the NE sense of shear. The offset occurred where the high angle veins are in contact with foliation parallel aplite dikes and quartz veins. The shear sense obtained from the quartz c-axes fabrics from these quartz veins indicates a relative top to the NW sense of shear, *90° to the shear sense obtained from the macroscopic offset.* The foliation-parallel veins vary in thickness from 1 cm to 40 cm and the shearing within them has offset the high angle veins by up to 1 m. Within most of the thicker foliation-parallel veins, the sheared high angle

veins can be traced across the shear zone and are homogeneously thinned and rotated towards parallelism with the foliation, suggesting a homogeneous distribution of strain and ductile deformation. The foliation-parallel quartz veins contain coarse grains (from 1 to 3 mm) which are macroscopically elongate with their long axes trending to the NE, parallel to the apparent direction of offset, and contain on the surface a more prevalant biotite stretching lineation which trends to the NW.

1.3.3 *Aplite Dikes*

There are several distinct episodes of vein/dike emplacement within the granite that are constrained by field relationships to have occurred at various times during the development of the gneissic foliation. Aplite dikes are constrained to have been emplaced prior to the deformation that formed the gneissic foliation because they are also strongly folded and foliated, and the gneissic foliation is parallel to the hinge planes of the folded aplite dikes. Aplite dikes within the core region of the pluton and within the relatively undeformed border of the pluton east of the gneissic border zone are also relatively undeformed (Sylvester et al. 1978). The folding of the aplite in the gneissic border facies can be locally intense with isoclinal to more open folds (Fig. 7b). Fold vergence varies with orientation of the aplite dikes and there seems to be no dominant direction to which folds verge. Fold limbs are symmetrical with respect to the foliation and the hinge planes of the folds are parallel to the foliation. Aplite dikes are commonly much thicker, up to 40 cm, where they are at high angles to the foliation and thinner where they are subparallel to the foliation. The deformed aplite contains a lineation which is defined by fine to medium grained elongate grain shapes of quartz and feldspar which trend NW - SE.

1.3.4 *Quartz Veins*

At least two episodes of quartz vein emplacement are recognized within the gneiss. The earliest event postdates the emplacement of the aplite dikes and at least the initial development of the gneissic foliation. Early quartz veins cross cut aplite dikes and are mostly oriented parallel or subparallel to the gneissic foliation. *The parallel alignment of foliation and quartz veins indicates that the quartz veins were emplaced later than the development of the gneissic foliation.* Initial crack opening was probably controlled by the pre-existing planar fabric of the gneiss. Quartz veins are planar, usually no more than 3-5 cm wide, and rarely extend for more than 3 or 4 m in any outcrop. They are also commonly observed within the interior of aplite dikes that are oriented parallel to the foliation. Quartz veins usually display a strong mylonitic foliation which is almost always parallel to the gneissic foliation. A lineation is well defined on the surface of the veins by fine grained biotite which is aligned parallel to the lineation in the gneiss and locally resembles a slickenside surface. Rare quartz veins are oriented at high angles (30 - 40°) to the foliation, and contain their own *vein-parallel foliation* (Fig. 8a). The high angle veins represent a small percentage of the early quartz veins, but were observed throughout the western margin of the pluton.

Field relationships indicate that the early foliation-parallel quartz veins have not simply been rotated into parallelism with the foliation during the deformation event. The aplite dikes, which seem to be randomly oriented, responded to the deformation by folding and developing a foliation. The quartz veins cross cut the folded aplite dikes and are not folded, suggesting that they were emplaced later than the initial foliation and folding event. The gneissic foliation seems to have controlled the orientation of the crack opening and therefore controlled the orientation of quartz veins.

A second generation of quartz veins are less commonly observed and are randomly

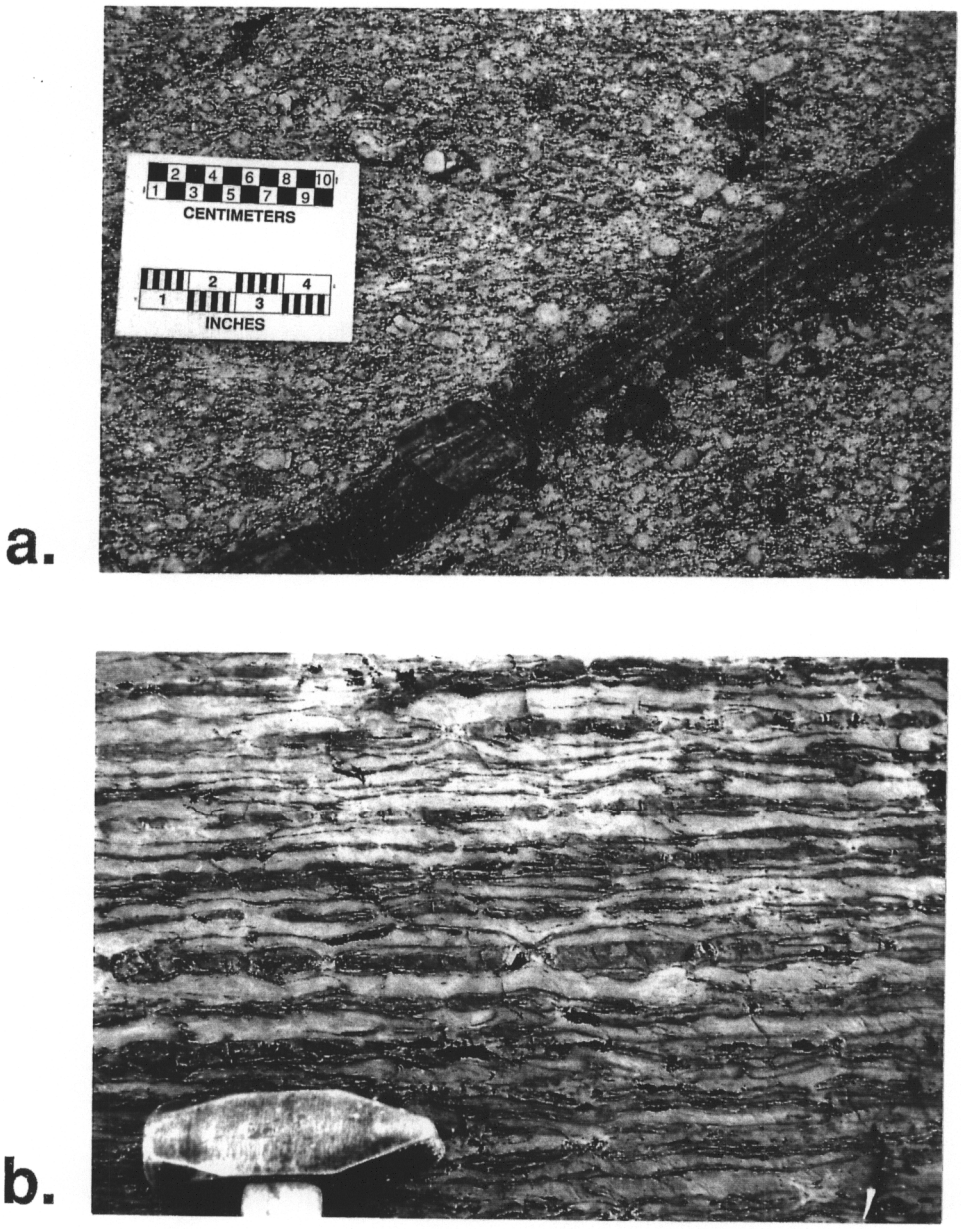

Fig. 8. Photographs of some of the rock units in the high strain zone. **a.** Mylonitic quartz vein at high angle to the gneissic foliation. Foliation is parallel to long axis of photo. **b.** Boudinaged layers of siltstone within marble of the Saline Valley Formation. Rock face is parallel to lineation. Head of hammer is 13 cm long.

oriented. They do not have a mylonitic foliation and crosscut the gneissic foliation and all other veins and dikes. Although these veins do not internally exhibit the mylonitic fabric, a lineation defined by biotite is commonly observed on the surface of the veins which is similar to the lineation on the surface of the early quartz veins.

1.3.5 *Skarn*

The Poleta siltstones, shales, and marbles at the contact are commonly metamorphosed to calc-silicate skarn that is best developed within one to two meters of the granite except at the eastern end of the pluton where metamorphism is static and sillimanite is found (Sylvester et al. 1978). At several localities within the skarn around the western margin, large (< 1m), equidimensional to elongate shaped boudins of garnet, epidote, and quartz are separated by sheaths of quartz mica schist. These boudins are equidimensional in the XY plane and are referred to as chocolate tablet boudins (Sylvester and Christie 1968). The garnet and epidote interiors are fractured but also pinch and swell while the mica sheaths are not fractured. The chocolate tablet boudins are elongate parallel to the foliation. A NW trending lineation defined by the alignment of fine to medium grained micas is observed on the surfaces of the phyllosilicate rich sheaths.

1.3.6 *Saline Valley Formation*

Locally within the Saline Valley Formation, interbedded siltstones are strongly boudinaged within limestone (Fig. 8b). Boudin shapes are symmetrical and their orientation with respect to foliation is symmetrical indicating pure shear (plane strain) deformation. At location 92 (Fig. 4), these structures are best developed in a section more than 20 m thick. The section is approximately 450 m from the contact on the ground, but

may be as close as 370 m above the projected pluton contact below, outside the zone of contact metamorphism (Nyman et al. 1992). Interbedded brown siltstone layers within the limestone are less than 1 cm thick and are symmetrically pulled apart within the foliation, in the direction of the lineation. In XZ cross section, the siltstone boudins are separated by fractures and commonly have sharp boundaries. Viewing the foliation surface (XY plane) from above, the siltstone layers seem to be 'torn' open, similar to how a layer of clay will tear when pulled apart. The 'tears' are elongate breaks, or cracks within the siltstone layer that are distributed throughout the siltstone layers, and that have the greatest separation in the central portion of the tear. The direction of crack opening is consistent throughout the siltstone layers and is oriented perpendicular to the orientation of the stretching lineation found throughout the western contact.

1.4 *Strain Path*

The sequence of deformational events is better understood within the gneissic border facies due to the dikes and veins which record incremental periods of deformation. The aplite dikes and quartz veins were emplaced at various stages in the development of the gneissic foliation, and therefore record different amounts of finite strain. There are no incremental strain markers in the metasedimentary units. Structural relationships observed within and near the high strain zone of the Papoose Flat pluton suggest two possible sequences of deformational events; 1) one period of noncoaxial deformation which is generally partitioned into pure shear and simple shear by rock type or, 2) an early, dominantly coaxial deformation which is later overprinted in some rock types by a component of simple shear deformation.

The following review of field relationships and their interpretations suggest that the exact timing of pure shear versus simple shear is unclear. Considering the tectonically rapid

emplacement and cooling of shallow level plutons (Paterson et al. 1992), the various components of deformation may be considered to be occurring synchronously. It is clear though, at least within the granite, that the pure shear component of the deformation was concentrated in the pluton's gneissic border facies and occurred, at least initially, prior to the component of simple shear deformation recorded in the quartz veins within the gneiss. Strain path partitioning may have occurred between rock types of differing rheology (see section V, 1.5 below). This strain path partitioning may have been contemporaneous with the component of pure shear recorded in the gneiss. Alternatively, the component of plane strain recorded in the quartz veins, and in the Saline Valley Formation, may post-date initial granite deformation.

1.5 *Interpretations of Field Relationships*

The macroscopic structures were described in detail above in order for the various types of strain, which vary drastically between the various rock types, to be analyzed separately (as below). The strain symmetry within the high strain zone varies with rock type and includes; pure shear plane strain (k=1), pure shear flattening (k=0), and approximately simple shear. The chronological order of development of the various types of strain is also key to understanding the structural evolution of the high strain zone, and is better understood by comparing the various structures and their spatial relationship to each other. The various types of strain, and the rocks they are found in, are discussed below.

I. *Early pure shear within the granite; plane strain or flattening?*

The symmetric aspect of the gneissic foliation viewed in XZ sections (Fig. 6 & 7a), i.e., the absence of shear sense indicators, does not preclude simple shear, but is most readily interpreted as a consequence of dominantly pure shear (plane strain or flattening)

deformation. During the present study S-C fabrics have been observed in only two outcrops compared to the many kilometers of gneiss and granite covered in field work, and their orientation indicates opposing senses of shear. This is in contrast to Paterson et al. (1991, p. 324) who state that shear sense indicators are located everywhere within and adjacent to the western half of the pluton.

Viewing the gneiss in XY sections, elongate potassium feldspar megacrysts are not preferentially aligned parallel to the NW trending mineral elongation lineation, and therefore may indicate flattening (K=0) strain. If the gneissic foliation represented a significant component of simple shear, or pure shear plane strain deformation, elongate bodies might be expected to have rotated into parallelism with the flow direction. The lineation within the gneiss is composed of elongate micas and quartz aggregates which anastamoze around the megacrysts. Biotite, muscovite, and quartz in the matrix can recrystallize at lower temperatures compared to potassium feldspar, possibly in response to a late variation in the strain path which did not recrystallize or rotate the larger more rigid feldspars.

The abundant aplite dikes are observed at all orientations with respect to the gniessic foliation and are intensely folded for over 15 km around the western margin of the pluton (Fig. 7b). Many folds do not display a vergence, although locally the folds do verge. There is no one dominant direction of fold vergence and the local vergence was probably controlled by the original orientation of the dike. The axial planes of the folds are parallel to the gneissic foliation and therefore the folding is probably related to the deformation that produced the foliation in the aplite dikes. It is possible, with assumptions, to discern the sense of shear from folds if the folds have a "regionally extensive consistent asymmetry" (Hanmer and Passchier, 1991, p. 66). If the well developed gneissic foliation represented a large component of simple shear, veins and dikes might be expected to have rotated, at least to some degree, into parallelism with the foliation during deformation. Folds might also be expected to display a dominant direction of vergence.

II. *Late simple shear within quartz veins;*

Quartz vein emplacement is inferred to have postdated at least the initial development of the gneissic foliation, and therefore the component of simple shear recorded in the quartz veins must have occurred later than the initial deformation that produced the gneissic foliation. The orientation of early quartz veins is almost always parallel to the gneissic foliation and therefore the orientation of crack opening was probably controlled by the strong gneissic fabric. Quartz veins, now mylonitized, crosscut and were locally emplaced within foliation parallel aplite dikes. The quartz veins were probably not rotated into parallelism with the foliation, as the aplite dikes have been, since the quartz veins cross cut the aplite dikes, and are not folded like the aplite dikes.

Mylonitized quartz veins are rarely observed oblique to the foliation, but occasionaly are found at angles up to 40° to the gneissic foliation and still contain their own vein parallel foliation (Fig. 8a) with strong crystallographic preferred orientations (PF 271 and PF 212, Figs. 10 & 11b, CHAPTER TWO). This cross cutting relationship also suggests that the deformation in the quartz veins is later than the deformation that produced the gneissic foliaton.

III. *Localized simple shear in quartz veins related to bulk pure shear;*

In three outrcops along the southeastern portion of the gneissic border facies, top to the NE shear took place along quartz veins and aplite dikes aligned parallel to the foliation, postdating the development of foliation. High angle quartz veins which initially crosscut the foliation parallel veins are offset across the foliation parallel veins. The high angle veins can be traced across the vein parallel shear zones where they are thinned and rotated into parallelism with the foliation.

The asymmetry of quartz crystallographic fabrics from three foliation parallel quartz

vein locations, and one sample from one of the outcrops discussed above (PF 400b, Fig. 11b, CHAPTER TWO), indicates a top to the NW sense of shear. The asymmetry of fabrics from six other vein locations indicates a top to the SE sense of shear. The number of sample locations that have quartz fabrics indicating a top to the NW sense of shear is almost the same as the number of sample locations that have quartz fabrics indicating a top to the SE sense of shear (see Fig. 12, CHAPTER TWO). The occurence of opposing shear sense indicators suggests a strong variation in flow direction which could be related to heterogeneous bulk pure shear deformation. For example, the quartz veins may have accomodated localized 'escape' of the granitic material during an event in which the maximum shortening direction was oriented perpendicular to the gneissic foliation.

IV. *Pure shear flattening and plane strain in the aureole;*

Chocolate tablet boudinage within the skarn rocks at the contact around the western margin of the pluton indicates approximate pure shear flattening (k=0). The mineral elongation lineation on the surface of the sheaths surrounding the boudins represents an approximate plane strain path (k=1), developed under pure shear or simple shear deformation. The intense deformation which flattened and extended the boudins probably occurred prior to or synchronously with lineation development, although a strain compatibility problem arises if they developed synchronously. The lineation is not believed to have developed first, since the intense flattening would probably have destroyed, or at least locally reoriented, the lineation.

V. *Synchronous pure shear plane strain and simple shear plane strain*;

There is a parallel alignment of the extension direction within the symmetrically boudinaged Saline Valley siltstones (Fig. 8b) and the orientation of the stretching lineation in the quartz veins and quartzites which suggests that they are related to the same

deformational event. This implies that simple shear plane strain within quartz rich units developed concurrently with pure shear plane strain in the siltstones.

VI. *Simple shear within the Harkless Formation;*

A strong component of top to the SE simple shear is well documented within the Harkless quartzites and is discussed in detail in chapter two. The component of simple shear within the Harkless schists is more locally developed than in the quartzites, but is observable throughout the high strain zone and will be discussed in chapter three.

The sequence of events recorded within the gneiss do not preclude the possibility that the pure and simple shear components of the overall deformation were contemporaneous, only that they were recorded within the gneiss at different times. It is possible that the simple shear component of the deformation recorded in the quartz veins developed later than the development of the gneissic foliation only because the quartz veins were emplaced after the formation of the gneissic foliation. Before the quartz veins were emplaced, there might not have been a rock type in the granite with the rheology necessary to accomodate simple shear, and the component of simple shear might have been accomodated elsewhere, perhaps within the aureole rocks. Once the quartz veins were emplaced, the existence of material anisotropy (which already existed in the metasedimentary units) might have favored noncoaxial flow (Lister and Williams 1983; Law et al. 1991), while the relatively isotropic granite, at least before significant deformation, favored accumulation of coaxial deformation.

Observations outlined above in sections V (and possibly IV) suggest that at least within the aureole, pure shear and simple shear were occurring contemporaneously. Since there is no evidence to indicate otherwise, the deformation within the aureole is considered to be concurrent with the development of the gneissic foliation. Strain path partitioning

between different rock types, and various combinations of; pure shear flattening (k=0), pure shear plane strain (k=1), and simple shear plane strain (k=1), is proposed to have resulted in the differences in strain symmetry observed in different rock types within the high strain zone.

CHAPTER TWO

C-AXIS FABRICS AND QUARTZ TECTONITE MICROSTRUCTURES

2.1 *Introduction*

C-axis fabrics were measured from quartz tectonites collected along 15 km of the intensely deformed western margin of the Papoose Flat pluton (Fig. 9). Sixteen c-axis fabrics were measured from quartz veins within the gneissic border facies of the pluton and sixteen c-axis fabrics were measured from Harkless quartzites in the aureole surrounding the pluton. Two c-axis fabric patterns were measured from quartz ribbons within the gneiss. Thirty-one out of the thirty-four fabric patterns indicate that strong crystallographic preferred orientations within the quartz veins and metasedimentary quartzites have developed in response to a deformation involving a large component of simple shear while the pluton was in its early stages of cooling (Law et al. 1992).

Asymmetric c-axis fabric patterns indicate a predominant top to the SE sense of shear in both quartz veins and quartzites, although vein fabric patterns are distinctly different than metasedimentary quartzite fabrics. Quartz vein fabrics from the gneissic border of the pluton are characterized by asymmetric single girdles with strong concentrations of c-axes parallel to the Y-axis of the sample coordinate system used in this paper. Quartzite fabrics within the narrow pluton aureole are characterized by asymmetric type I (Lister 1977) cross girdles with less strongly concentrated c-axis maxima.

Quartz tectonite c-axis fabrics were also examined in traverses (Fig. 9) perpendicular to the pluton/wall rock contact in order to examine the change in fabric with varying distance from the contact. Three traverses are located within the high strain zone and one traverse is located in the low strain zone.

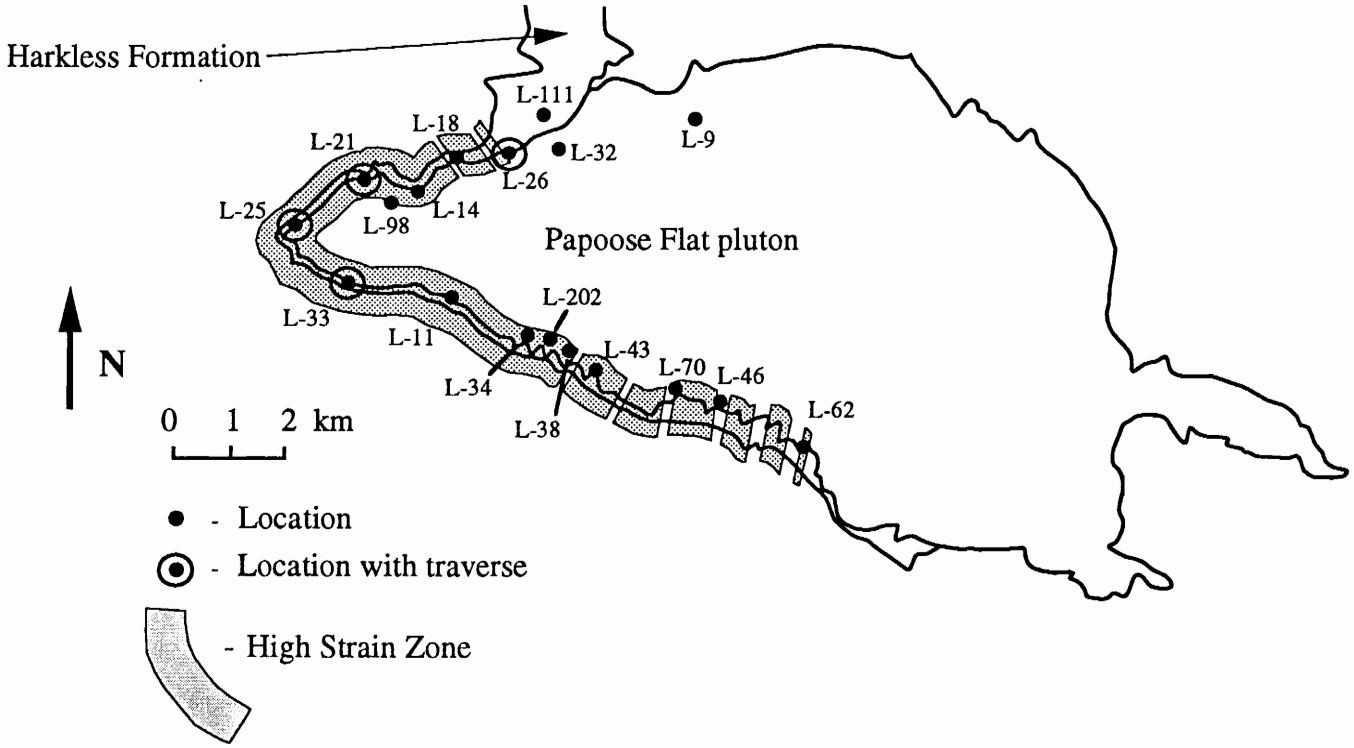

Fig. 9. Generalized outline of the high strain zone at the western margin of the Papoose Flat pluton and locations of quartz tectonite samples with measured c-axis fabrics from the Harkless quartzite and quartz veins within the pluton.

The differences in quartz fabrics are examined across the pluton-wall rock contact and along the contact from the highly strained western margin to the less intensely strained rocks farther east. The strong variation in fabrics across and along the pluton/wall rock contact can be related to one or any combination of four possible factors: 1) Quartz veins accumulated a greater amount of finite strain than the quartzites, which is associated with a greater degree of recrystallization, 2) The strain path was partitioned between quartzites and quartz veins, the quartzites having accomodated a stronger component of pure shear than the quartz veins, 3) A pre-deformation preferred orientation of c-axes within veins due to the processes involved in vein crystallization influenced the subsequent deformation fabric, or 4) Changes in temperature, strain rate, or other variables induced different slip systems to operate between the quartz veins and quartzites.

2.1.2 *Analytical Methods and Data Presentation*

Quartz c-axes were measured from thin sections using a Leitz optical microscope and universal stage following the techniques outlined by Turner and Weiss (1963, p. 202-203). A minimum of 200 c-axes were measured for each of the thirty-four thin sections used in this study. C-axis plots were contoured using the Macintosh computer program designed by Neil Mancktelow of the Geologisches Inst., ETH, Zurich, Switzerland. Maximum concentrations of c-axes (per unit area of the lower hemisphere projection) were calculated using the Turbo-Pascal computer program of Starkey (1989). C-axis plots were contoured with the Mancktelow program because of the ease and swiftness in manipulating the variables (contour interval, projection view, line width) involved in producing the plots. The maximum concentrations of c-axes were calculated using the program of Starkey (1989), because his program does not smooth the peaks in the concentrations like the Mancktelow program does.

All projections used for c-axis presentation are perpendicular to foliation and parallel to lineation. These lower hemisphere projection planes are always viewed to the north and east as the lineation trends north and west. The face perpendicular to foliation (XY) and parallel to lineation (X) is termed the XZ plane and Y is orthogonal to the XZ plane, although in this paper the visible lineation (X) and foliation (XY) are not assumed to be parallel to the principal axes of finite strain. The term 'fabric' in this paper is used to refer to the fabric pattern that a preferred orientation of quartz c-axes will exhibit when plotted on a lower hemisphere projection plane.

Descriptions of quartz fabrics and microstructures are divided between quartz tectonites within the pluton and those within the metasedimentary units. Generally, fabric patterns from the quartz veins within the pluton are dominated by asymmetric single girdles while fabrics from the aureole quartzites are typically asymmetric type I cross girdles. The terminology used in this paper to describe the quartz c-axis fabric patterns has been defined by Lister (1977). 'Girdles' are roughly planar concentrations of c-axes plotted on a lower hemisphere projection plane that intersect the YZ plane along the Y axis and typically are oriented much closer to the Z axis than the X axis. Cross girdles are composed of two planar concentrations that intersect along the Y axis. Type I cross girdles are parallel to the YZ plane when close to Y. Closer to the Z axis, the great circle girdle becomes a small circle girdle central about the Z-axis. Type II cross girdles are composed of two great circle girdles that intersect along the Y-axis.

2.2 *Quartz Tectonites Within the Pluton*

2.2.1 *Quartz Vein Microstructures*

The microstructure of the mylonitic quartz veins is fairly constant throughout the high strain zone. In XZ sections the microstructures are strongly indicative of dynamic recrystallization during a deformational event involving a component of simple shear. Individual grains within quartz veins are characterized by straight to lobate grain boundaries and equidimensional to slightly elongate grain shapes. The main foliation is defined by changes in grain size associated with an alignment of the minor secondary phases, usually micas and elongate feldspars. Oblique grain shape fabrics are locally developed. Grains are only slightly elongate where they define a variably developed oblique grain shape fabric, which is typically at c. 50° to 60° to the macroscopic foliation. It is also common to observe large areas where grain boundaries are similary aligned at high angles to the foliation but in both directions with respect to the lineation (see Lister and Snoke, 1984, fig. 14). Grain boundaries also commonly intersect at triple junctions with 120° angle intersections. Quartz grains exhibit slight undulatory extinction, little to no subgrain development, and vary in size from 0.5 to 2.0 mm in diameter and average around 1.0 mm in diameter. Deformation lamellae are locally abundant, but vary in number and intensity with location around the pluton. Within the gneiss, elongate polycrystal ribbons of quartz are sporadically developed around feldspar grains adjacent to the borders of the veins.

2.2.2 *Quartz Vein Fabrics*

Sixteen quartz veins from the gneissic border facies collected at twelve different locations around the pluton were measured for c-axis preferred orientations (Fig. 10). Six locations are from the north side of the pluton and six locations from the south side. Fifteen fabrics exhibit strong preferred orientations associated with high strain. Fourteen veins were oriented parallel to the gneissic foliation and two were oblique. The following discussion of fabrics covers all of these veins.

C-axis concentrations can be as high as 46 times uniform distribution, the most intense point maxima centered around the Y-axis (e.g., PF 14, fig 11a), but have an average maximum of 30 times uniform distribution. Most fabric girdles are narrow and are usually defined by a linear series of elliptical concentrations of c-axes that do not cross the XZ plane (e.g., PF 152, Fig. 11b).

The c-axis fabrics from the quartz veins have characteristically strong Y-axis parallel concentrations (Y-axis maxima) and are mainly asymmetric single girdles (Figs. 11a & 11b). Out of the thirteen fabrics with discernable girdles, eleven are asymmetric single girdles, and two are asymmetric type I cross girdles. Out of the remaining three fabrics, two display elongate Y-axis point maxima which trend toward the Z-axis in the Z-Y plane. The fabric from the remaining sample, PF 169b, has an irregular shaped maxima distributed around the Y-axis (Fig. 11b).

Out of the twelve locations sampled (Fig. 10), fabric asymmetry from six locations (L-32, L-26, L-14, L-33, L-34, L-70, Figs. 10,12a) indicates a relative top to the southeast sense of shear and asymmetry from four locations (L-9, L-21, L-202, L-38, Figs. 10, 12b) indicates a relative top to the northwest sense of shear. Samples from the remaining two locations, L-46 and L-98 (Fig.10) display fabrics with no discernable asymmetry.

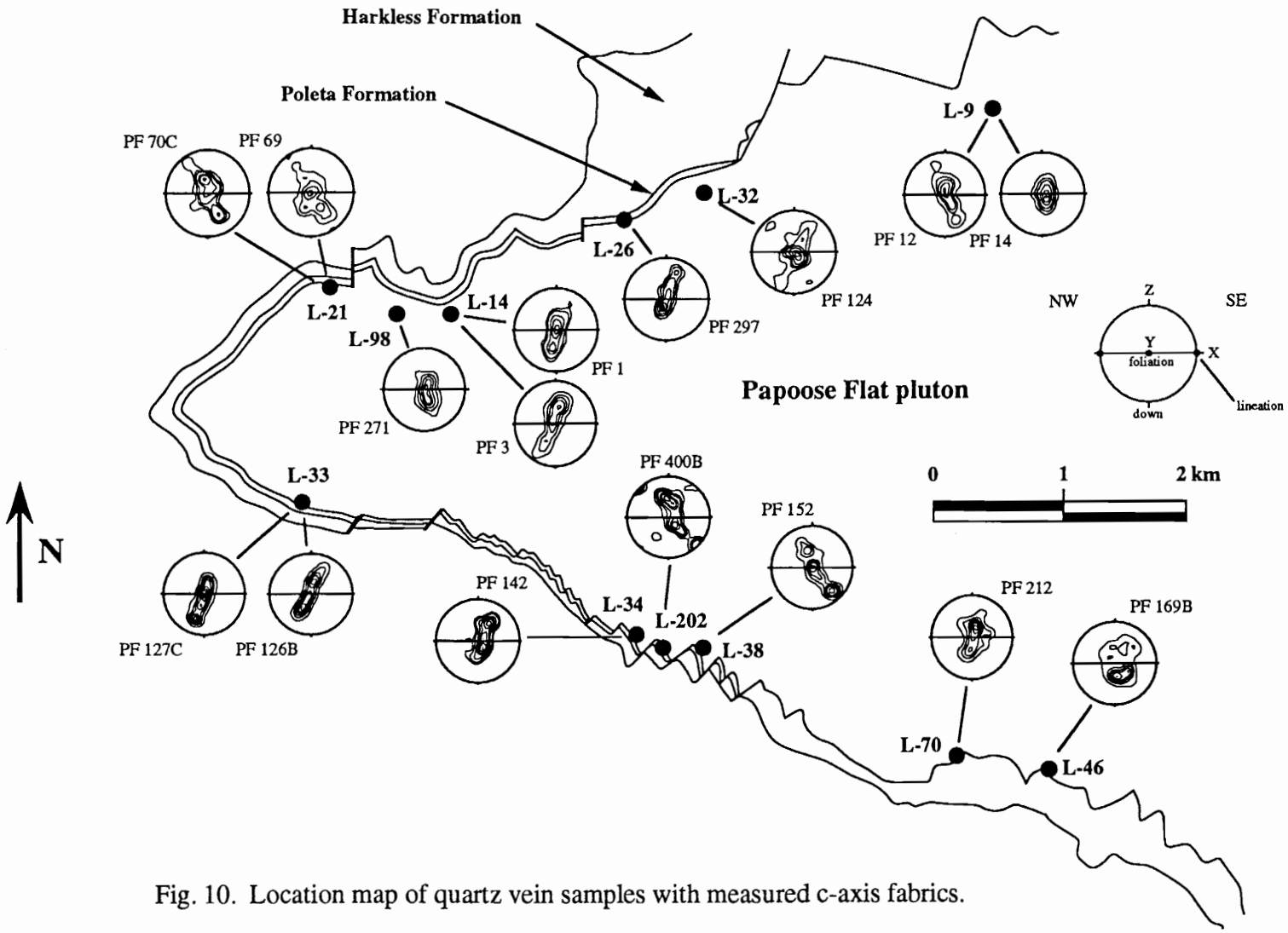

Fig. 10. Location map of quartz vein samples with measured c-axis fabrics.

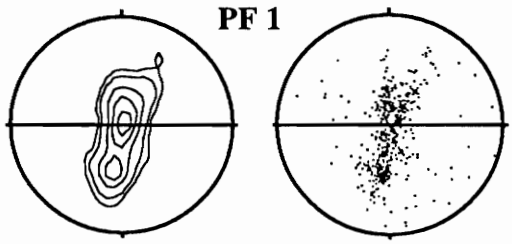

Contoured at 1 2 3 ... times uniform
Max. Con.=34 times unif.
525

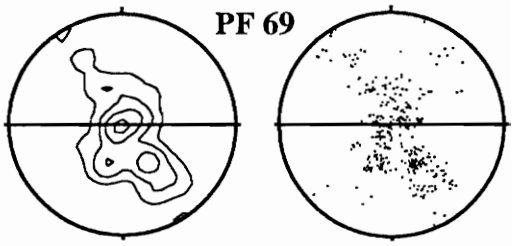

Contoured at 1 3 6 10 times uniform
Max. Con.=32 times unif.
400

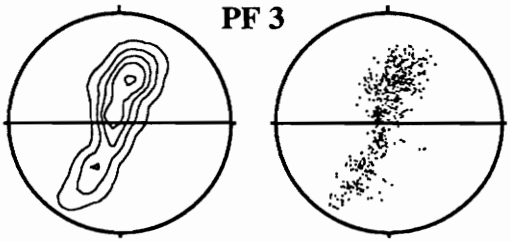

Contoured at 0 1 3 5 7 10 times uniform
Max. Con.=27 times unif.
600

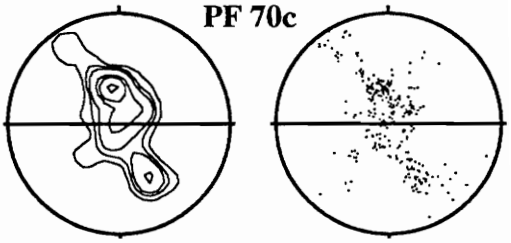

Contoured at 1 2 3 6 8 12 times uniform
Max. Con.=27 times unif.
327

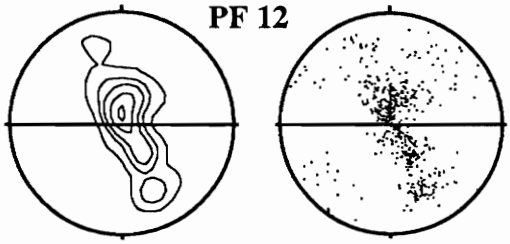

Contoured at 1 3 5 8 11 times uniform
Max. Con.=25 times unif.
600

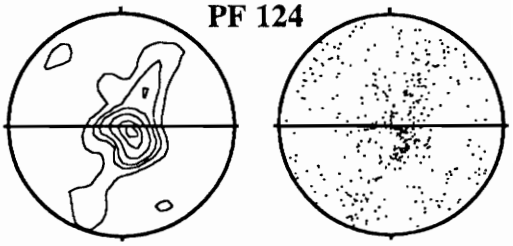

Contoured at 1 2 3 ... times uniform
Max. Con.=30 times unif.
502

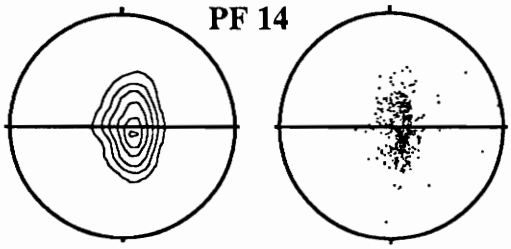

Contoured at 1 3 6 11 16 20 times uniform
Max. Con.=46 times unif.
500

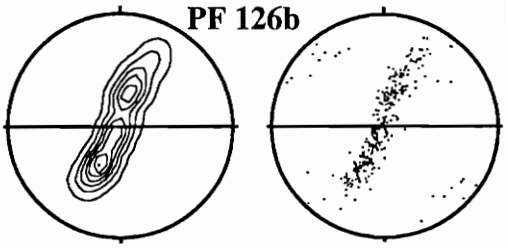

Contoured at 1 3 5 ... times uniform
Max. Con.=30 times unif.
356

Fig. 11a. Contour and scatter plots of quartz vein c-axes. Lower hemisphere projections, viewed towards the the ENE.

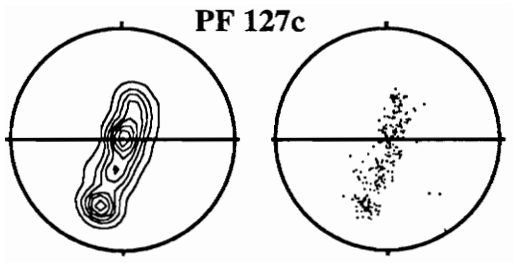

Contoured at 1 3 5 ... times uniform **300**
Max. Con.=34 times unif.

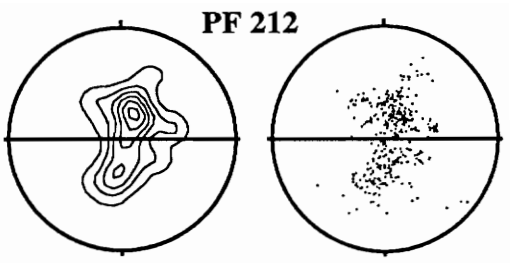

Contoured at 1 3 5 ... times uniform **400**
Max. Con.=22 times unif.

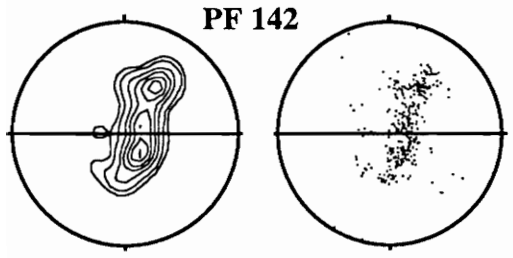

Contoured at 1 2 4 ... times uniform **400**
Max. Con.=24 times unif.

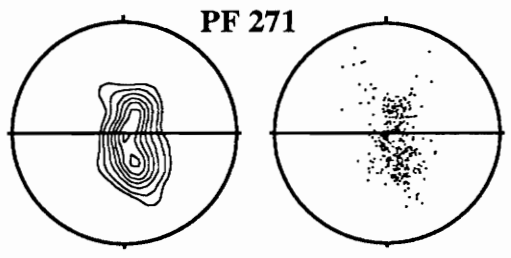

Contoured at 1 2 4 ... times uniform **400**
Max. Con.=30 times unif.

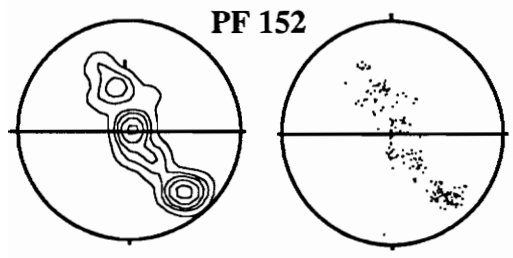

Contoured at 1 0 3 5 8 12 times uniform **258**
Max. Con.=38 times unif.

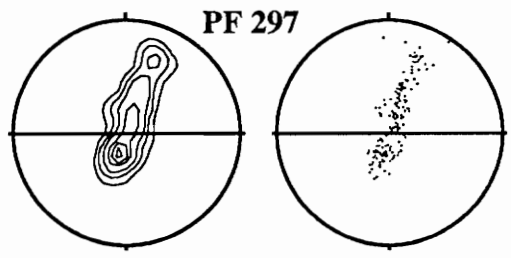

Contoured at 1 3 6 ... times uniform **200**
Max. Con.=30 times unif.

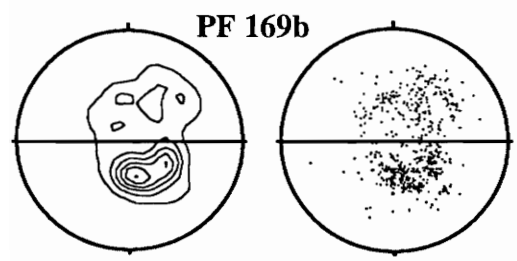

Contoured at 1 3 5 ... times uniform **600**
Max. Con.=24 times unif.

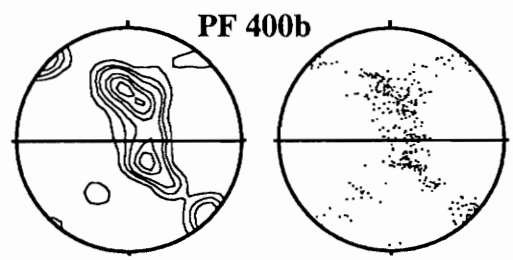

Contoured at 1 2 3 ... times uniform **400**
Max. Con.=20 times unif.

Fig. 11b. Contour and scatter plots of quartz vein c-axes. Lower hemisphere projections, viewed towards the ENE.

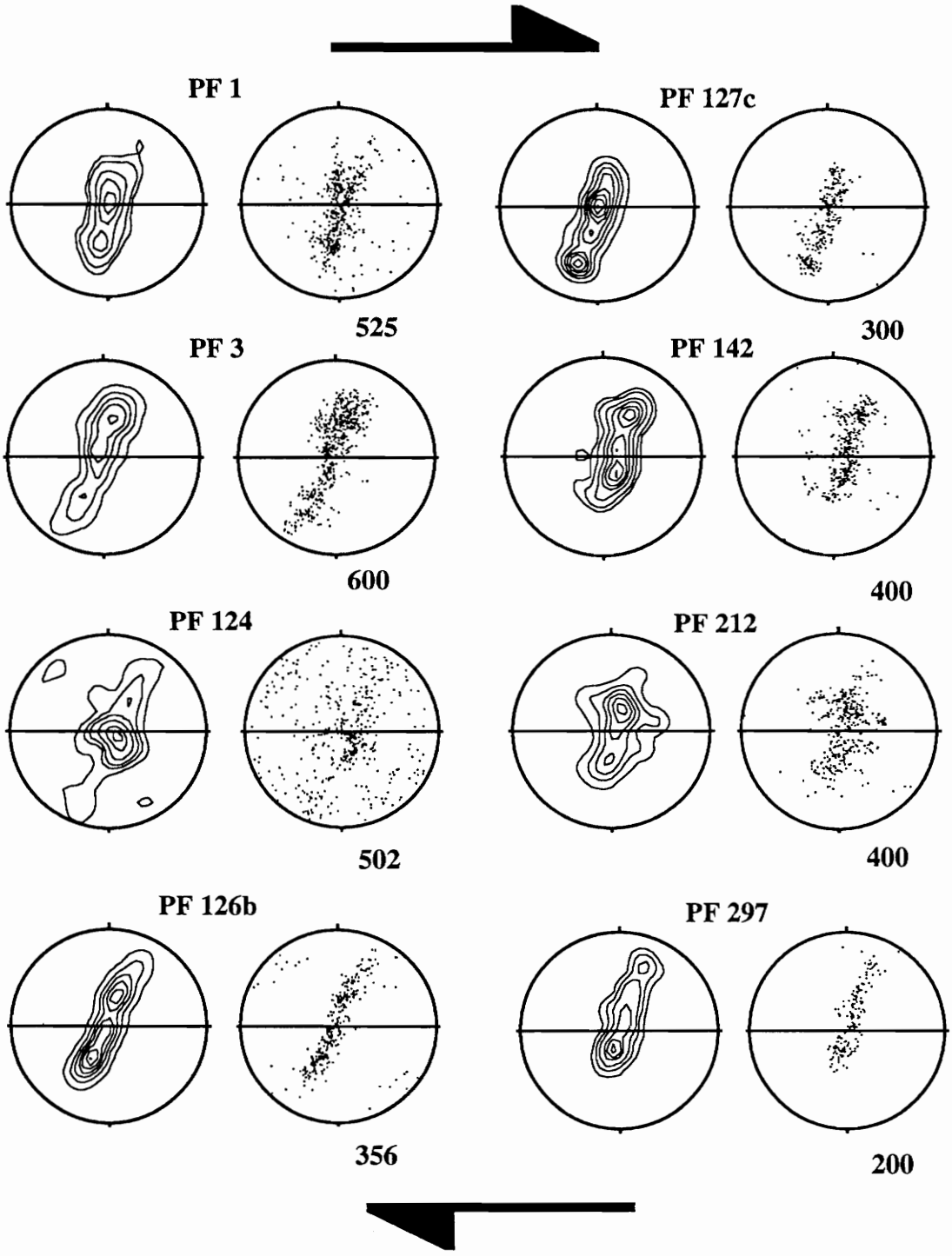

Fig. 12a. Quartz vein c-axis fabrics (viewed towards the ENE) that are asymmetric and indicate a relative top to the SE sense of shear. See Fig. 10 for location of samples.

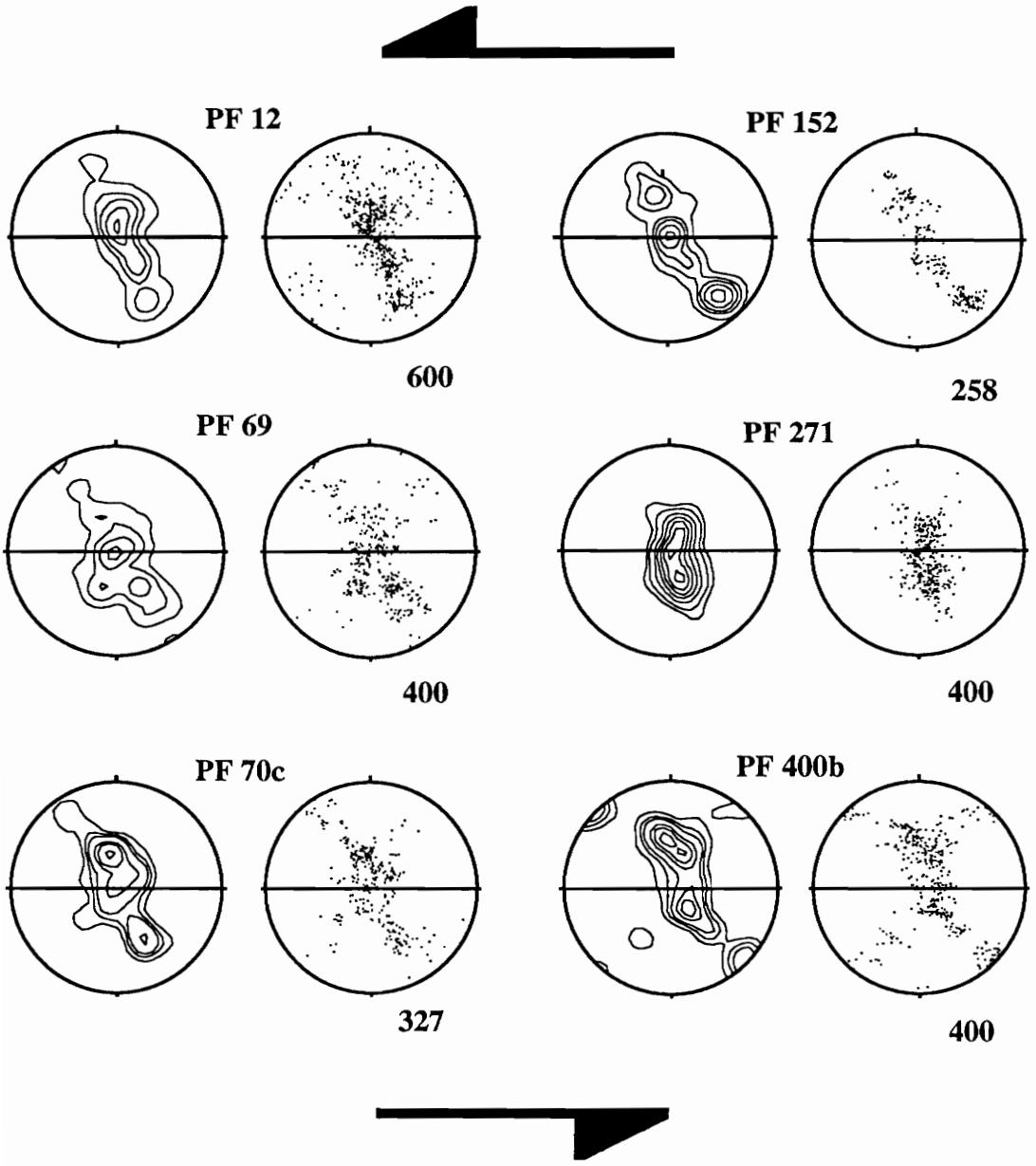

Fig. 12b. Quartz vein c-axis fabrics (viewed towards the ENE) that are asymmetric and indicate a relative top to the NW sense of shear. See Fig. 10 for location of samples.

No correlation between shear sense and geographic location around the pluton has been detected. The samples with fabrics that indicate NW directed shear were collected at both the northern and southern border of the pluton (Fig. 10). The shear sense indicated by the asymmetric fabric patterns is always consistent with the shear sense indicated by the angular relationship between the principal foliation and the oblique grain shape fabric (in the samples where the oblique fabric was observed).

2.2.3 *High Angle Quartz Veins*

Over 95% of the mylonitic quartz veins observed in the field have an orientation that is parallel or subparallel to the gneissic foliation. Due to their similar orientation, the foliation in the veins was difficult to distinguish in attitude from the gneissic foliation. Rare quartz veins at high angles (20-45°) to the gneissic foliation are uncommon, but they were observed throughout the high strain zone. The high angle veins have their own vein-parallel mylonitic foliation (Fig. 8a).

The relationship between the high angle quartz veins and the gneiss is potentially important for use in determining the timing relationship between development of the gneissic foliation and formation/deformation of the veins. Data on the sequence of events can help to constrain the bulk deformation path, i.e., whether the strain was partitioned and the noncoaxial deformation in the quartz veins occurred synchronously with the apparent coaxial deformation that produced the gneissic foliation in the granite, or if the deformation in the quartz veins was a later phenomena. Quartz fabric development is related to various parameters that could also help constrain the deformational environment, i.e., the orientation of shear zone boundaries and the instantaneous stretching axes (Lister and Price 1978). Two of the high angle veins have been sampled from opposite margins of the pluton and their fabrics measured.

High angle vein sample PF 271 (Fig. 11b) was collected from the northern margin of the pluton (Fig. 10) and is from a vein which dips 24° more steeply to the NW than the gneissic foliation. The c-axis fabric is similar to other vein fabrics with a strong Y-axis maxima and concentrations symmetrically disposed at 15-20° away from the Y-axis towards the Z-axis within the Y-Z plane. High angle vein sample PF 212 (Fig. 11b) was collected from the southern border of the pluton (Fig. 10) from a vein which dips 35° more steeply to the southeast than the gneissic foliation. The fabric resembles the fabric of PF 271 with strong Y-axis parallel and subparallel maxima, but differs in that a slight asymmetry indicates a top to the SE sense of shear.

2.2.4 *Quartz Ribbon Microstructures*

The well developed foliation in the gneiss is partly defined by ubiquitous quartz ribbons which are relatively planar but locally anastomose around the coarser potassium feldspar megacrysts. Much of the quartz in the gneiss is concentrated within the ribbons where it is significantly coarser grained than the surrounding matrix quartz. Grain size varies from .25 mm to 1.5 mm in length and width, but depends on ribbon width, where single elongate grains commonly span the width of the ribbon. Quartz grain boundaries outside of the ribbons are vague and it is difficult to distinguish feldspar from quartz grains. Within ribbons, grain boundaries are sharp and vary between straight and lobate.

2.2.5 *Quartz Ribbon Fabrics*

C-axes were measured from ribbon quartz samples collected from the northern and southern border of the pluton. C-axes were measured in sections of ribbon that are relatively planar. The crystallographic orientation of individual grains that 'wrap' around larger, more rigid mineral phases has probably been affected by the oblique angle the ribbon is oriented with respect to the foliation. Therefore, sections of ribbon that anastomoze around larger phases were not measured.

The fabric PF 145, collected at the southern border of the pluton (L-34, Fig. 9), is from a quartz ribbon and displays a symmetrical cross girdle with two strong point maxima parallel and subparallel to Y-axis (Fig. 13). The girdles are less well defined traced away from the point maxima towards the XZ plane.

The fabric PF 68 is from the northern border of the pluton (L-21, Fig. 9) and displays one of the more poorly developed fabrics (Fig. 13). There is a broad central concentration of c-axes around the Y-axis and vague vestiges of a cross girdle towards the periphery. The grains are very coarse and planar sections of ribbons are not common, perhaps indicating a lower degree of strain in this portion of the gneiss.

2.3 *Quartz Tectonites within the Harkless Formation*

2.3.1 *Microstructure*

Harkless quartzites within the high strain zone are completely recrystallized and contain no relict detrital grains. The quartzites display different textural features than the quartz veins. Grain size is generally much finer than in the quartz veins (down to 50

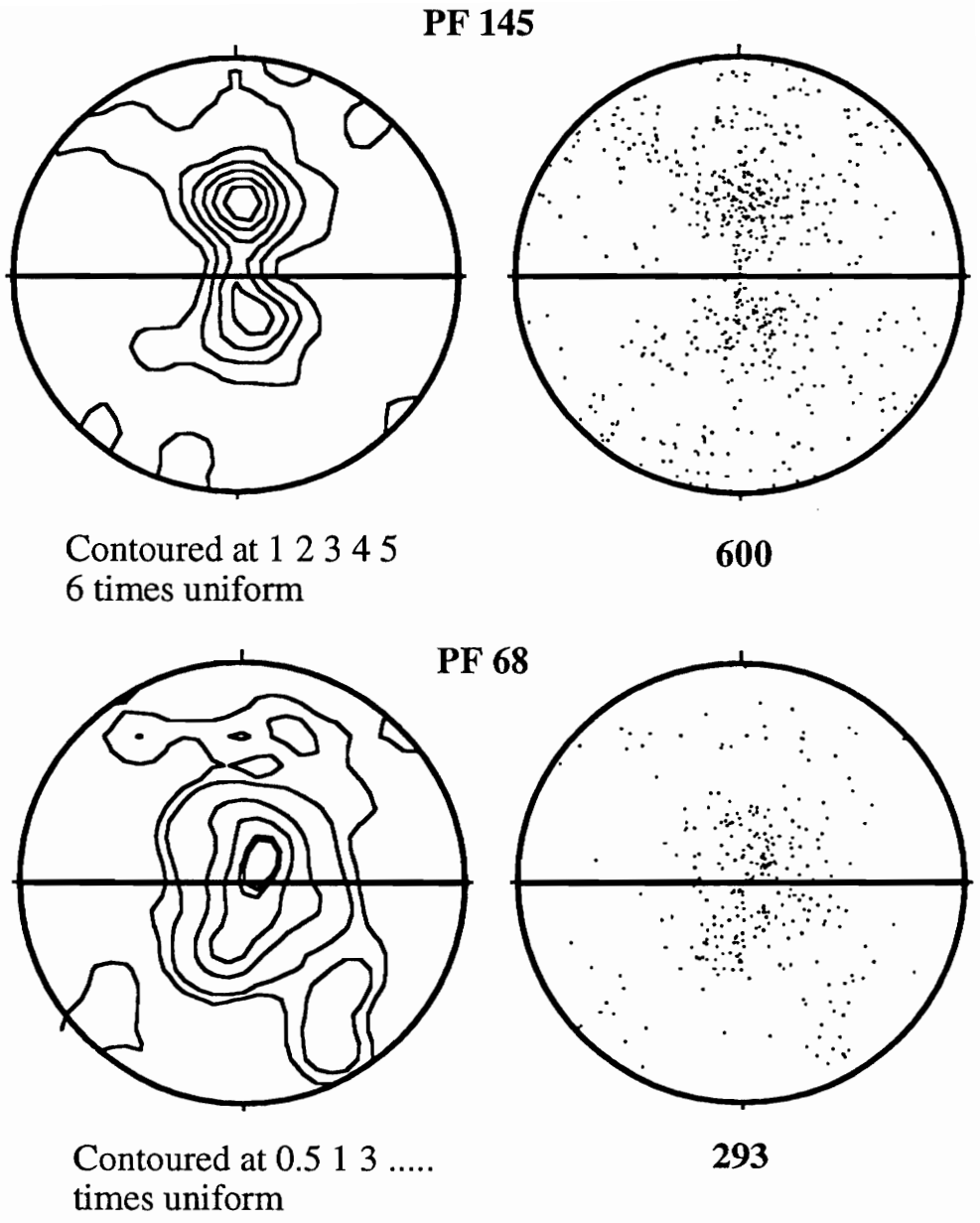

Fig. 13. Contour and scatter plots of quartz c-axes in ribbon grains within the gneiss. Lower hemisphere projection. Viewed towards the ENE.

μm), but is often controlled by mica content. In addition, the grains are usually more constant in size and equant in shape within the quartzites. Lobate grain boundaries are observed but straight grain boundaries are more common. Subgrains are rare. The absence of mica is at times associated with the development of a preferred alignment of elongate grains oriented oblique to the foliation. This oblique grain shape fabric is only observed where there are coarse grains within the more monominerallic quartzites. The oblique grain shape alignment is only well developed in the one sample (PF 8) from location 11 (Fig. 9), which is an old flagstone quarry on the south side of the pluton. The oblique angle is oriented at approximately 35° to the foliation and the sense of obliquity indicates a top to the SE sense of shear.

On the north side of the pluton at location 26 (Fig. 9), where the strain is gradational between the high strain zone to the west and the less deformed strata to the east, possible relict detrital grains are observed 70 m above the contact within the Harkless Formation. The majority of grains in this transitional area still exhibit microstructures indicative of recrystallization and a strong crystallographic preferred orientation has developed. The relict detrital grains are coarser in grain size, exhibit more internal strain features (deformation bands and irregular extinction), are occasionally polycrystalline, and are more elongate than the surrounding recrystallized matrix grains. Micas are more homogeneously distributed, but remain aligned parallel to the foliation, and anastomose around the coarser, relict detrital grains.

2.3.2 *Quartzite Fabrics*

Sixteen samples from the Harkless Quartzite representing eleven locations around the pluton were measured for c-axis preferred orientation. Six locations are from the aureole north of the pluton, four locations are from the aureole south of the pluton, and one

location is from the aureole at the western margin, or 'nose' of the pluton (Fig. 14)

Thirteen out of the sixteen fabrics are either asymmetrical Type I or Type II cross girdles (Fig. 15a & 15b). Out of the three remaining fabrics, PF 75 (Fig. 15a) is a well defined aysmmetric single girdle and PF 170b and PF 293 (Fig. 15b) have very weak preferred crystallographic orientations, having been collected outside of the high strain zone in the more eastern part of the aureole.

In contrast to the vein fabrics, the quartzite fabric girdles typically display maxima straddling the XZ plane. In relation to the vein fabrics, c-axis concentrations are also less intense between the Y-axis maxima and the XZ plane. C-axis concentrations in the quartzites are as high 34 times uniform distribution (e.g., PF 135, Fig. 15b), but average 20 times uniform distribution and vary with both distance from the pluton and location with respect to the high strain zone.

Eleven of the sixteen fabrics are well developed asymmetric cross girdles indicating a top to the SE sense of shear. Out of the remaining five fabrics, PF 75 (Fig. 15a), is a well developed single girdle with asymmetry also indicating a top to the SE sense of shear. Two fabrics, PF 90 and PF 159 (Fig. 15a & 15b), are weakly asymmetric displaying a top to the NW sense of shear. PF 90 is from the western 'nose' of the pluton, and PF 159 was collected from the south side of the pluton. The sense of asymmetry is, in PF 90, much more clearly displayed in the regenerated c-axis fabric from x-ray data (Law et al. 1992, fig. 13). The remaining two fabrics display little asymmetry and are from samples collected outside of the high strain zone. PF 170b (Fig. 15b) displays a trend towards a small circle distribution centered about the Z-axis (flattening, k=0, strains?) and is from a sample collected in the central part of the southern border. PF 293 (Fig. 15b) displays a trend towards a small circle distribution centered about the X-axis (constrictional, $K=\infty$, strains?) and is from a sample collected along the central northern border where the strain is low enough so that trace fossils are preserved. Deformed skolithos tubes were measured

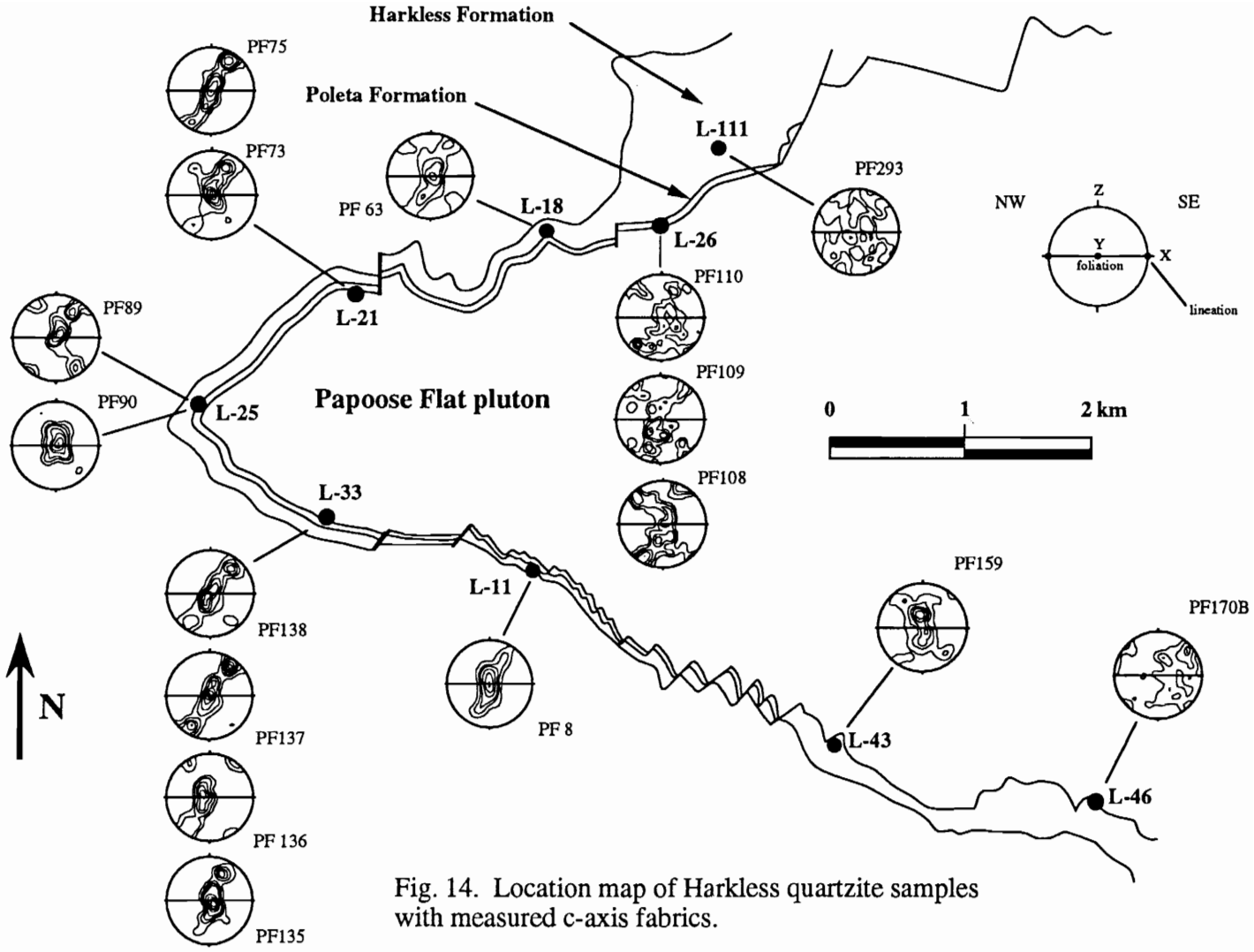

Fig. 14. Location map of Harkless quartzite samples with measured c-axis fabrics.

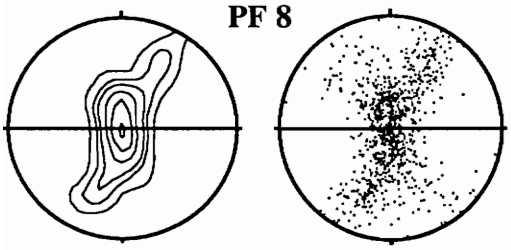

Contoured at 1 2 3 ... times uniform **1000**
Max. Con.=20 times uniform

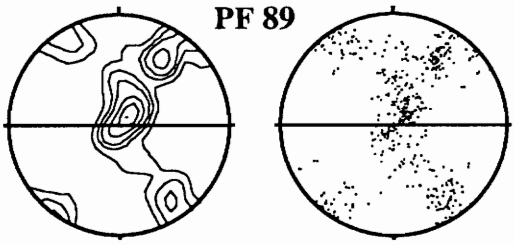

Contoured at 1 2 3 5 7 8.6 times uniform **500**
Max. Con.=20 times uniform

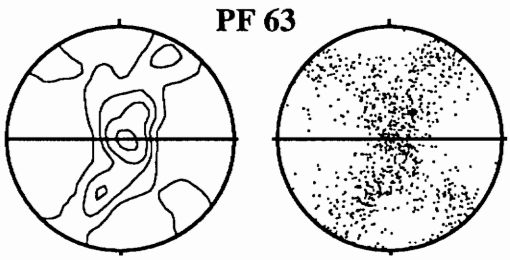

Contoured at 1 2 3 5 6 times uniform **993**
Max. Con.=14 times uniform

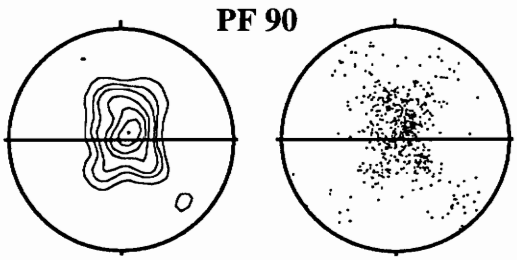

Contoured at 1 2 3 5 7 10 12.5 times uniform **600**
Max. Con.=24 times uniform

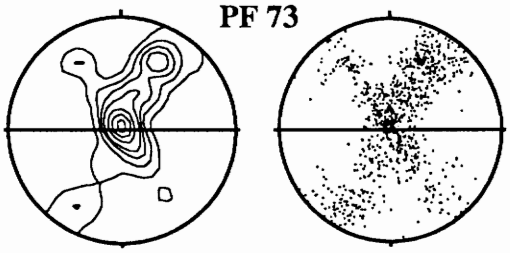

Contoured at 1 2 3 4 6 8 10 times uniform **993**
Max. Con.=31 times uniform

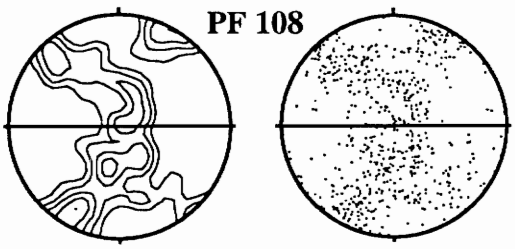

Contoured at 0 1,1.5,2,2.5,2.93 times uniform **600**
Max. Con.=8 times uniform

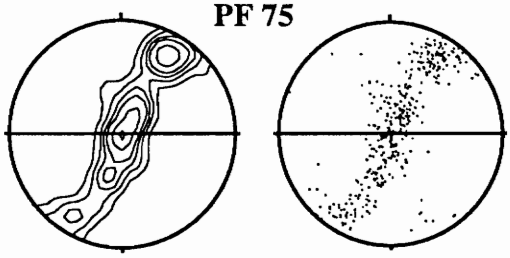

Contoured at 1 2 3 4 6 8 times uniform **400**
Max. Con.=22 times uniform

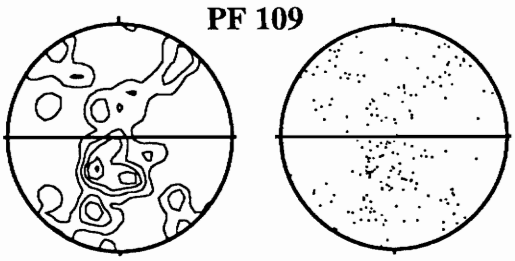

Contoured at 1 2 3 4 5 times uniform **200**
Max. Con.=10 times uniform

Fig. 15a. Contour and scatter plots of Harkless quartzite c-axes. Lower hemisphere projection, viewed towards the ENE.

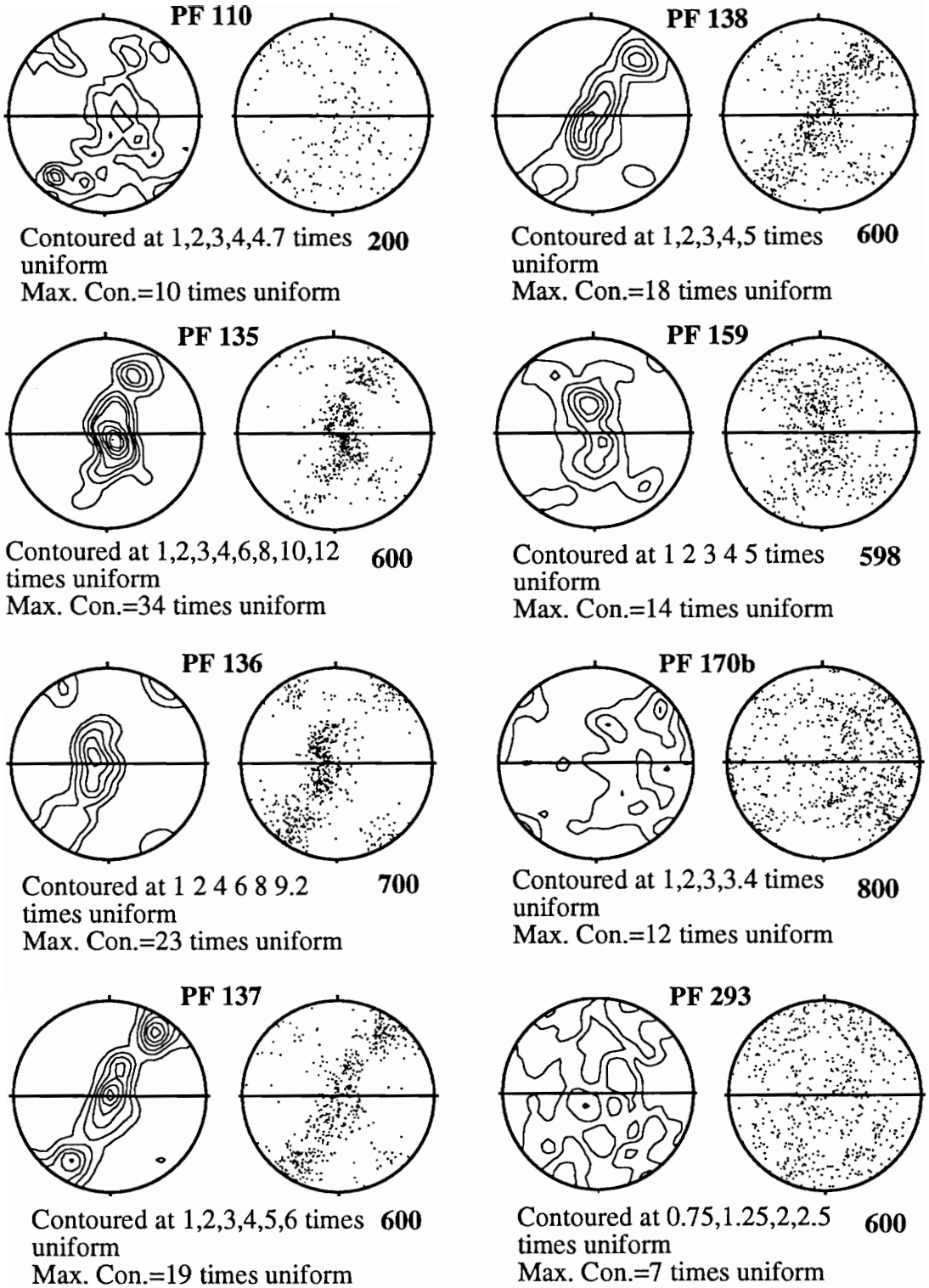

Fig. 15b. Contour and scatter plots of Harkless quartzite c-axes. Lower hemisphere projection, viewed towards the ENE.

on sample PF 293 with aspect ratios on bedding surfaces of between 4:1 and 3:1 (Location 111, Fig. 9). The orientation of the elongate tubes are parallel to the stretching lineation observed throughout the high strain zone. The possible implications of patterns PF 170b and PF 293 will be discussed in the following sections.

2.4 *Discussion of Fabrics and Microstructures*

2.4.1 *Introduction*

Out of the thirty-four quartz fabrics measured, twenty display an asymmetry indicating a top to the southeast sense of shear, while seven display an asymmetry indicating a top to the northwest sense of shear. Out of the twelve quartz vein locations, four (or possibly five) have samples with fabrics indicating a top to the NW sense of shear, and six locations have samples with fabrics indicating a top to the SE sense of shear (Figs. 10 & 12).

C-axis fabrics from the gneissic quartz veins are characteristically asymmetric single girdles with strong Y-axis point maxima. In contrast, fabrics from the aureole quartzites are characterized by asymmetric cross girdles which commonly display maxima straddling the XZ plane. The switch in quartz fabric pattern from pluton to aureole coincides with a strong decrease in the maximum concentration of c-axes within the fabrics. Within the high strain zone, the maximum concentration of c-axes consistently decreases with distance from the pluton/wall rock contact.

The strong variation in fabrics from vein to quartzite across the pluton-wall rock contact and along the contact moving out of the high strain zone can be related to one, or any combination of, four possible factors: 1) quartz veins accumulated a greater amount of finite strain than quartzites, which is associated with a greater degree of recrystallization, 2)

different slip systems operated due to differences in temperature, strain rate, or other variables, 3) the strain path was partitioned between quartzites and quartz veins, the quartzites having accomodated a stronger component of pure shear than the quartz veins, or 4) a pre-deformation preferred orientation of c-axes within the veins due to the processes involved in primary crystallization of vein quartz influenced the subsequent deformation fabric.

The data suggests that factors 1. and 2. were involved in producing the observed fabric variation. An increase in the amount of finite strain was involved in producing the variation in quartz tectonite fabric intensity with decreasing distance from the pluton/wall rock contact, and different operative crystallographic slip systems, combined with an increase in finite strain, helped to produce the variation in fabric pattern from quartzite to quartz vein. Factors 3. and 4. might also have been involved in producing the fabric variation, but there are no independent data or observations that reinforce these possibilities.

It is not possible, without TEM analysis, to determine the crystallographic slip systems that operated to produce observed c-axis fabric patterns (see discussion by Law 1990). Transmission electron microscope analysis of slip systems is based on observing dislocations and their abundance. However, as discussed by White (1979), Ord and Christie (1989), and Law (1990), dislocations observed under the TEM may be produced during uplift rather than being associated with the intracrystalline slip mechanisms responsible for the fabric formation. Numerical and geometrical simulations of fabric development by crystal plastic deformation using prescribed slip systems closely approximates many natural fabric patterns (e.g. Lister et al. 1978; Lister and Paterson 1979; Etchecopar and Vasseur 1987). The effects of dynamic recrystallization have also been modelled (Jessel and Lister 1990), and may add to the applicability of fabric simulation to natural examples. Correlations between the natural and simulated fabric

patterns, along with observations of the metamorphic conditions interpreted to exist at the time of fabric development (e.g., Lister and Dornsiepen 1982; Hobbs 1985; Schmid and Casey 1986; Law et al. 1990) allows an interpretation of the active slip systems based on the fabric patterns measured within the quartz tectonites surrounding the Papoose Flat pluton. It is proposed that *an increase in the finite strain, from quartzite to quartz vein, combined with a difference in operative crystallographic slip systems, from dominantly prism <a> slip in the vein material to basal <a> + rhomb <a> + prism <c> slip within the quartzites, produced the variation in fabric patterns across the pluton/wall rock contact.*

The eight fabrics indicating a top to the NW sense of shear imply that there was a considerable amount of flow to the NW. All the strong fabrics indicating a top to the NW sense of shear are from the gneissic quartz veins. The two asymmetric fabrics measured from the Harkless quartzite that indicate a top to the NW sense of shear are very weakly asymmetric in comparison to the quartz vein fabrics that indicate a top to the NW sense of shear. Quartz veins comprise an extremely small volume fraction of material within the gneiss, but out of the ten locations with asymmetric fabrics, four locations (almost 50%) have veins with fabrics indicating top to the NW sense of shear (Fig. 12). This variation of flow direction in the quartz veins suggests that the deformation within the gneiss is locally heterogeneous, and may suggest that the overall deformation in the gneiss best approximates pure shear. For example, the quartz veins may have accomodated localized 'escape' of the granitic material to the NW and SE during an event in which the maximum shortening direction was oriented perpendicular to the gneissic foliation.

Within the low strain zone, deformation is more intense in the pluton than in the metasedimentary units (based on the quartz tectonite fabrics and on the intensity of foliation and amount of attenuation in the surrounding rocks). This observation is best explained by modelling the forces that caused the deformation as coming from the interior of the pluton and being directed outward, rather than coming from outside of the pluton and being

directed into the pluton.

2.4.2 *Fabric Variation Related to Finite Strain*

There are no passive markers whereby the finite strain can be calculated at various distances from the pluton/wall rock contact within the high strain zone. Finite strain is examined in a relative sense through fabric variation traced outwards from the pluton. The quartz fabrics vary around the pluton-wall rock contact in principally two ways; 1) fabrics change from single girdle to cross girdle and, 2) the maximum concentration of c-axes within the fabrics decreases significantly with distance from the pluton/wall rock contact.

The fabric variation correlates well with the observed macroscopic changes in foliation development. Foliation is best developed at the contact and decreases in intensity of development into the pluton, where the gneissic border changes into a foliated granite, and away from the pluton where attenuation of the metasedimentary units decreases with increasing distance from the contact.

2.4.3 *Review*

Schmid and Casey (1986) have suggested that symmetric cross girdle fabric patterns will progressively change into asymmetric cross girdles and finally into asymmetric single girdle patterns with either an increasing component of simple shear or with an increase in strain during simple shear deformation (Fig. 16). Bouchez and Duval (1982) observed a transition from double maxima to single maxima fabrics associated with an increase in strain in experimentally deformed ice. Similarly, Dell'Angelo and Tullis (1989) also documented a shift from symmetrical fabrics to asymmetrical fabrics in their non-coaxial experiments with increasing shear strain in quartzites. Both experiments

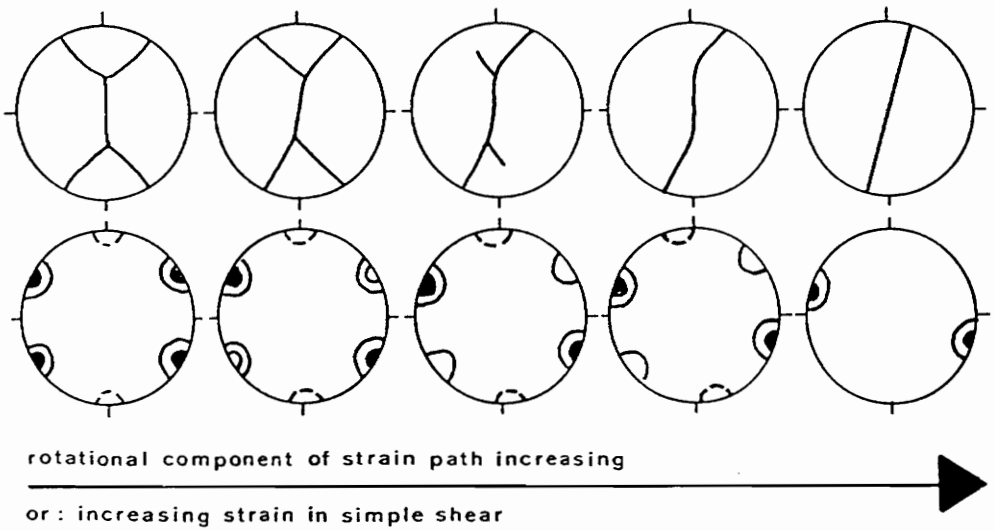

Fig. 16. Illustration portraying the c-axis and a-axis fabric transition for quartz tectonite undergoing dextral shear. C-axis fabric represented by skeletal outline. A-axis fabric represented by schematic contour intervals. From Schmid and Casey (1986).

involved crystal plastic deformation with large components of simple shear.

Hudleston (1977) examined the transition from double maxima to single maxima fabrics and back again to double maxima fabrics across a shear zone within glacial ice from the Barnes Ice Cap, Canada. Hudleston (1977) related the transition from double to single maxima fabrics to an increase in shear strain towards the center of the shear zone. Shear strain was obtained by measuring the angle between elongate air bubbles and the shear zone boundary, which progressively decreased towards the center of the shear zone.

In Lister and Hobb's (1980) Taylor-Bishop-Hill computer simulations of fabric development under varying strain paths, coaxial and noncoaxial strain histories produced similar, although diffuse, fabrics until high strains were accumulated. Only after an imposed shear strain of approximately 2.0 (which corresponds to a shortening of approximately 60%) were the fabrics noticably asymmetric in models simulating non-coaxial deformation. It should be noted that in Lister and Hobb's (1980) simulations, single girdle fabrics were never developed, although, Jessel (1988), and Jessel and Lister (1990), succeded in simulating the transition from double maxima to single maxima fabrics in computer models incorporating simultaneous crystal slip and dynamic recrystallization.

From the above experimental, theoretical, and observational based work (Huddleston, 1977; Lister and Hobbs, 1980; Bouchez and Duval,1982; Schmid and Casey, 1986; Jessel, 1988; Dell'Angelo and Tullis, 1989), the degree of crystallographic preferred orientation is, at least in part, related to finite strain. The higher the strain in simple shear deformation, the greater the propensity to form single girdle fabrics, and the greater the preferred orientation of c-axes. It should be noted that fabrics do not necessarily record finite strain, and more than likely only record the latter increments of strain.

In the quartz tectonites surrounding and within the Papoose Flat pluton, the highest maximum concentration of c-axes is found within the quartz veins closest to the pluton/wall rock contact. The c-axis concentrations within the gneissic quartz veins have an average

maximum concentration of 30 times uniform distribution, but can be as high as 46 times uniform distribution (e.g. PF 14, Fig. 11a). The c-axis concentrations within the Harkless quartzites have an average maximum concentration of 19 times uniform distribution, but can be as high as 34 times (e.g., PF 135, Fig. 15b).

The intensity of c-axis concentrations decreases significantly across the contact into the Harkless quartzites and then decreases more gradually within the Harkless quartzites as the distance from the pluton increases. A correlation is made between the amount of finite strain, the type of girdle(s) developed, and the degree to which c-axes are concentrated in the quartz tectonites surrounding and within the Papoose Flat pluton. The quartz veins within the gneissic border of the pluton exhibit the highest degree of strain, strain magnitude decreases with increasing distance from the pluton, and the Harkless quartzites furthest from the pluton exhibit the least amount of strain. Fabric intensity within quartz veins also seems to decrease with increasing distance into the pluton, although there is not enough c-axis data within the pluton to be conclusive.

2.5 *Traverses*

Samples were collected from four traverses traced perpendicular to the pluton/wall rock contact in order to examine the variation in c-axis fabrics associated with varying distance from the pluton (Fig. 9). Of the three traverses that cross the contact, all veins fabrics are single girdles and most quartzite fabrics either resemble, or are cross girdles. All three of the traverses within the high strain zone display quartzite fabrics that decrease in maximum concentration with increasing distance from the pluton. Fabrics from the three high strain traverses also have a more concentrated Y-axis maxima from samples located closer to the pluton. Fabrics from samples collected farther from the pluton have concentrations that are more spread towards the XZ plane. The fourth traverse, at location

26 (Fig. 9), is on the north side of the pluton in the low strain zone. The strain at location 26 seems to remain at a high level within the quartz veins, although it drops off significantly within the Harkless quartzites. Fabrics from location 26 switch from single to cross girdle at the contact, although the fabrics do not exhibit consistent changes in maximum concentration of c-axes or in degree of c-axes parallel to the Y-axis with varying distance from the contact.

2.5.1 *Traverse # 1; High Strain Zone*

Traverse #1 is at location 33 (Figs. 9 & 17), where the first quartzites within the Harkless Formation occur 12 m above the contact. A sample from this horizon was measured for crystallographic prefered orientation along with three other Harkless quartzite samples collected at greater distances from the contact. Two quartz veins within the granite adjacent to the contact were also sampled and measured for c-axis preferred orientations. While the quartzites are characterized by asymmetric cross girdle fabrics, the quartz veins display asymmetric single girdle fabrics. Both the veins and quartzites display fabric asymmetry indicating a top to the southeast sense of shear (Law et al. 1992).

Quartzite PF 135, collected 12 m above the contact, has a maximum c-axis concentration of 34 times uniform distribution. PF 136 was collected at 17 m above the contact, PF 137 at 20 m above, and PF 138 at 21 m above, and their maximum concentration decreases from 23 to 19 to 18 times uniform distribution respectively (Fig. 17).

The two quartz veins, PF 126b and 127c, were both collected 1 m below the contact and display maximum c-axis concentrations of 30 and 34 times uniform distribution, respectively. Both fabrics are well developed single girdles with an asymmetry indicating a top to the southeast sense of shear. Both contain c-axis maxima

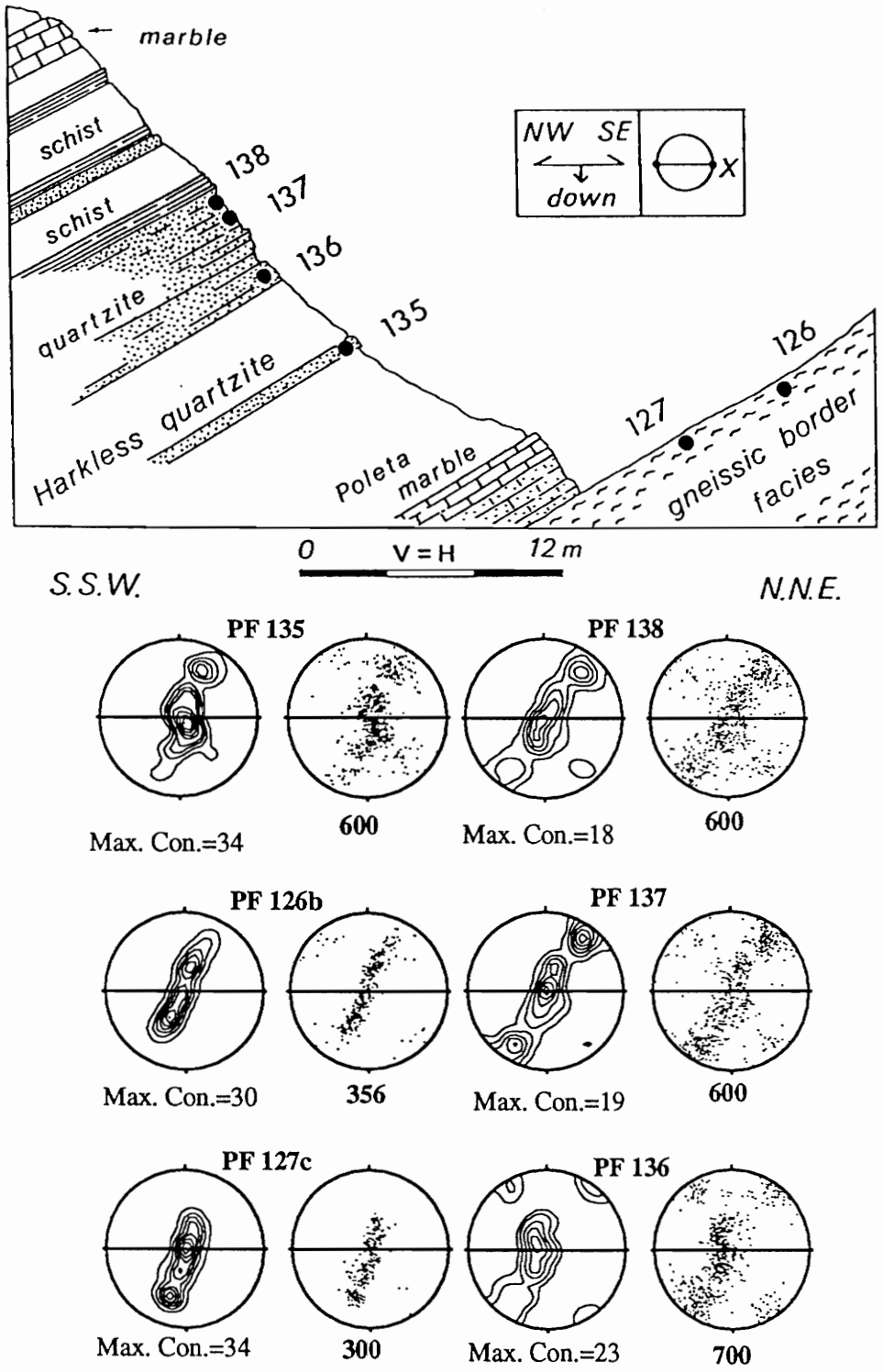

Fig. 17. Cross section along Traverse One (high strain zone) with quartz c-axis fabrics from samples collected along traverse. Note; a) the switch in fabric pattern from single girdle fabrics within the pluton to fabrics resembling cross girdles within aureole quartzites, and b) the decrease in maximum concentration of c-axes from samples collected farther from the pluton/wall rock contact. This is adapted from Traverse B of Law et al. (1992).

parallel to the Y-axis of the sample coordinate system.

Quartzite fabric PF 135 displays the same maximum concentration of c-axes as quartz vein PF 127c, and yet while PF 135 was collected 12 m above the contact, PF 127c was collected 1 m below the contact. One possibility that explains the similar concentration is that PF 135 might have experienced a similar amount of finite strain as PF 127c, possibly due to homogeneous simple shear. PF 135 closely resembles a single girdle fabric and the maximum concentration of c-axes is located parallel to the Y-axis (Fig. 15b & 17).

2.5.2 *Traverse #2; High Strain Zone*

Fabrics from the two quartzites measured along traverse #2 were collected at location 25 (Fig. 9 & 18) and are distinctively different from each other. PF 90 was collected at the first quartzite horizon located 30 m above the contact and exhibits a strong Y-axis maxima c-axis fabric. A slight asymmetry to the NW is detected in the lower concentration portions of this fabric. PF 89 was collected 2 m above PF 90 and displays a cross girdle which is slightly asymmetric to the SE. PF 90 has a maximum c-axis concentration of 24 times uniform distribution and PF 89 has a maximum concentration of 20 times uniform distribution (Fig. 18).

2.5.3 *Traverse #3; High Strain Zone*

Location 21 is situated on the NW margin of the pluton where two quartzites and two quartz veins have been analyzed for fabric development (Fig. 9 & 19). The first quartzite, PF 73, is located 30 m above the contact and displays a c-axis fabric that, at least in terms of density distribution, is strongly asymmetric to the SE with a strong Y-axis

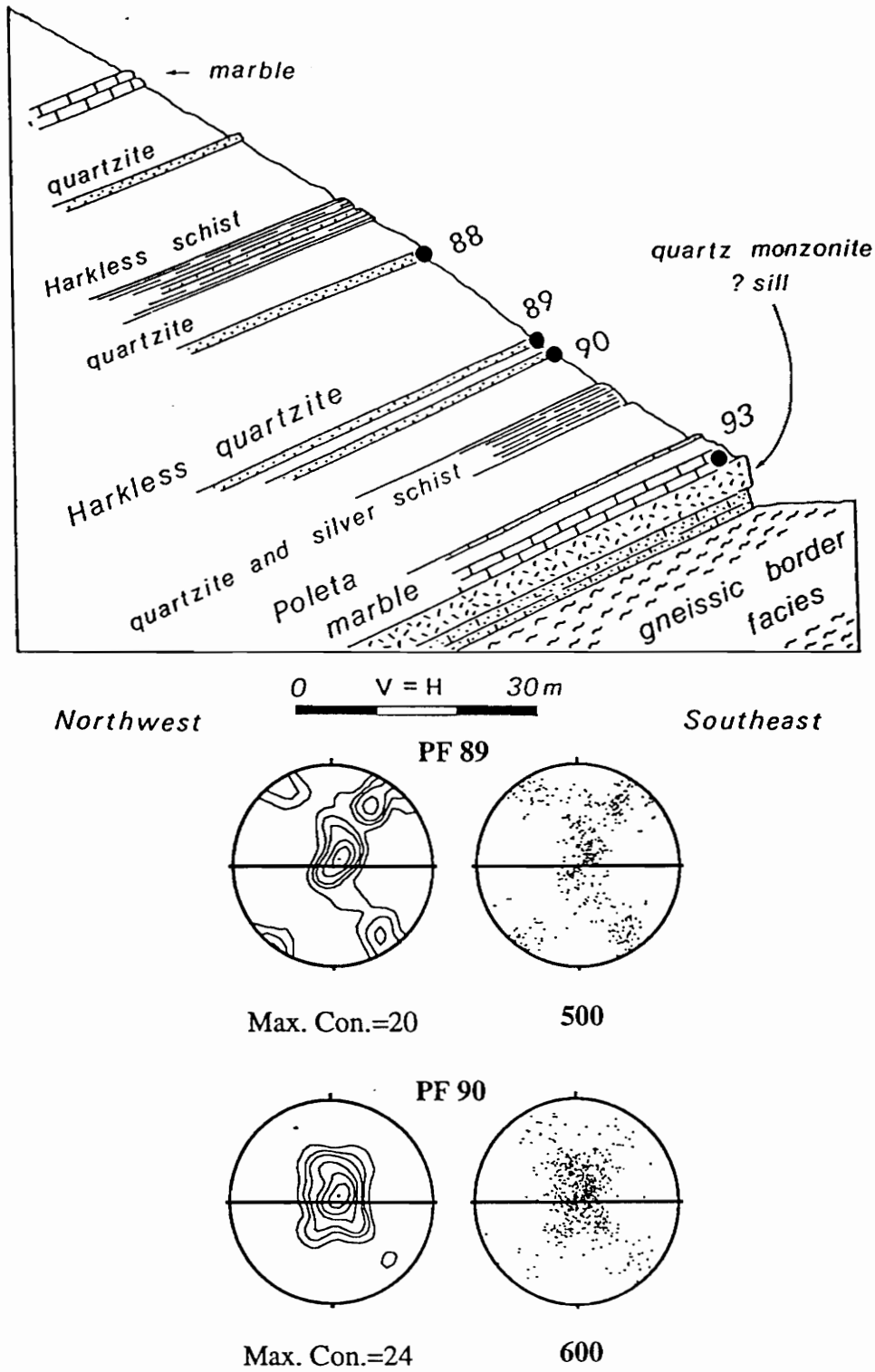

Fig. 18. Cross section along Traverse Two (high strain zone) with quartz c-axis fabrics from samples collected along traverse. Note decrease in maximum concentration of c-axes from PF 90 to PF 89, moving farther from the pluton/wall rock contact. This is adapted from Traverse C of Law et al. (1992).

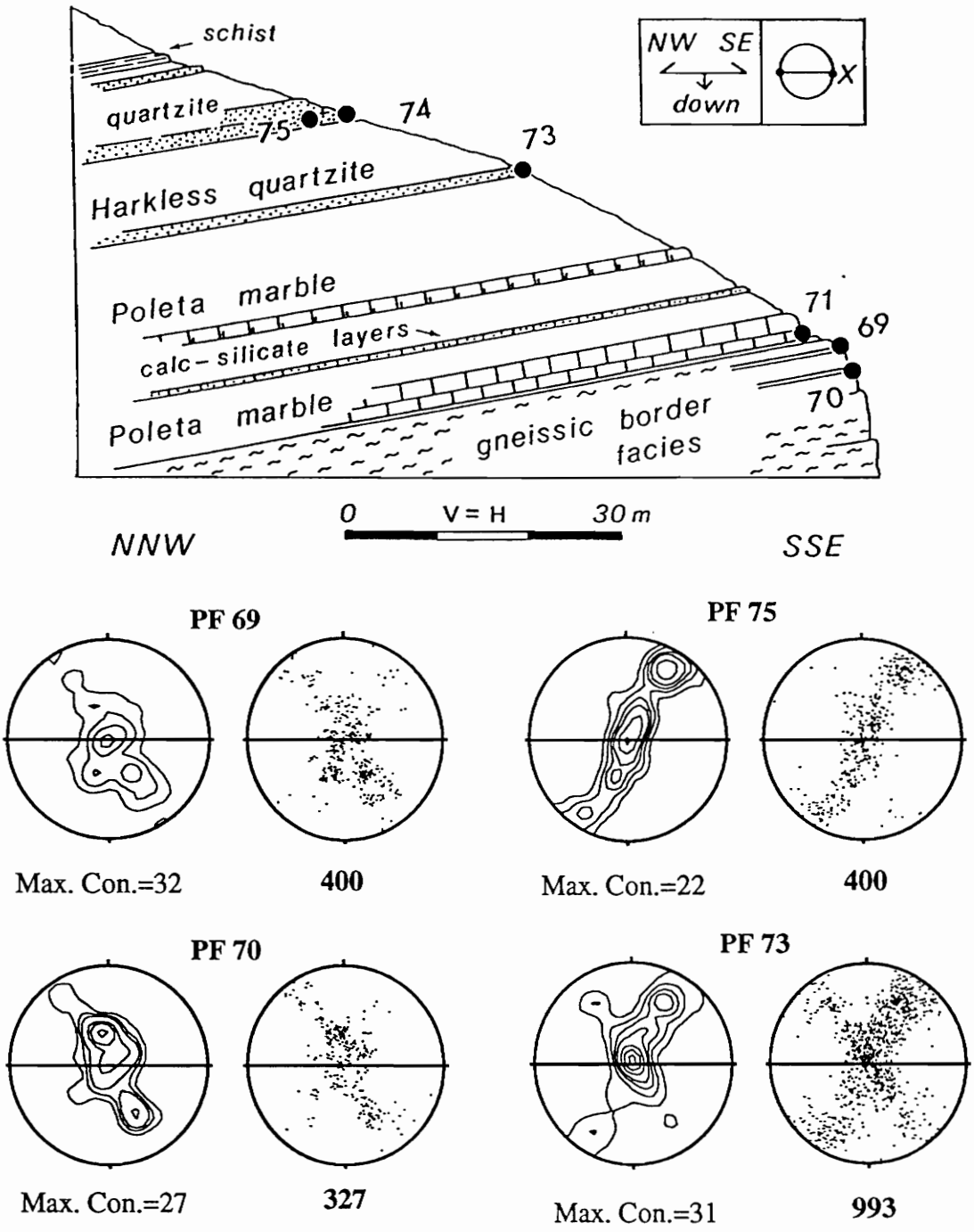

Fig. 19. Cross section along Traverse Three (high strain zone) with quartz c-axis fabrics from samples collected along traverse. Note decrease in maximum concentration of c-axes from samples collected farther from the pluton/wall rock contact, both into and away from the pluton. Also note switch in asymmetry of fabrics from samples collected across the contact. This is adapted from Traverse D of Law et al. (1992).

maxima (Fig. 11a & 19). PF 73 has a maximum c-axis concentration of 31 times uniform distribution. PF 75 was collected 38 m above the contact and displays a fabric that is also strongly asymmetric to the SE, but with c-axes more evenly distributed along a single girdle. PF 75 has a maximum concentration of 22 times uniform distribution.

PF 69 and PF 70c are quartz veins located 0.5 and 3 m below the pluton/wall rock contact respectively. Both display strongly asymmetric c-axis fabrics indicating a top to the NW shear sense. PF 69 has a fabric that is slightly more concentrated parallel to the Y-axis than PF 70c and has a higher maximum concentration of c-axes. PF 69 has a maximum c-axis concentration of 32 times uniform distribution while a 27 times uniform distribution was detected in PF 70c (Fig. 19). Quartz veins PF 69 and PF 70, and quartzite PF 75 are characterised by single girdle c-axis fabrics, while quartzite PF 73 displays a cross girdle c-axis fabric.

2.5.4 *Traverse #4; Low Strain Zone*

Traverse #4 is situated in the low strain zone at location 26 (Fig. 9 & 20), close to where the Harkless Formation loses its conformity with the pluton and strikes more regionally to the NW. Strain remains high within the quartz vein (PF 297, Fig. 20). The first Harkless quartzites are located 72 m above the pluton (Fig. 20), in contrast to the high strain zone where the first quartzites can be found 12 m above the pluton. The quartzites are composed of recrystallized grains and larger elliptical grains that are interpreted to be relict deformed detrital grains. Approximately 800 m farther east along strike than traverse #4, at location 111 (Fig. 9), relict sedimentary grains within the Harkless quartzites are more obvious and numerous amongst the recrystallized grains as the strain intensity rapidly diminishes. Defomed skolithos tubes are also observed at location 111 that have aspect ratios between 4:1 and 3:1 where they intersect foliation/bedding surfaces. The elongation

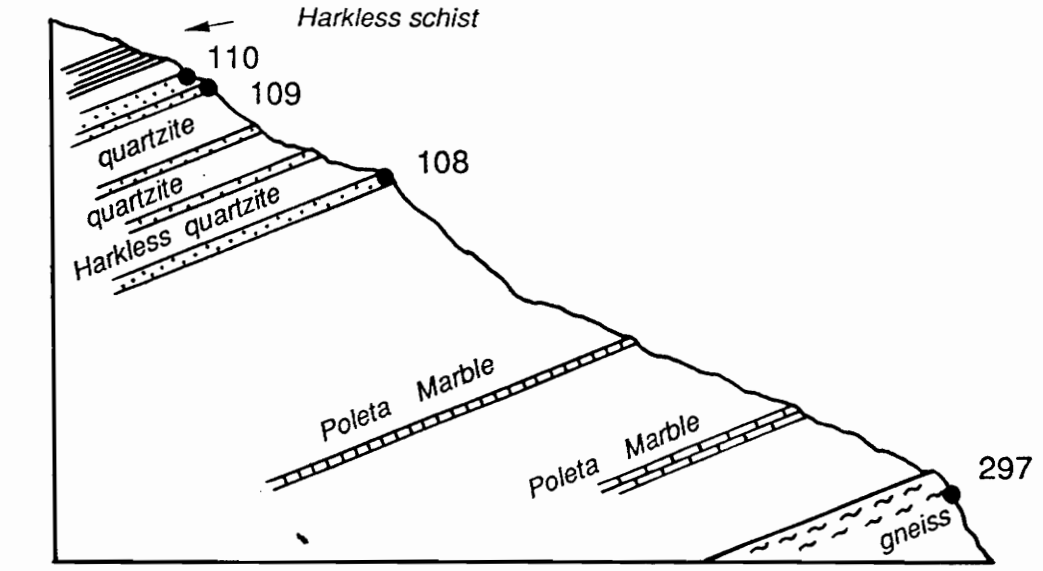

North 0 V=H 30m South

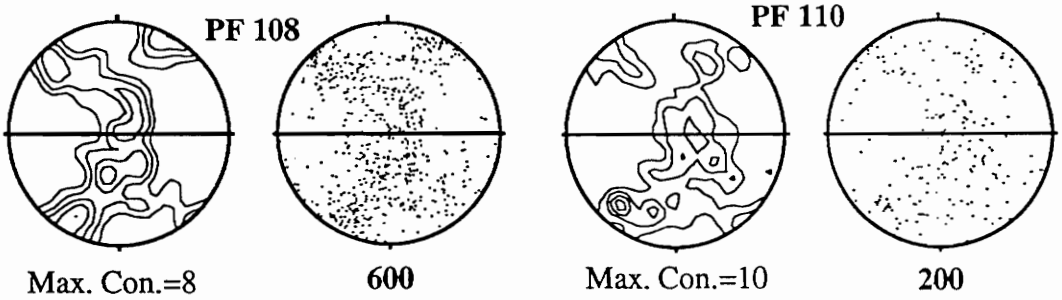

Max. Con.=8 600 Max. Con.=10 200

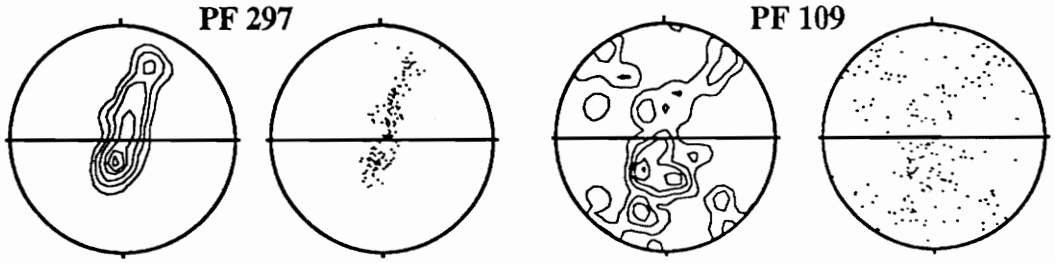

Max. Con.=30 200 Max. Con.=10 200

Fig. 20. Cross section along Traverse Four (low strain zone) with quartz c-axis fabrics from samples collected along traverse. Note; a) the decrease in maximum concentration of c-axes and the weaker preferred orientation from samples collected above the pluton/wall rock contact and, b) the greater distance between the pluton and the Harkless quartzites here (in the low strain zone) versus the same distance in the other three traverses (high strain zone).

direction of the tubes is oriented parallel to the stretching lineation observed throughout the western margin of the pluton. In contrast, nowhere to the west within the high strain zone are sedimentary structures observed.

Three quartzite fabrics and one quartz vein fabric were measured at location 26 (Fig. 20). The quartzite fabrics are weakly asymmetric cross girdles and indicate a top to the southeast sense of shear. The quartz vein, PF 297, was collected 6 m below the pluton/wall rock contact and displays a strongly asymmetric single girdle, also indicating a top to the SE sense of shear.

The quartz vein, PF 297, has a maximum c-axis concentration of 30 times uniform distribution. PF 108 is from the first quartzite horizon above the contact. This quartzite horizon is situated 72 m structurally above the pluton. PF 108 is the most well defined cross girdle of the three quartzites and displays a maximum concentration of c-axes which is 8 times uniform distribution. PF 109 was collected 96 m structurally above the pluton and exhibits a fabric that is more of a diffuse cross girdle, but has a maximum concentration of 10 times uniform distribution, slightly higher than PF 108. PF 110 was collected 1 m above PF 109 and has a fabric that is slightly more diffuse than PF 109. PF 110 has a maximum concentration of 9 times uniform distribution (Fig. 15b & 20).

In contrast to traverses #1-3, a decrease in maximum concentration of c-axes moving away from the contact is not observed at traverse #4 (Fig. 20), although the fabric patterns do become more diffuse farther from the contact. This may be indicative of the heterogeneous nature of the deformation within the low strain zone, although the difference in maximum concentrations between the three quartzites is not great enough to be conclusive.

2.6 *Strain Related Recrystallization*

In the section 2.5 above, fabric type and degree of maximum concentration of c-axes have been related to finite strain. In the following section, it will be shown that there is a similar relationship between the amount of finite strain and degree of recrystallization.

2.6.1 *Review*

Two groups of models for explaining crystallographic preferred orientation may be distinguished (see review by Hobbs 1985) - those involving stress-induced recrystallization and those involving intracrystalline deformation. Over the last fifteen years, attention in crystallographic fabric studies of quartz has focussed on the influence of crystal slip on fabric evolution, with particularly influential advances being made by G.S. Lister and co-workers (e.g. Lister et al. 1978, Lister & Hobbs 1980) using a modified version of the Taylor-Bishop-Hill model of homogeneous strain and a minimum of five independent slip systems in each grain.

In these slip-induced fabric simulation studies, each potential crystallographic slip system has its own critical resolved shear stress, CRSS, (the minimum resolved shear stress needed to activate a particular slip system). Within an aggregate of grains, some grains will, at any given instant in time, have their potential slip systems oriented at high angles to the principal stress directions, and will therefore have only low resolved shear stresses on these potential slip systems. Schmid & Casey (1986, p. 283-284) have argued that these 'hard orientation' grains "... *deform less than the surrounding aggregate and they have to use alternative slip systems which are harder to activate. Since these locked grains are local stress raisers their dislocation density will be higher than that of the surrounding*

grains. Thus they will be preferentially affected by syntectonic recrystallization driven by the build-up of distortional lattice energy. The subgrain rotation mechanism will create new grains with a different lattice orientation more favourable for easy slip, whereas the grain boundary migration mechanism will lead to the preferential consumption of grains with a high distortional lattice energy ...". A similar selective recrystallization model to explain progressive fabric evolution in experimental deformation of ice has previously been proposed by Bouchez & Duval (1982).

Jessell (1988a & b) and Jessell & Lister (1990) have recently incorporated both progressive subgrain rotation and grain boundary migration into a radically modified version of Lister's earlier Taylor-Bishop-Hill model of slip-induced quartz fabric evolution. As pointed out by Gleason et al. (in press) the fundamental assumption of homogeneous strain in the Taylor-Bishop-Hill model required Jessell and Lister (1990) to assume that there is a direct correlation between a high resistance to deformation and a high dislocation density, and thus that grains oriented poorly for slip will, as suggested by Schmid & Casey (1986), be removed by grain boundary migration. For progressive simple shear deformation, the fabric simulations of Jessell and Lister (1990, p. 358) suggest that contemporaneous crystal slip and dynamic recrystallization will result in a change in fabric pattern with increasing shear strain. This change in fabric pattern is characterized by a gradual transition from diffuse cross-girdle quartz c-axis fabrics (which at low shear strains appear to be symmetrically oriented with respect to finite strain axes) to an intensely developed single girdle fabric oriented oblique to the finite strain axes at high shear strains.

The assumption that quartz grains oriented poorly for slip will be selectively recrystallized has recently been questioned by Gleeson et al. (in press). Based on a series of experimental coaxial quartzite deformation tests, Gleeson et al. have documented evidence indicating that, contrary to the suggestion of Schmid & Casey (1986), it is the quartz grains oriented poorly for slip that have lower dislocation densities and are therefore

favoured for growth indicating, in turn, that these samples have experienced homogeneous stress rather than strain. This alternative view of selective dynamic recrystallization has not, to date, been incorporated into any simulation models for crystal fabric development.

The relationship between amount of strain, degree of recrystallization, and pattern of fabric developed has been discussed before by Law (1986, p 121). Law (1990) notes from field observations that a significant increase in the degree of recrystallization coincides with the spatial transition from mylonites with symmetrical cross girdle fabrics to mylonites with asymmetrical single girdle fabrics. Other workers, such as Bouchez and Duval (1982) and Dell'Angelo and Tullis (1989), have also observed an increase in the degree of recrystallization with increased strain in their experimental studies. Computer simulations of quartz fabrics using the Taylor-Bishop-Hill model (e.g. Lister and Hobbs, 1980) were unable to reproduce single girdle fabrics commonly observed in natural tectonites until Jessel (1988), and subsequently Jessel and Lister (1990) incorporated dynamic recrystallization into the model.

This relationship between the amount of strain, degree of recrystallization, and type of fabric developed is also observed at the margins to the high strain zone around the Papoose Flat pluton. In the low strain zone, quartzites have not been completely recrystallized and deformed relict sedimentary grains remain. The c-axis fabrics are weak (traverse #4, Fig. 20) in comparison to the high strain zone c-axis fabrics (traverses #1-3, Figs. 17-19). In the high strain zone, all quartz tectonites seem to have been completely recrystallized and any finite strain markers have been destroyed (evidence exists for cycles of dynamic recrystallization in the high strain zone tectonites).

2.6.2 *Recrystallization and Strain in the High Strain Zone versus the Low strain Zone*

The quartz tectonites at traverses #1 and #4 (Figs. 17 & 20) are used as end members in terms of finite strain accumulation and degree of recrystallization. The rocks at traverse #1 exhibit the greatest degree of attenuation and strain and the rocks at traverse #4, at least within the Harkless quartzites, exhibit the lowest amount of attenuation and strain. The Harkless quartzites at traverse #1 are approximately 9 m thick, their stratigraphic base is located 12 m above the pluton/wall rock contact, and exhibit fabrics that are well defined (Fig 17). In contrast, the Harkless quartzites at traverse #4 are approximately 25 m thick, their stratigraphic base is located 72 m above the pluton/wall rock contact, and display fabrics that are poorly defined (Fig. 20) in comparison to the high strain zone fabrics. The quartzite fabrics from traverse #1 are nearly single girdles, display strong Y-axis maxima, and are from completely recrystallized rocks. The quartzite fabrics from traverse #4 are diffuse cross girdles with little or no concentration at the Y-axis, and are from incompletely recrystallized rocks. *Finite strain seems to be correlated with the degree of recrystallization and the type of fabric produced.*

The same correlation can be made between quartz veins and quartzites. The vein fabrics are usually stronger in maximum concentration, are single girdles, have strong Y-axis maxima, and the veins commonly display signs of dynamic recrystallization. The quartzite fabrics are mostly weaker in maximum concentration, are cross girdles, display Y-axis maxima when close to the contact, and display, at least within the low strain zone, microstructures indicative of remnant deformed sedimentary grains.

2.6.3 *Finite Strain related to Volumetric Differences*

Outside of the high strain zone, quartz veins display well developed fabric patterns (e.g., PF 297, Figs. 11b & 20) characteristic of the high strain zone, while the quartzite fabric patterns (e.g., PF 108, 109, 110, Figs. 15a, 15b & 20) are less well developed as attenuation of the metasedimentary rocks becomes less intense and recrystallization is less complete. The strain is distributed and can be explained by differences in the volume of rock undergoing deformation. Quartz veins are almost negligible in total volume compared to the Harkless quartzites. Assuming that the pluton and the aureole rocks are accomodating the same bulk noncoaxial deformation (same amount of pure shear and simple shear components), and assuming that within the gneiss, the strain is partitioned and the quartz veins are accomodating the majority of simple shear, quartz veins will accomodate a far greater amount of simple shear compared to the quartzites. For example, in a deck of cards with only 5 cards, each card will have to be translated farther from his neighbor for the deck to accomodate the same bulk translation as in a deck with 50 cards.

The quartz veins are typically 1-3 cm in thickness within the gneiss and are probably accomodating most of the simple shear within the granite (see chapter one). In the previous section, it was argued that the fabric variation is due to the quartz veins having accumulated a greater degree of strain than quartzites. The strain within several 3 cm thick veins will be much more intense than for any 3 cm thick sequence within a 30 m sequence of quartzite undergoing the same bulk deformation. The Harkless quartzites are 9-40 m thick and are presumably distributing the strain over a much larger volume of rock. The deformed aureole also contains micaceous schists and marbles which have also accomodated a component of simple shear (Law et al. 1991). Therefore, even in the low strain zones, the quartz veins are still accomodating a much greater amount of strain per

volume of quartz than the quartzites (e.g. Fig. 20).

2.7 *Fabric Variation Related to Differences in Operative Slip Systems*

Temperature is one of the main variables, along with strain rate and chemical environment, controlling which slip systems operate during deformation (Nicholas and Poirer 1976; Hobbs 1985; Law 1990). It is the slip system or combination of slip systems which operate that controls development of a particular fabric pattern (assuming the fabric formed by crystal plastic processes). Basal slip is associated with low temperatures and or high strain rates while prism and rhomb slip are usually associated with higher temperatures and or lower strain rates (Nicholas and Poirer 1976, p. 201; Hobbs 1985). Prism slip is inferred to have occurred where quartz c-axis fabrics contain Y-axis maxima and basal slip is inferred where c-axis maxima are at high angles to the XY plane of finite strain, i.e., maxima clustering around the Z-axis (Schmid and Casey 1986; Law 1990, Law et al. 1990, Law et al. 1992). Y-axis maxima are generally associated with amphibolite to upper amphibolite conditions in areas affected by regional metamorphism and are typically associated with higher temperatures of deformation than fabrics characterised by girdles with concentrations close to the Z-axis (Bouchez et al. 1983; Schmid and Casey 1986; Law et al. 1992).

Jessel and Lister (1990, p. 360) have used computer models to simulate quartz c-axis fabrics produced by crystal plastic deformation and dynamic recrystallization under varying temperature conditions. A constant maximum shear strain was acheived in each simulation while they varied parameters supposed to mimic change in temperature. At low temperatures, c-axis maxima were concentrated at right angles to the shear plane. With runs at increasing temperatures, the c-axis maxima became aligned parallel to the Y-axis.

The highest temperatures within the aureole of the Papoose Flat pluton have occurred at the contact and decreased with increasing distance from the pluton (Nyman et

al. 1992). Field observations support this hypothesis. A thin skarn is commonly observed at the contact and is associated with an amphibolite facies assemblage (Ms+And+Bt+Qtz+Pl±Grt) which then rapidly gives way to a greenschist facies assemblage (Chl+Qtz±And) less than two hundred meters from the contact.

The quartz c-axis fabrics around the pluton should also reflect the change in temperature. Different slip systems operate at different temperatures in response to the change in critical resolved shear stresses needed for the various slip systems to operate at different temperatures (Lister and Paterson 1979; Lister and Dornsiepen 1982; Hobbs 1985). Quartz vein fabrics are typically dominated by a Y-axis maxima and probably indicate a dominance of prism <a> slip due to the relatively high temperatures within the pluton. Y-axis maxima are also observed in fabrics from quartzites adjacent to the pluton (Figs. 17 & 18). The microstructure of the quartz veins is also indicative of high temperatures (see Lister and Snoke 1984, p. 632). Exterior of the pluton, quartzite fabrics commonly contain maxima adjacent to the XZ plane and a more equally distributed spread of c-axes. The change in fabrics with distance from the pluton could be in response to a change in the critical resolved shear stress of the various slip systems as temperature decreased with distance from the pluton. Basal <a> slip became the more favored slip system at lower temperatures, farther from the pluton, and the c-axes rotated into higher angles with the shear plane.

2.8 *Strain Path Partitioning*

The difference in fabrics between the quartz veins and quartzites could also be due to a difference in strain path (Schmid and Casey, 1986). It is possible that the metasedimentary units and the granite record the same bulk strain path, but that within the granite the strain is partitioned according to rheology. For example, in a regime of general

shear, the more competent granite may have deformed coaxially and the less competent quartz veins deformed noncoaxially (cf. Lister and Williams 1983; Law et al. 1992). The competency contrast is not as great between the marbles, schists, and quartzites within the aureole, and therefore the general shear may not be partitioned into pure and simple shear components by rock type in the aureole metasediments. All the metasedimentary units may, relative to the gneiss and quartz veins, record the approximately same combination of pure and simple shear, and therefore have fabrics reflecting components of both pure and simple shear deformation. The quartz veins, having accomodated primarily simple shear deformation, would therefore be expected to display fabrics more indicative of strict simple shear deformation.

However, in Chapter Three, it will be argued that strain partitioning may have occurred *within* the metasedimentary units. For example, aysmmetric structures, i.e., shear bands, are best developed within the almost pure micaceous layers within the schists, which are able to accomodate simple shear more easily than pure shear (Bell, 1985). In contrast, the andalusite-quartz-mica schists are more commonly characterised by a single schistosity, parallel to lithologic layering, with no observable shear sense indicators, suggesting a major component of pure shear deformation.

There is no evidence to suggest that the degree of crystallographic preferred orientation (maximum concentration of crystallographic axes), is related to differences in strain path, although it has been demonstrated that strain accumulates more rapidly during pure shear deformation than simple shear deformation (Pfiffner and Ramsay 1982). This is in contrast to the strain distribution detected within the quartz tectonites surrounding the Papoose Flat pluton. The more highly strained quartz tectonites display fabrics indicative of noncoaxial deformation (i.e. single girdle fabrics, high maximum concentration of c-axes) while the least strained quartz tectonites have fabrics indicative of coaxial deformation (i.e cross girdle fabrics, lower maximum concentration of c-axes). If finite strain were

more rapidly accumulated by pure shear deformation, then the rocks that have accumulated the greatest amount of strain should have structures indicative of pure shear deformation. This line of reasoning suggests that the variation in fabric intensity across the pluton-wall rock contact is probably not due to differences in strain path.

2.9 *Original Preferred Orientation Affecting the Deformation Fabric*

Undeformed quartz veins commonly display a crystallographic preferred orientation due to the processes involved in crack opening and associated vein crystallization (Frondel 1962). As the crack opens, fibers of the vein material will often grow perpendicular to the orientation of the crack. This type of growth will, to some degree, control the crystallographic orientation of the vein material. In this situation, quartz c-axes may be preferentially aligned perpendicular to the orientation of the crack before any deformation produces a preferred crystallographic orientation. A subsequent reorientation of the crystal axes might be affected by the original preferred orientation. Hobbs (1985, p. 477) states that a 40% shortening is sufficient strain to produce gross changes in a preexisting fabric, but it is not presently known if the older fabric can be completely reoriented. Law (pers. comm.) has observed that mylonitized quartz veins from various regions around the world (e.g. Mancktelow 1990) usually have stronger fabrics than mylonitized quartzites, and these fabrics are more apt to be single girdles than cross girdles. Therefore, an original preferred orientation could have aided in producing the observed variation in fabric patterns between quartz veins and quartzites within and around the Papoose Flat pluton.

CHAPTER THREE

PORPHYROBLAST-MATRIX RELATIONSHIPS

3.1 *Introduction*

A constant angle between planar inclusion trails within cores of andalusite porphyroblasts and lithologic layering is observed within the Harkless schist surrounding the Papoose Flat pluton. The Harkless schist is concordant with the western margin of the pluton and is thinned to approximately 10% of its original thickness within the aureole of the pluton (Sylvester et al. 1978). Foliation is parallel to lithologic layering and a mineral stretching lineation lies within the foliation plane.

Andalusite porphyroblasts consist of two distinct domains based on differences in inclusion trail density and orientation: A) a core region with a high density of planar inclusion trails (S_{ic}) which are oriented at a statistically constant angle (~40°) to the external foliation (S_e) and, B) a rim region with a low density of inclusion trails (S_{ir}) that continue in orientation from S_{ic} and curve into parallelism with the external foliation, S_e (Fig. 21).

Three models are proposed to explain the porphyroblast-matrix relationships:

1) S_{ic} represents a pre-intrusive foliation (?cleavage) which was originally planar and oblique to lithologic layering in the Harkless shales. Andalusite porphyroblasts nucleated in the surrounding shales during heating accompanying intrusion of the Papoose Flat pluton and incorporated the fabric as planar inclusion trails. Initial growth of andalusite porphyroblasts was pre-tectonic. Rotation of the external foliation around the

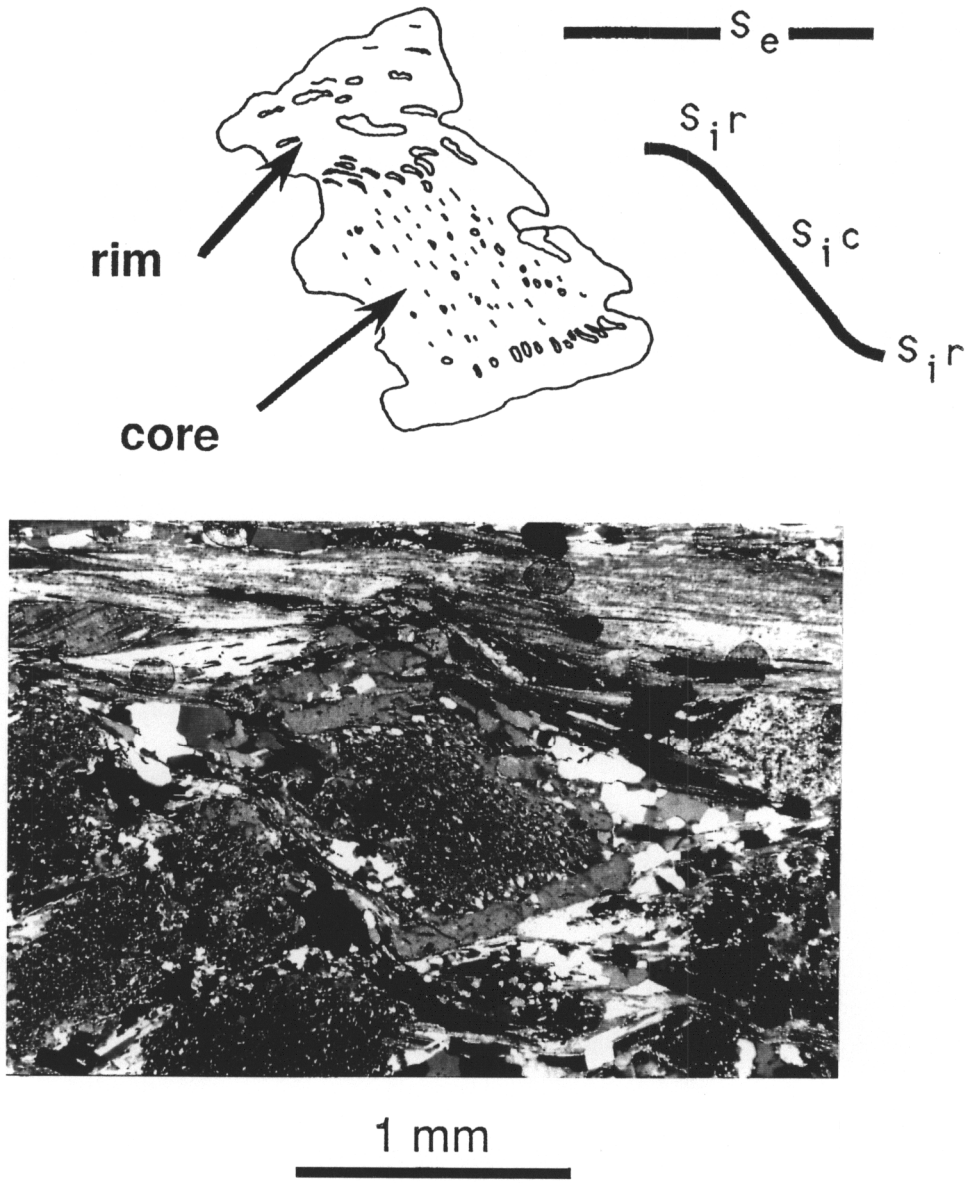

Fig. 21. Drawing and photo of andalusite porphyroblast within the Harkless schist. Note the two distinct domains within the porphyroblast; a) a core region with a high density of planar inclusion trails (Sic), which are oriented at approximately 40° to the external foliation (Se), and b) a rim region with a low density of inclusion trails (Sir), that continue in orientation from Sic and curve into parallelism with Se.

porphyroblasts and into parallelism with lithologic layering occurred during the late stages of porphyroblast growth and therefore only the porphyroblast rims record the deformation event. Rims are therefore syn-tectonic. Porphyroblasts have not rotated with respect to compositional layering.

2) Andalusite porphyroblasts nucleated on the limbs of microfolds deforming an earlier cleavage within the Harkless shales/schists. Fold limbs were preserved as inclusion trails in the porphyroblasts. The microfolds developed early to synchronous with intrusion, and were destroyed outside porphyroblasts during subsequent or continued deformation. Porphyroblasts are either syn- or post-tectonic relative to the microfolding and pre-tectonic relative to the present foliation. Neither porphyroblasts nor foliation have rotated with respect to compositional layering.

3) All andalusite porpyroblasts rotated the same amount during late stages of intrusion. The intrusion and contact metamorphism initially caused andalusite to nucleate within the Harkless shales. Andalusite porphyroblasts statically overgrew the bedding plane foliation, which was progessively being metamorphosed into an amphibolite grade foliation. Late in the growth history of the porphyroblasts, a strong component of simple shear rotated all andalusite porphyroblasts the same amount. Andalusite continued to grow and incorporate the foliation as inclusion trails during the rotation event. Porphyroblast cores are pre-tectonic, rims are syn-tectonic. The external foliation did not rotate with respect to compositional layering.

Model number one is favored for the following reasons: A) the planar and constant orientation of inclusion trails and the unlikeliness of a constant amount of porphyroblast rotation, B) the apparent coaxial nature of the deformation (see sections 3.6.2 & 3.6.3)

and, C) the geometry and nature of inclusion trail patterns from core to rim and the relationship of the inclusion trails to the external foliaton.

3.1.2 *Analytical Methods*

Sixty-four schist and phyllite samples collected from the Harkless and Poleta Formations from thirty-two locations around the Papoose Flat pluton were examined for microstructures. Fifty-nine thin sections were cut parallel to the lineation and perpendicular to foliation and five thin sections were cut perpendicular to lineation and perpendicular to foliation. All thin sections were examined for: 1) number of foliations and their orientation; 2) cross cutting relationships between foliations and porphyroblasts; 3) inclusion trails in cores and rims of andalusites and relationship to matrix foliation; and 4) degree of sericitization of andalusite porphyroblasts. Twelve samples were chosen for measurement of inclusion trail orientations. These sample locations were chosen because they: a) are evenly spaced around the western margin of the pluton (Fig. 22), and b) contain well preserved porphyroblasts.

3.2 *The Harkless Schist*

3.2.1 *Description of the Harkless Schist*

The Harkless Schist is concordant to, and attenuated around, the Papoose Flat pluton for over 18 km along the western margin (Fig. 22). The Harkless Formation varies from 0 to 75 m in distance from the pluton (measured perpendicular to the pluton wall rock contact) depending on the intensity of the attenuation of the underlying units and on how high into the section the pluton intruded. Only along the central-southern margin of the

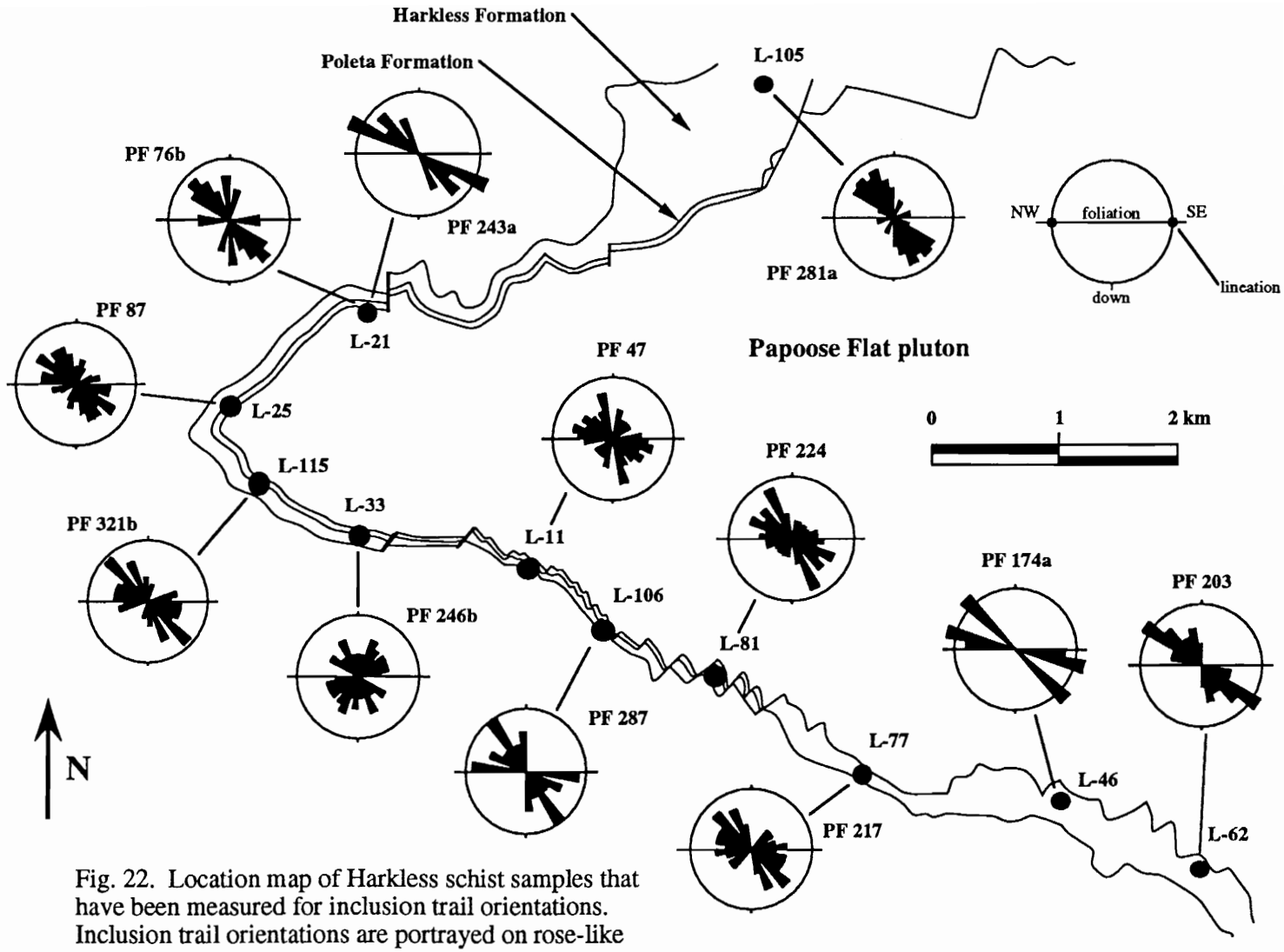

Fig. 22. Location map of Harkless schist samples that have been measured for inclusion trail orientations. Inclusion trail orientations are portrayed on rose-like diagrams.

pluton does the granite actually intrude the Harkless Formation (Nelson et al. 1977). The degree of stratigraphic attenuation of the aureole rocks varies, but the regional thickness of 570 to 700 m for the Harkless Formation is reduced to roughly 45 m around the western margin of the pluton (Sylvester et al. 1978).

The Harkless schist contains Qtz+And+Ms+Bt+Pl±Chl±Grt, minor opaque minerals, and various amounts of sericite replacing andalusite. Andalusite is typically anhedral with a high density of planar inclusion trails in the core region which give the porphyroblasts a poikiloblastic character. Inclusions are typically small single crystals of quartz and opaque minerals with minor amounts of mica and feldspar crystals. Most andalusite porphyroblasts have some sericite on the rims and it is common to observe andalusite completely replaced by sericite. Rare unaltered andalusite porphyroblasts, or porphyroblasts that have some portion of their rims preserved, commonly exhibit curvature of inclusion trails that coincides with a sharp decrease in density of inclusions at porphyroblast rims. The change in density and orientation of inclusion trails within andalusite porphyroblasts also commonly coincides with an increase in grain size of inclusions.

The schistose foliation is defined by sub-parallel alignment of elongate muscovite, biotite, and chlorite grains and is oriented subparallel to the lithologic layering. Muscovite is typically found in either very fine grained elongate masses or is deformed and exhibits wavy undulatory extinction and subgrain formation. Biotite is less deformed and more equidimensional in grain outline than muscovite and is commonly partially altered to chlorite. Quartz and plagioclase grains are equidimensional to slightly elongate and are concentrated in pressure shadows around andalusite porphyroblasts.

The foliation anastomoses around andalusite porphyroblasts and is locally included within the rims of porphyroblasts. Smaller andalusite grains that have inclusion trails at oblique angles to the general trend of inclusion trails are thought to represent fragments of

originally larger grains.

3.2.2 *Inclusion Trail Orientations*

Measurements of the orientation of andalusite core inclusion trails (Sic) have been plotted for twelve different locations around the pluton (Figs. 22 & 23). These orientations were measured from XZ thin sections and therefore represent a two dimensional perspective of the angular relationship between the matrix foliation, Se, and the core inclusion trails, Sic. Thin sections were cut parallel to lineation and perpendicular to foliation and viewed to the north and east.

A constant angular relationship of ~40° is observed between the orientation of Se and the orientation of Sic measured from thin sections regardless of position around the pluton (Figs. 22 & 23). The one exception out of twelve measurements is sample PF 246b (Fig. 22 & 23) which was taken from a thin schistose layer within the Harkless quartzite at Location 33 (Fig. 22) on the south side of the pluton. This sample has the largest spread of orientations of inclusion trails of the twelve samples measured. The schist here also exhibits asymmetric microstructures indicative of a strong component of simple shear. Evidence for a strong component of simple shear was not observed in any other sample of Harkless schist that was measured for inclusion trail data. Therefore, the strong component of simple shear is interpreted to be responsible for rotating the porphyroblasts and causing the spread in inclusion trail orientation of PF 246b.

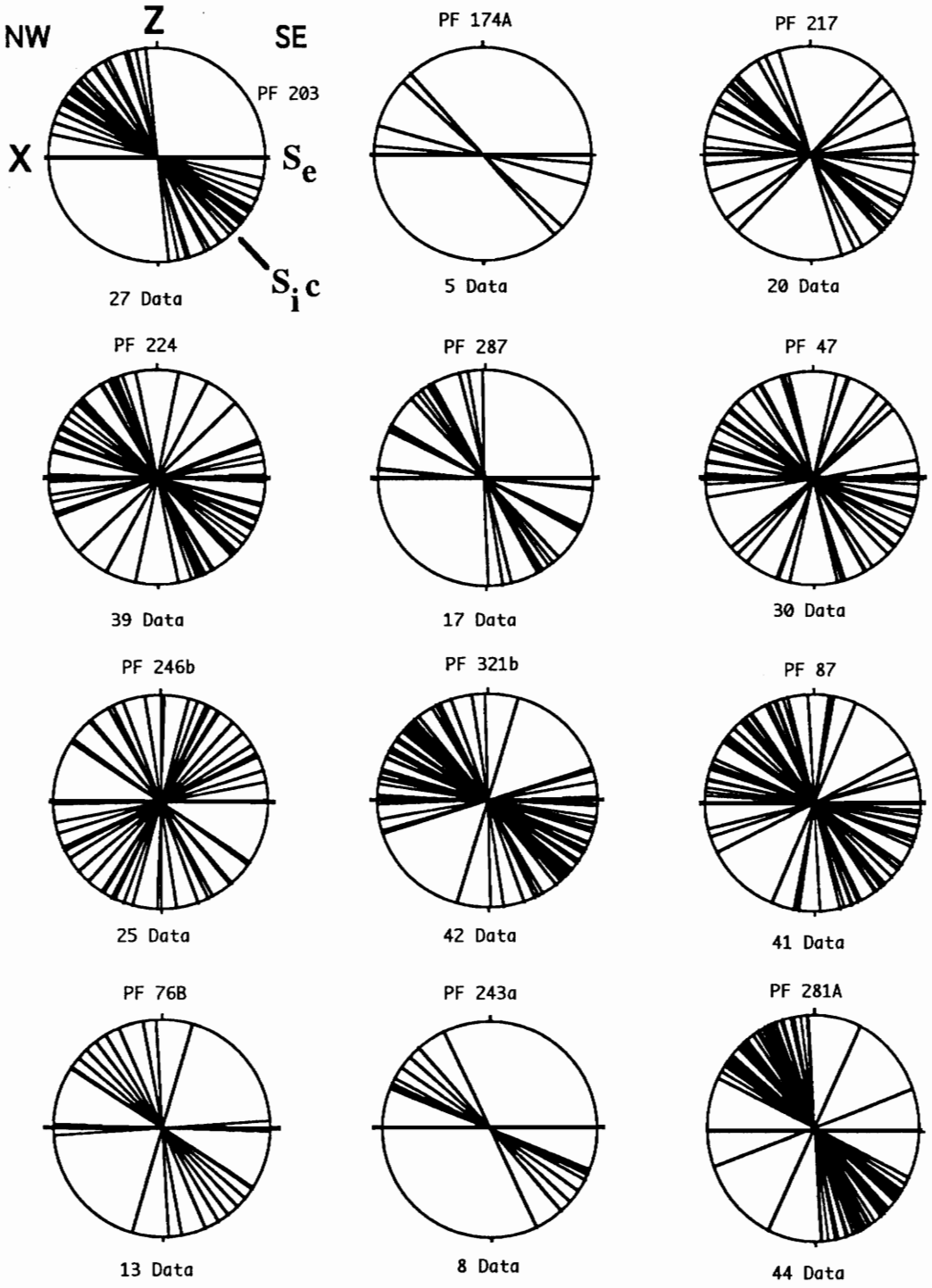

Fig. 23. Dip of Sic relative to Se. Black lines represent intersection of Sic with thin section. Thin sections cut parallel to NW trending lineation and perpendicular to foliation (Se).

3.3 *Si to Se Relationships*

3.3.1 *Review*

Inclusion trails are considered to be foliations that have been included in porphyroblasts as the porphyroblasts grew (Ramsay 1962; Zwart 1962; Spry 1969; Vernon 1989; Hanmer and Passchier 1991). The foliation within the porphyroblast is generally termed Si while the foliation in the surrounding matrix is termed Se (Spry, 1969). Si to Se relationships are used in determining the type of deformation and tectonic setting and are also used in deciphering the timing relationship between deformation and metamorphism (Ramsay 1962; Zwart 1962; Spry 1969; Rosenfeld 1968; Vernon 1978, 1989; Fyson 1980; Bell et al. 1986; Bell & Johnson 1989; Vissers 1989; Johnson 1990; Hanmer and Passchier 1991). Interpretation of some of the many different Si to Se relationships has always been controversial. However, over the last ten years, interpretation of even the most basic relationships between Si and Se has (primarily due to the work of T. H. Bell and co-workers), been brought into question.

The traditional school of thought held that a foliation which passed continuously from matrix to porphyroblast without deflection (Si parallel to Se) represented growth of the porphyroblast after foliation development, and an angular relationship between Si and Se was thought to represent deformation postdating porphyroblast growth (Zwart 1962; Spry 1969; Vernon 1978). Porphyroblasts were termed 'post-tectonic' in the former case and 'pre-tectonic' in the latter case (Zwart 1962). Although, Ramsay (1962, p. 323) illustrated at an early stage how a parallel alignment of Si in many porphyroblasts indicated that the matrix foliation was deforming around non-rotating porphyroblasts, most authors agreed that an angular relationship between Si and Se indicated that pre-tectonic

porphyroblasts had rotated during deformation (Rosenfeld 1970; Williams and Schoneveld 1981; Olesen 1982). Spiral shaped inclusion trails were commonly interpreted as a rotation of porphyroblasts during growth, and were termed 'syn-tectonic' (Rosenfeld 1968; Spry 1969; Schoneveld 1977).

More recently, Si to Se relationships have been reexamined and several authors (Bell 1985; Steinhardt 1989; Johnson 1990; Bell et al. 1992) have suggested that it was the matrix foliation, and not the porphyroblast, which rotated to produce the observed angular relationships between Si and Se. The ideas of Bell and co-workers are not accepted by all geologists (see Passchier et al. 1992), but most authors now agree that porphyroblast-matrix relationships are not easily interpreted, and that detailed microstructural analyses along with other quantitative analyses are needed in order to fully understand Si to Se relationships (Vernon 1989; Hanmer and Passchier 1991).

3.3.2 *Nonrotation of Porphyroblasts*

Ramsay (1962 p. 323) has illustrated how deformation in the *flattening* field might explain the nonrotation of porphyroblasts during an event that rotates the foliation around the porphyroblast (Fig. 24). Growth of the porphyroblast during flattening (Ramsay 1962) could produce the 'S' shaped pattern of inclusion trails so commonly interpreted as a rotation of porphyroblasts. Ramsay (1962) came to this conclusion by an examination of the parallel alignment of porphyroblast inclusion trails over a significant area.

Bell (1985) proposed that rigid bodies within a less viscous matrix do not rotate during *noncoaxial deformation* unless special circumstances exist, and that it is the matrix foliation that deforms around the porphyroblast due to deformation partitioning. In noncoaxial deformation, Bell (1985, p. 112) argues that porphyroblasts partition the deformation around themselves due to their coarse grain size and rigidity relative to the

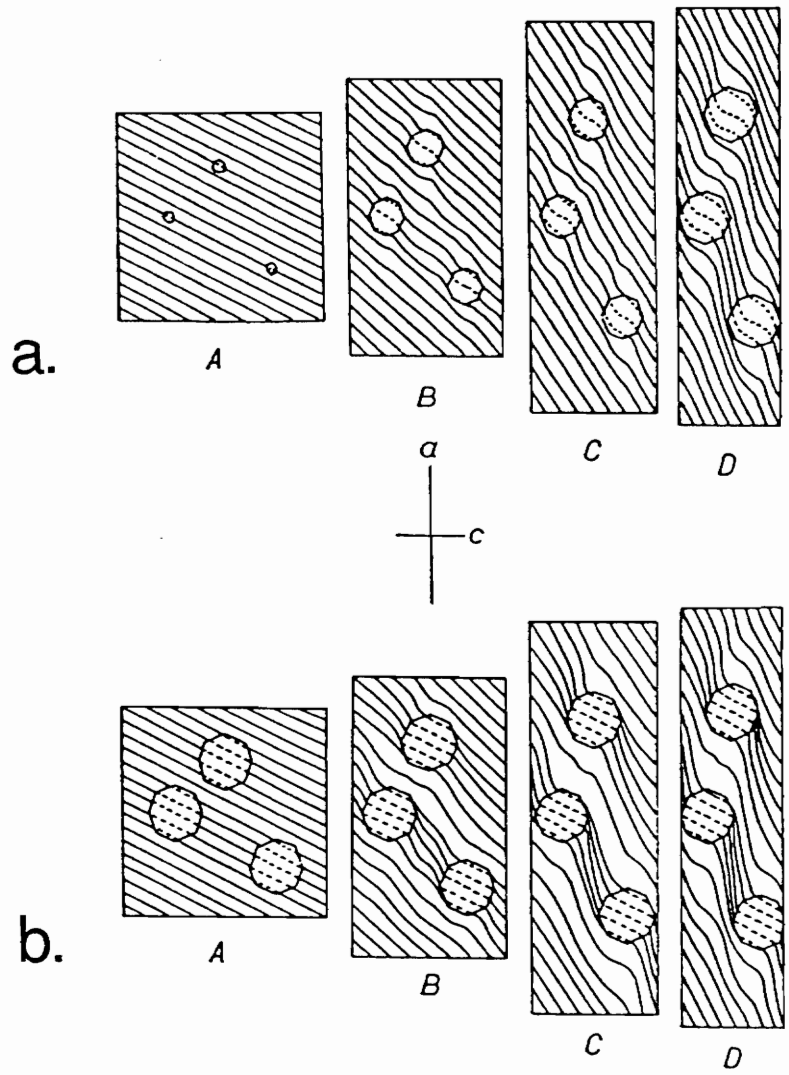

Fig. 24. Development of an angular relationship between porphryoblast and matrix foliations. Constant angle between internal foliation, Si, and external foliation, Se, indicates that porphyroblasts have not rotated and that the deformation is largely a flattening event. a) Syntectonic growth of porphyroblasts during flattening. b) Pretectonic growth of porphyroblasts before flattening. From Ramsay (1962).

surrounding matrix. Porphyroblast-controlled deformation partitioning produces elliptical zones of either no strain, or coaxial deformation, immediately surrounding porphyroblasts. Noncoaxial deformation is concentrated in phyllosilicate rich layers which anastomose around the coaxial zones (Fig. 25).

Bell et al. (1986) also suggest that deformation partitioning controls where porphyroblasts will nucleate. Bell (1986) considers that porphyroblasts cannot nucleate in zones experiencing high shear strain. Heterogeneous deformation localizes dissolution and solution transfer within high strain zones, preventing porphyroblast growth. In rocks undergoing crenulation, metamorphic segregation concentrates phyllosilicates in the limb regions where they can deform more easily and porphyroblasts nucleate in the hinge zones where more coaxial defomation is concentrated. The porphyroblasts grow as the folds tighten and a spiral-shaped inclusion trail is produced. The only evidence for the rotation of the foliation is usually preserved within the porphyroblast. The matrix foliation can be completely reoriented.

3.3.3. *Rotation of Porphyroblasts*

Although there is evidence that under certain circumstances porphyroblasts may not rotate during deformation in natural tectonites (Bell 1985; Steinhardt 1989; Johnson 1990; Bell et al. 1992), direct experimental studies (Schoneveld 1977; Passchier and Simpson 1986; Van den Driessche and Brun 1987) have clearly demonstrated that more rigid objects can rotate during simulated deformation. Many observation-based papers also cite examples of porphyroblasts that are interpreted to *have rotated* during deformation (Rosenfeld 1968; Schoneveld 1977; Olesen 1982; Vissers 1989; Hanmer and Passchier 1991; Paterson et al. 1991) of natural tectonites.

Rotation of rigid objects in a more ductile matrix subjected to noncoaxial

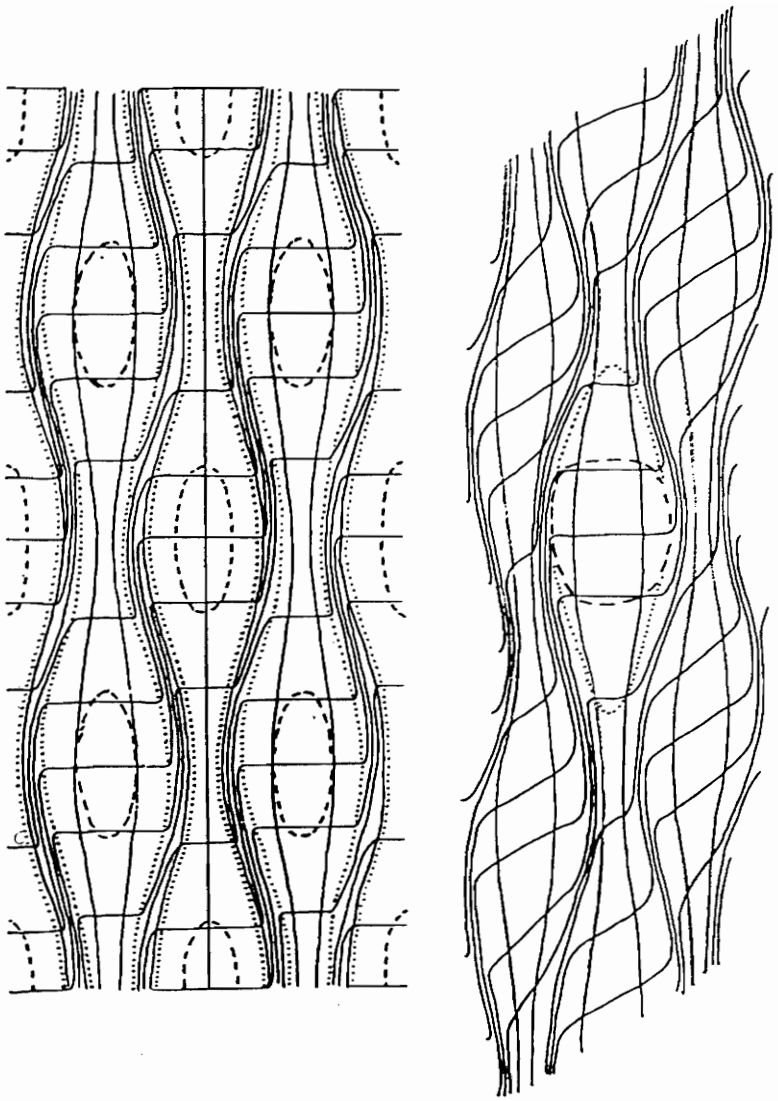

Fig. 25. The Bell (1985) model for deformation partitioning in a rock which has undergone non-coaxial progressive bulk inhomogeneous shortening. In the diagram on the left, the different zones and their strain paths are delineated as follows; 1. No strain occurred within the dashed ellipses. 2. progressive shortening strain dominated the zones between the dashed and dotted lines. 3. progressive shortening plus shearing strain occurred between the dotted lines. The diagram on the right, which has the same partitioning of deformation as the diagram on the left, illustrates how rotation of porphyroblasts (dashed line) will not occur if the porphyroblasts do not deform. From Bell (1985).

deformation has been observed experimentally (Passchier and Simpson 1986; Van Den Driessche and Brun 1987), and the resulting structures closely resemble structures observed in naturally deformed rocks. In these experiments, the porphyroclast is allowed to deform. A mantle of less rigid material surrounds the more rigid clast in order for wings or tails to form as the clast rotates. Mantles of less rigid material are incorporated into the experiment in order to model recrystallization and grain size reduction of the grain boundaries as the rock deforms (Hanmer and Passchier 1991). These experiments do not necessarily preclude the Bell model, because Bell (1985) explains that porphyroblasts in a rock undergoing deformation will not rotate as long as they do not deform internally. Presumably, if porphyroblasts do deform, this implies that deformation partitioning on the scale that Bell proposes did not occur. Strict simple shear is the only environment where Bell proposes that rotation of porphyroblasts can occur, because the deformation cannot be partitioned into coaxial and noncoaxial components (Bell 1985; Bell et al. 1986; Bell and Johnson 1990).

Recent work which combines the evidence for rotation of porphyroblasts with independent modern kinematic analysis is not common. Vissers (1989) examined poikiloblastic garnets from the Betic Zone in Southern Spain which exhibit rotation structures that indicate the same sense of shear obtained from the analysis of asymmetric quartz c-axis fabrics. Rotation is also believed to occur where porphyroblasts interfere with one another during deformation (Fyson 1980; Oleson 1982; Bell 1985; Vernon 1989).

Whether rigid objects rotate or remain fixed during defomation is clearly still controversial (Bell et al. 1992; Passchier et al. 1992). The possibility that both rotation and non-rotation of porphyroblasts can occur depending on the specific combination of variables that make up the deformation environment (i.e., the amount of pure shear versus simple shear defomation, the strain path, the viscosity contrast between porphyroblast and matrix, the P-T conditions, etc.) is plausible considering the amount of evidence for both

cases.

Paterson et al. (1991, p. 326) argued that the non-parallel alignment of inclusion trails from porphyroblast to porphyroblast is evidence that some porphyroblasts have rotated within the aureole of the Papoose Flat pluton, although they also argued (p. 326) that the parallel alignment of some inclusion trails indicates that some porphyroblasts have not rotated.

3.4 *Models*

The following three models attempt to explain the sequence of deformational and metamorphic events that may have taken place in order to produce the observed porphyroblast-matrix relationships. The three models differ greatly in their sequence of deformational versus metamorphic events, their strain paths, and also in respect to whether the matrix foliation and/or the porphyroblasts, have, or have not, rotated.

Model 1

S_{ic} represents a pre-intrusive foliation (?cleavage) which was originally planar and oblique to lithologic layering in the Harkless shales. Andalusite porphyroblasts nucleated in the surrounding shales during heating accompanying intrusion of the Papoose Flat pluton and incorporated the fabric as planar inclusion trails. Initial growth of andalusite porphyroblasts was pre-tectonic. Rotation of the external foliation around the porphyroblasts and into parallelism with lithologic layering occurred during the late stages of porphyroblast growth and therefore only the porphyroblast rims record the deformation event. Rims are therefore syn-tectonic. Porphyroblasts have not rotated with respect to compositional layering.

The evidence for Model #1:

Model one was conceived because, in order to achieve a constant orientation of Sic around the pluton, it was found that the metasedimentary units must be 'unwrapped' from concordancy with the pluton and placed into a planar reference frame. 'Unwrapping' of the metasedimentary units 'unspins' (sensu Lister and Williams 1983) the porphyroblasts and brings Sic from all locations on the western margin (both the north and south sides) of the pluton into parallelism (Fig. 26). Once the units are planar, the constant orientation of Sic indicates that the porphyroblasts have not rotated with respect to the lithologic layering, since rotation of porphyroblasts should produce a random spread of Sic orientations (Jamieson 1988).

The 'unwrapping' of Se into a planar reference frame rotates the porphyroblasts with respect to geographic coordinates. This type of rotation is in reference to external coordinates when discussing the microstructures within the schist, and is therefore more properly termed 'spinning' (Lister and Williams, 1983, p. 10). The term 'rotation' is used when in reference to internal coordinates. For example, the porphyroblasts have not 'rotated' with respect to the matrix foliation, but they have rotated with respect to geographic coordinates. The 'unwrapping' of the metasedimentary units brings Sic into a constant orientation, which is inclined at approximately 40° to the lithologic layering. This implies that the porphyroblasts initally overgrew a foliation that was oriented at 40° to the sedimentary layering.

In this model, which assumes that porphyroblasts did not rotate with respect to the lithologic layering, the granitic magma is envisioned as being initially intruded as a sill and statically metamorphosing the Harkless shales, causing andalusite to nucleate and grow. The Harkless shales contained a pre-existing tectonic (?) fabric, possibly a slaty cleavage, oriented at 40° to the compositional layering, which was incorporated into the andalusite porphyroblasts as inclusion trails. This pre-existing fabric in the Harkless shales may be

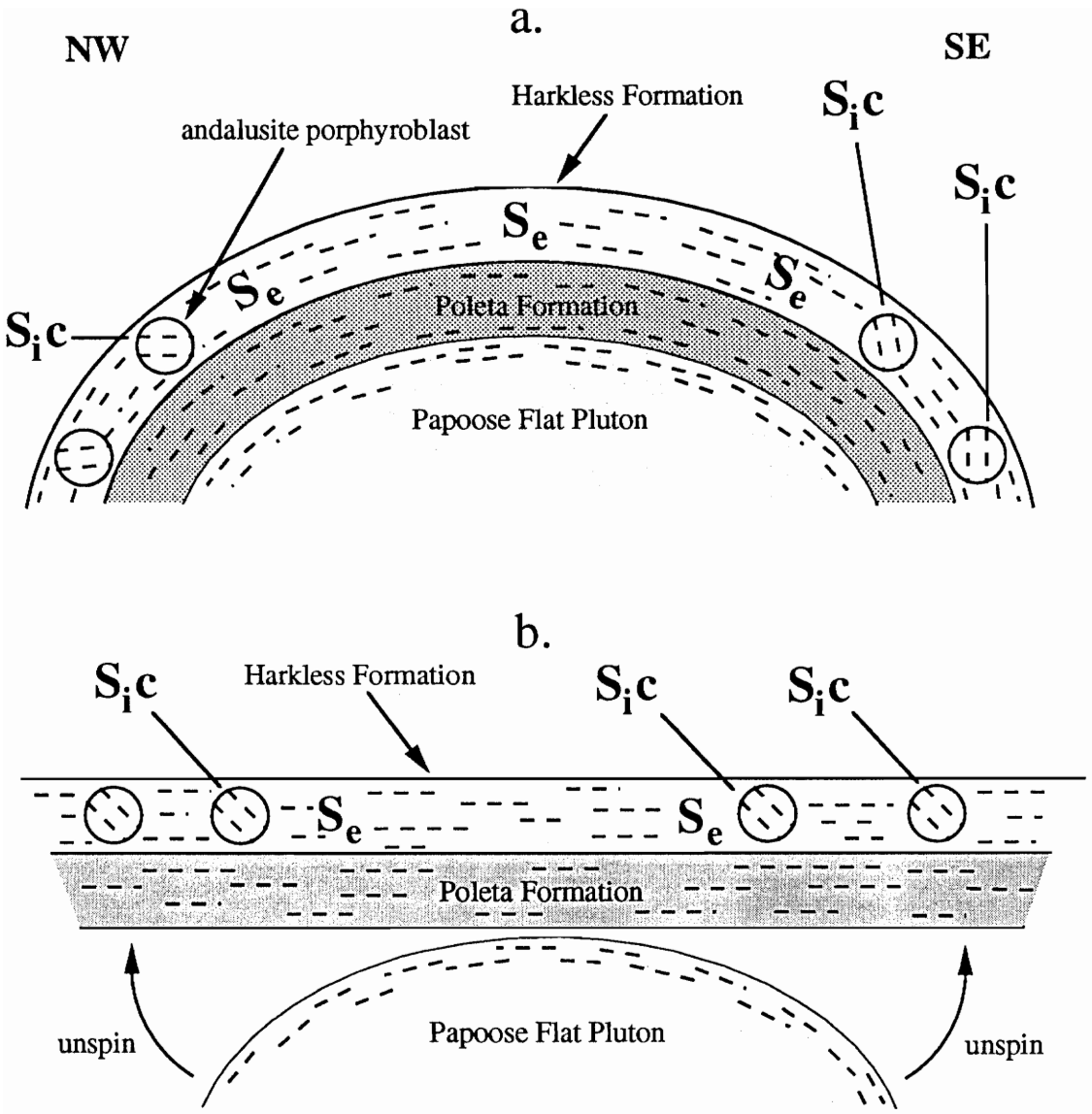

Fig. 26. **a.** Schematic cross section, before erosion to current level, from NW to SE through the western portion of the Papoose Flat pluton and the overlying metasedimentary rocks in pluton aureole. Note the various orientations of Sic from the NW margin to the SE margin.

b. "Unwrapping" the overlying metasedimentary rocks into a planar reference frame "unspins" Sic from all locations within the Harkless Formation into a parallel alignment.

the NW striking cleavage that Dunne et al. (1978), Sylvester and Babcock (1975), and the author have observed elsewhere in the Inyo Mountains. Evidence for Sic being an earlier fabric that is only preserved within porphyroblasts is best observed at location 105 (Fig. 22) in the low strain zone where deformation and metamorphism are less intense. From examination of the Harkless phyllite/schist at location 105, it is clear that the inclusion trails within the andalusite porphyroblasts are the same material as the matrix material, yet in a different orientation (Fig. 27).

The strike of the plane of inclusion trails (calculated from andalusite porphyroblast inclusion trails measured in orthogonal sections, XZ & YZ) is approximately N35°E, and they dip 50° to the SE. Assuming that inclusion trails in the cores of andalusite porphyroblasts represent the NW striking cleavage that Dunne et al. (1978), Sylvester and Babcock (1975), and the author have observed in the Inyo Mountains, the strike of the cleavage/inclusion trails must have been rotated a minimum of 45° in response to the deformation associated with the intrusion of the pluton, to be presently oriented at N35E°. This amount of cleavage/inclusion trail rotation is not unfeasible considering the amount of rotation that the metasedimentary units may have undergone during intrusion of the Papoose Flat pluton. The regional strike of the sedimentary units, including the Harkless Formation, north of the pluton is to the NNW. Within the northwestern portion of the aureole of the Papoose Flat pluton, the same metasedimentary units strike ENE to NE.

Subsequent to initial intrusion and static metamorphism, 'inflation' or 'doming' of the granitic 'mush' rotated the cleavage into parallelism with compositional layering as attenuation of the metasediments occurs. During the later 'doming' event, the cleavage is transposed into a well defined foliation and metamorphosed into an amphibolite grade assemblage. This event is recorded in the rims of andalusite porphyroblasts where inclusion trails curve from the planar interior region into parallelism with the exterior foliation. In the rims, inclusions become more similar in shape and composition to the

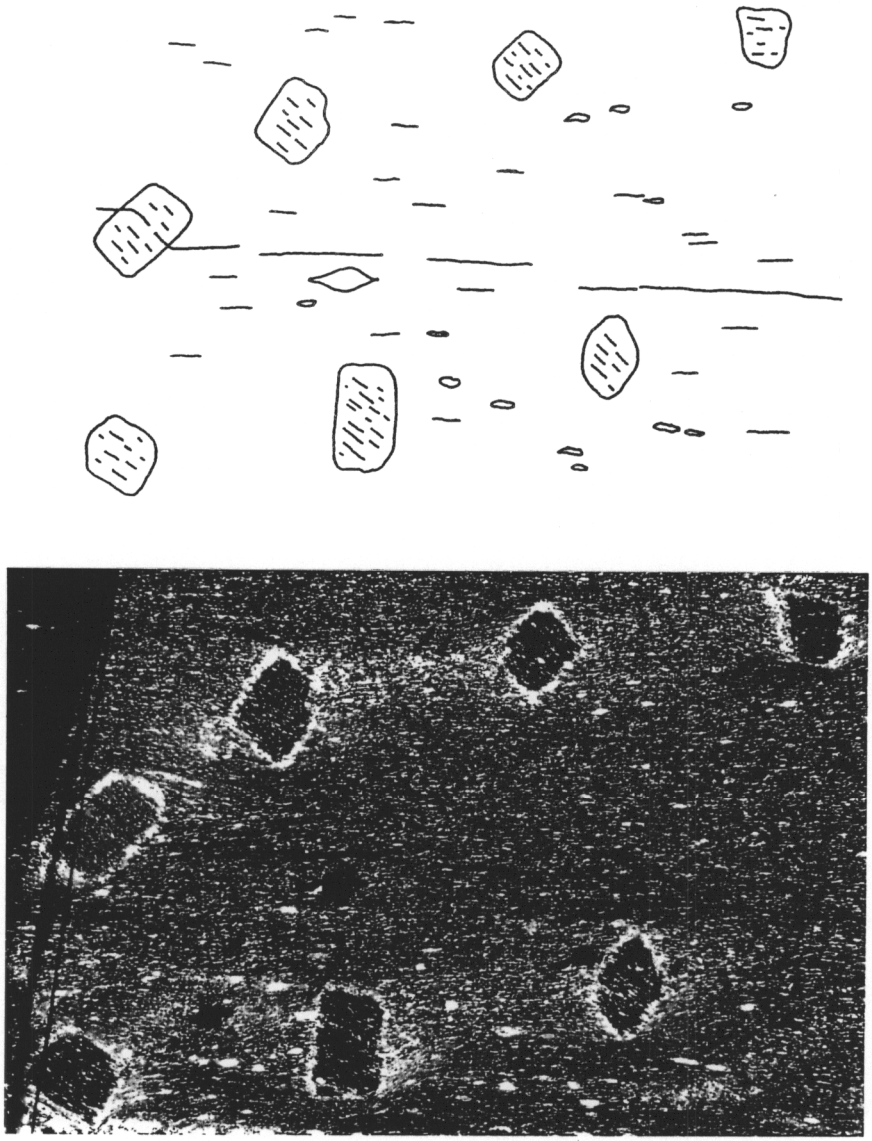

Fig. 27. Photomicrograph and drawing of sample PF 281, collected at Location 105, 250 m from the pluton. Area of photo is 6.5 mm by 5.0 mm. Photo is parallel to lineation and perpendicular to foliation, view is to the NE. Note; A) the parallel alignment of the inclusion trails in the andalusite porphyroblasts, B) how inclusion trails are the matrix material which has been overgrown by andalusite porphyroblasts. Compare these porphyroblasts with the core region in the porphyroblast in Fig. 21.

mineral phases making up the matrix foliation. Inclusions in the core regions are primarily composed of fine grained quartz blebs and opaque minerals that are extremely similar in shape and texture to the matrix in the relatively undeformed Harkless shales (compare Figs. 21 & 27). Inclusions in the rim regions are coarser grained, quartz grains usually have larger aspect ratios, opaque minerals are less abundant, and muscovite and biotite porphyroblasts of varying grain size are included. The observation that the inclusion trails in the rim regions of the porphyroblasts curve into parallelism with the matrix foliation indicates that at least *the last period of porphyroblast growth was syndeformational* (Rosenfeld 1968; Spry 1969; Vernon 1989; Hanmer and Passchier 1991).

Fyson (1980), argued for a similar interpretation of planar inclusion trails around a granitoid pluton in the NW Territories, Canada, and proposed that inclusion trails can be used as "fossil directions". In this model, inclusion trails in porphyroblasts are the only record of previous foliations which have been destroyed outside of the porphyroblasts. Fyson analyzed inclusion trails in biotite grains from Archean metasedimentary rocks around a granitoid pluton and observed that S_i in biotite was parallel to an S_2 foliation outside of the biotite, and therefore was probably the same foliation (Fig. 28a). Where a later S_3 foliation is the dominant fabric, which overprints and destroys S_2, S_i in biotite is the only remnant of the S_2 foliation (Fig. 28b). Fyson (1980) concluded that the inclusion trails preserved in biotite porphyroblasts represent a foliation in the rocks that existed prior to pluton emplacement, and that subsequent deformation to form S_3 has only minimally rotated the biotite porphyroblasts.

Vernon (1989) observed a similar relationship adjacent to the Bathhurst Batholith near Sydney, Australia. Cordierite porphyroblasts adjacent to the batholith contain planar inclusion trails which are at a constant angle to the matrix foliation. Vernon interpreted S_i to be the remains of an earlier cleavage obliterated within the matrix of the aureole, but still preserved outside the aureole within the country rocks. He also noted that the parallelism

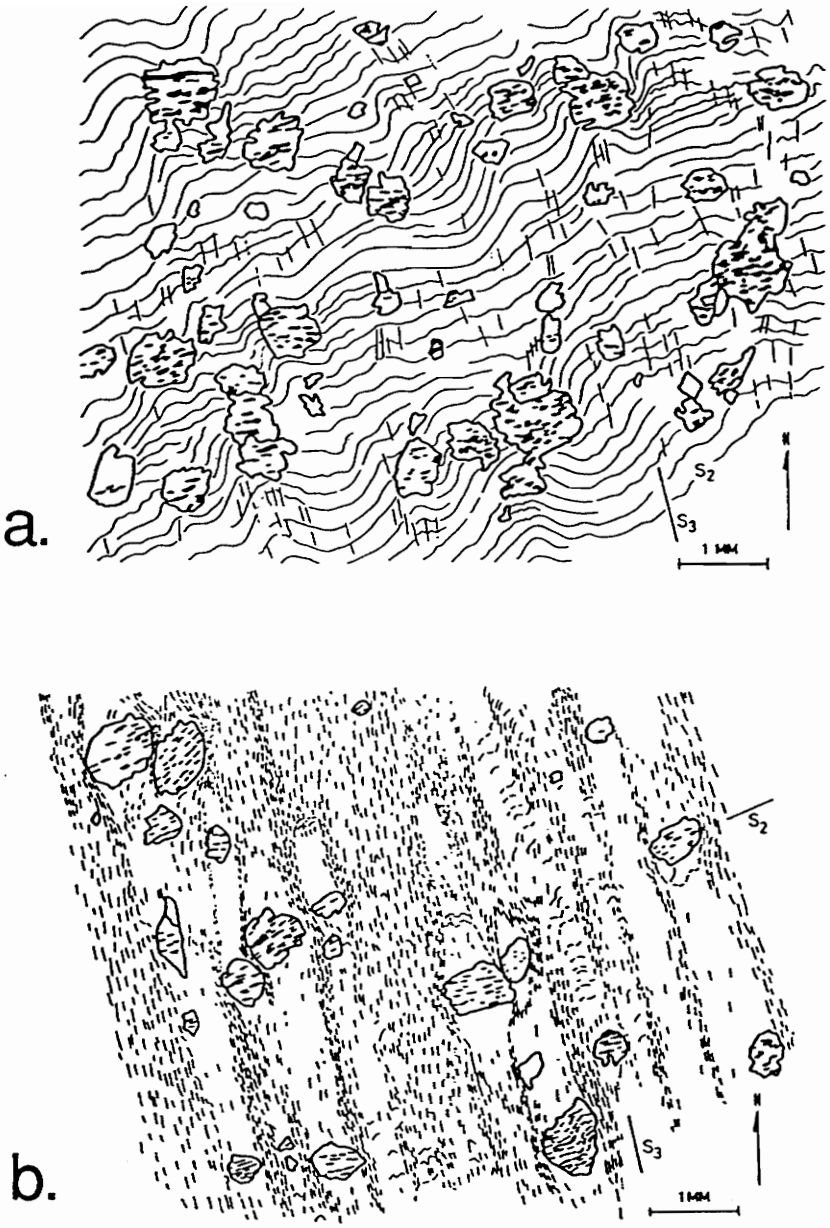

Fig. 28. Porphyroblast-matrix relationships from schists collected near granitoid plutons in the NW Territories, Canada. In **a**. S2 is the dominant foliation in the rock, which biotite porphyroblasts have overgrown. The S3 foliation is poorly developed. The drawing in **b**. is of a sample collected where S3 is the dominant foliation and S2 is preserved in biotite porphyroblasts as inclusion trails. From Fyson (1980).

of Si in porphyroblasts surrounding the intrusion suggested that rotation of the porphyroblasts had not occurred during subsequent deformation.

The evidence against model #1:

It has not been conclusively demonstrated that the inclusion trails in andalusite porphyroblasts are the preserved remnants of the NW striking cleavage observed throughout the Inyo Mountains.

Model 2

Andalusite porphyroblasts nucleated on the limbs of microfolds deforming an earlier cleavage within the Harkless shales/schists. Fold limbs were preserved as inclusion trails in the porphyroblasts. The microfolds developed early to synchronous with intrusion, and were destroyed outside porphyroblasts during subsequent or continued deformation. Porphyroblasts are either syn- or post-tectonic relative to the microfolding and pre-tectonic relative to the present foliation. Neither porphyroblasts nor foliation have rotated with respect to compositional layering.

The evidence for model #2:

In this model NE striking crenulations developed in response to the same event which produced the noncoaxial deformation observed in the quartz and marble-rich units surrounding the pluton. The shear sense obtained from the 'crenulated fabric' matches with the shear sense exhibited by the quartz fabrics and microstructures. An over-thrusting event towards the southeast, which occurred during or soon after intrusion, has been suggested before by Law et al. (1990, 1992) and by Paterson et al. (1991). The porphyroblasts nucleated on the short limbs of the crenulatations as intrusion and metamorphism took place (Fig. 29). Continued defomation destroyed the crenulated fabric

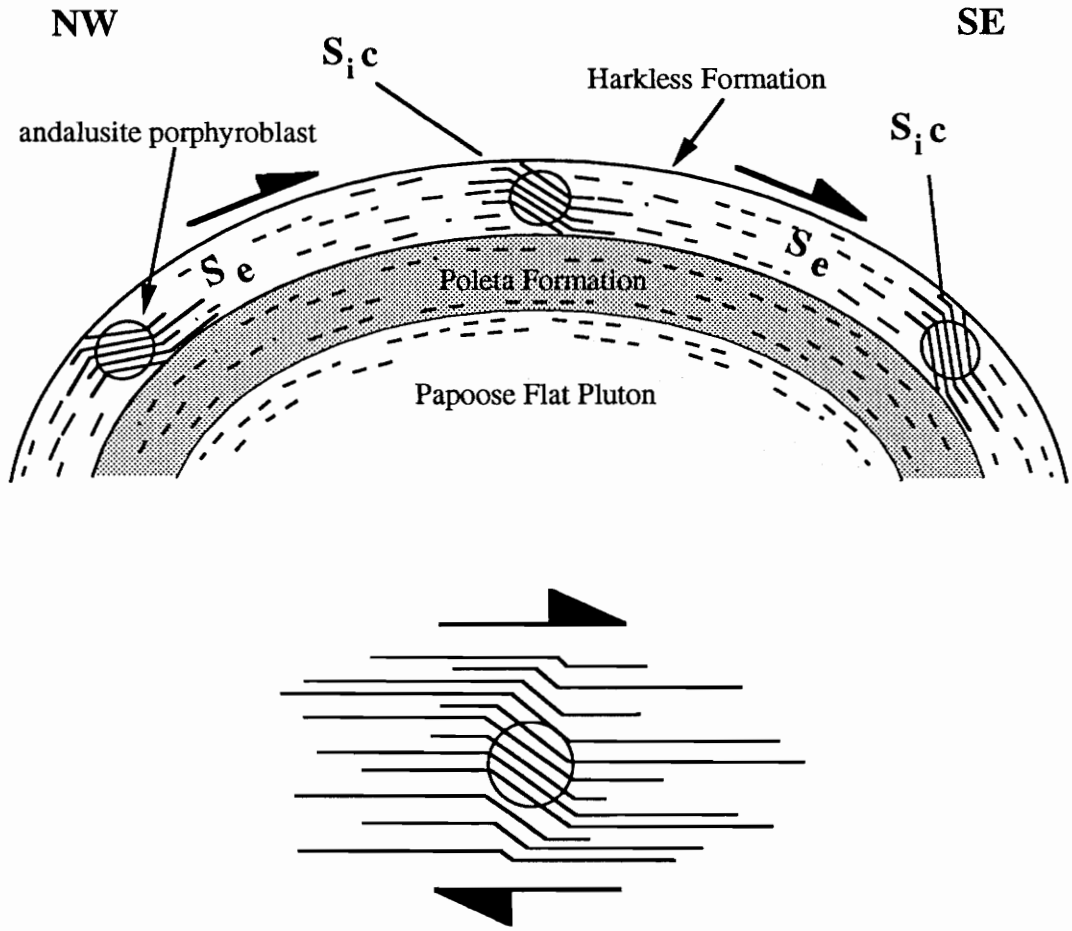

Fig. 29. Diagram portraying crenulation cleavage model for the possible formation of the angular Sic to Se relationship. Andalusite porphyroblasts nucleate in zones of microfolded foliation associated with top to the SE simple shear. Microfolds deform an earlier bedding parallel foliation. Subsequent deformation destroys microfolds outside of porphyroblasts.

outside of the porphyroblasts.

The evidence against Model #2:

A) In Bell's (1986) model it was suggested that porphyroblasts nucleate in the hinge zones of the crenulated fabric where coaxial deformation is concentrated, not in the limb zones (Bell, 1986). No crenulated hinges, or curved inclusion trails, are observed in the cores of andalusite porphyroblasts. The inclusion trails in the core regions of the porphyroblasts are always planar.

B) All crenulations have the same interlimb angle regardless of geographic position around the pluton.

C) The rim regions of porphyroblasts, regardless of size of the porphyroblast, always preserve the hinges of the 'crenulated' fabric. The distance between hinges recorded in porphyroblasts varies with the size of the porphyroblast. For example, small porphyroblasts with rims preserved show the same hinge-limb-hinge geometry as large porphyroblasts with rims preserved, although the distance between hinges in the small porphyroblast will be much less than in the large porphyroblast. This implies that the distance between hinges is variable and that porphyroblasts always stopped growing after overgrowing the hinge regions, regardless of how far apart the hinges were.

D) In some porphyroblasts where the rim regions are preserved, andalusite has overgrown the 'crenulated cleavage' so that the porphyroblast preserves the cleavage from one crenulation or hinge to the next crenulation/hinge and the limb in between. Within these porphyroblasts the inclusions always become coarser grained and less numerous on either side of the limb region begining with the hinges. The increase in inclusion grain size

always coincides with the change in orientation of inclusion grains, or 'hinges' of the crenulated fabric. The change in metamorphic conditions that produced the increase in inclusion grain size would have had to coincide with the exact time that porphyroblasts grew just large enough to encompass both hinges of the crenulated fabric, regardless of size of porphyroblast. The increase in inclusion grain size is never observed to occur within the straight part of the inclusion trails, or 'limb' region.

Model 3

All andalusite porpyroblasts rotated the same amount during the late stages of intrusion. The intrusion and contact metamorphism initially caused andalusite to nucleate within the Harkless shales. Andalusite porphyroblasts statically overgrew the bedding plane foliation, which was progessively being metamorphosed into an amphibolite grade foliation. Late in the growth history of the porphyroblasts, a strong component of foliation parallel simple shear rotated all andalusite porphyroblasts the same amount. Andalusite continued to grow and incorporate the foliation as inclusion trails during the rotation event. Porphyroblast cores are pre-tectonic, rims are syn-tectonic. The external foliation did not rotate.

Observations that support Model #3:

Model #3 is simpler than models #1 and #2 in that only one foliation-forming event is needed to explain the Si to Se geometry. Other oblique foliations are not needed. Andalusite porphyroblasts overgrew a foliation which was initially parallel to the compositional layering (?bedding) and subsequent non-coaxial deformation rotated the porphyroblasts. Porphyroblast growth must have continued through the rotation event as the trace of Sic to Sir to Se is continuous. The foliation only rotated where the porphyroblast had overgrown the foliation.

Other authors have observed similar relationships and have cited porphyroblast

rotation as the mechanism for development of the angular relationship. Olesen (1982) observed a similar and roughly constant angular relationship between a planar Si and Se within garnet bearing phyllites from the Norwegian Caledonides (Fig. 30), and interpreted this relationship as indicating a rotation of the garnet porphyroblasts late in their growth history. He concluded that all garnet porphyroblasts had rotated approximately the same amount during a deformational event involving components of both pure and synchronous simple shear deformation.

Evidence against Model #3:

A) All porphyroblasts would have rotated the same amount regardless of; a) the heterogeneity of the simple shear component and b) the size and/or shape of porphyroblasts. Jamieson (1988, p. 207) has stated that, "...a model involving matrix re-orientation is much more plausible than one requiring all porphyroblasts to have rotated the same amount regardless of size, position in rock, or crystal form." Bell et al. (1986) has reinterpreted Olesen's (1982) data to represent rotation, or 'reactivation', of the original foliation around the garnet porphyroblasts, and concluded that the garnets themselves had not rotated.

B) If andalusite porphyroblasts have rotated, the sense of rotation from core to rim is switched on 5-10 % of the porphyroblasts within almost all samples. Porphyroblasts that have Sic oblique to the regional inclusion trail orientation, i.e., Sic dipping to the NW and not to the SE, contain a curvature of inclusion trails from core to rim that indicates a "top to NW sense of rotation". 90-95% of the porphyroblasts contain curvatures of inclusion trails that indicate a "top to the SE sense of rotation".

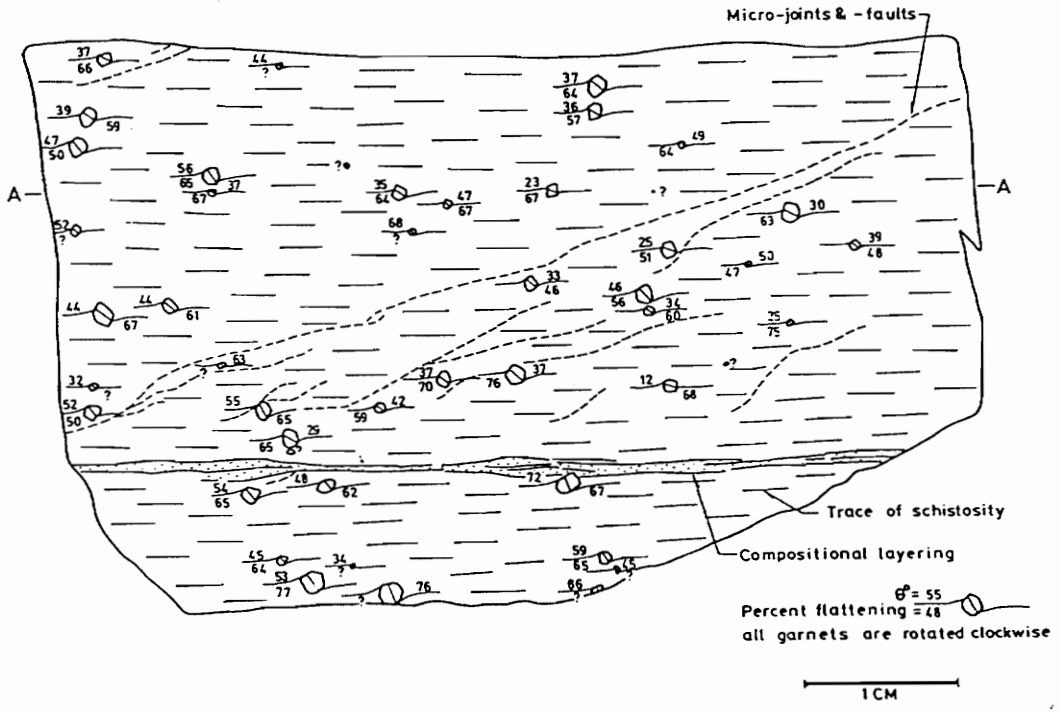

Fig. 30. Sketch of large thin section from a garnet bearing phyllite collected in the Norwegian Caledonides. Note that the garnet porphyroblasts have a similar orientation of inclusion trails. Olesen (1982) interpreted this porphyroblast-matrix relationship as indicating rotation of garnet porphyroblasts. Bell et al. (1986) interpreted this relationship as indicating rotation of the matrix foliation around the porphyroblasts. From Olesen (1982).

C) Northeast of the high strain zone, the Harkless Formation is much less deformed and metamorphosed and loses concordancy with the pluton while striking more regionally to the northwest. Here the apparent angle of porphyroblast 'rotation' is the same as in the high strain zone. It might be expected that if the porphyroblast rotation is related to the same deformational event that attenuated the aureole rocks, the amount of rotation would be related to the intensity of deformation.

D) Within the high strain zone, the Harkless Formation has been thinned from its regional thickness of approximately 570 m to its present state of approximately 45 m (Sylvester et al., 1978). If strict simple shear is largely responsible for this attenuation, then 1) the shear zone boundaries must have been oriented oblique to the lithological layering and, 2) there should have been a massive amount of top to the SE flow within the Harkless Formation. In the experimental work of Passchier and Simpson (1986), the angle of rotation of the model porphyroblast was approximately half the shear strain in all simple shear experiments. The shear strain needed to thin the Harkless Formation by 90% would be very large and probably cause porphyroblasts to rotate more than 40°, assuming the same relationship between shear strain and porphyroblast rotation as in Passchier and Simpson's (1986) experiments. Obviously, direct correlation between experimental work and real rocks cannot be made, but even if the model approximates the real system, a loss of over 500m by flow to the SE is a massive amount of translation of matrix rock around the porphyroblasts. Note that Law et al. (1992) have argued that if attenuation of stratigraphy is associated with a shearing event, then components of both simple shear and coaxial thinning must have been involved.

In light of the above arguments in favor of model #1 and against models #2 and #3 , the

remainder of this paper will discuss porphyroblast-matrix relationships assuming that model # 1 is the most applicable sequence of deformational and metamorphic events. The following data and observations of the relationship between porphyroblast inclusion trails and matrix foliation support the hypothesis that pure shear is the principal strain path for attenuation of the Harkless Formation and that this deformation was synchronous with the late stages of metamorphism.

3.5 *Syndeformational Metamorphism*

The portion of andalusite porphyroblasts that overgrew a planar foliation makes up a considerable portion of the cross-sectional area of the porphyroblasts examined (Fig. 21). The observations that; 1) Sic is planar and, 2) the core region makes up a considerable portion of the porphyroblast, suggests that for a considerable period of time during the growth period of andalusite, there was no ongoing deformation. The observation that the inclusion trails in the rims (Sir) of the andalusite porphyroblasts smoothly curve from the orientation of Sic into parallelism with the orientation of Se suggests that the period of andalusite rim growth was syn-tectonic. This relationship between Sir and Sic and Se yield evidence for a strong component of coaxial deformation (see Section 3.6) within the Harkless schist, and also record the synchroneity of the deformation with the second period of andalusite growth.

Where rims of andalusite porphyroblasts are preserved, the rim region is texturally much different than the core region. Inclusions in the rims are coarser grained and also less densely concentrated than in the planar core regions (Fig. 21). The transition is sharp between core and rim regions, yet the transition is always observed as a progressive curvature of inclusions from core-parallel to matrix-parallel. No evidence of truncation of inclusion trails between core and rim regions is observed.

The planar matrix foliation, Se, is mainly defined by muscovite, and to a lesser extent biotite, which are oriented subparallel to the lithologic layering except when in contact with andalusite porphyroblasts. Se anastomoses around the subhedral andalusite porphyroblasts and, when in contact, is parallel to the porphyroblast grain boundaries. The rim inclusion trails, Sir, are not parallel to the average attitude of the anastomosing matrix foliation, Se. Sir is parallel to the local Se adjacent to the porphyroblast, which has been rotated into parallelism with the porphyroblast grain boundary due to the deformation (Fig. 31). *The anastomosing foliation, Se, is recorded in the rims of andalusite porphyroblasts (Sir) and indicates that the growth of andalusite rims is synchronous with the deformation that produced the present orientation of the foliation.*

3.6 *Strain Path Model for the Harkless Schist*

3.6.1 *Simple Shear*

The interpretation that the deformation which attenuated the Harkless schist was dominantly pure shear (? plane strain, k=1) is supported by examining the samples where simple shear deformation is recorded and how this deformation has affected porphyroblast-matrix relationships. Sample PF 246b, which distinctly has the most random orientation of Sic of the twelve samples measured (Figs. 22 & 23), comes from the location that displays the most well developed microstructural evidence for a strong component of simple shear deformation. The foliation is composed of groups of deformed elongate muscovite porphyroblasts that are asymmetrically distributed around andalusite porphyroblasts, and where there is little interference from andalusite porphyroblasts, muscovite 'fish' (Fig. 32) indicate a top to the SE sense of shear. *This implies that where there was a strong component of simple shear, rotation of equidimensional porphyroblasts*

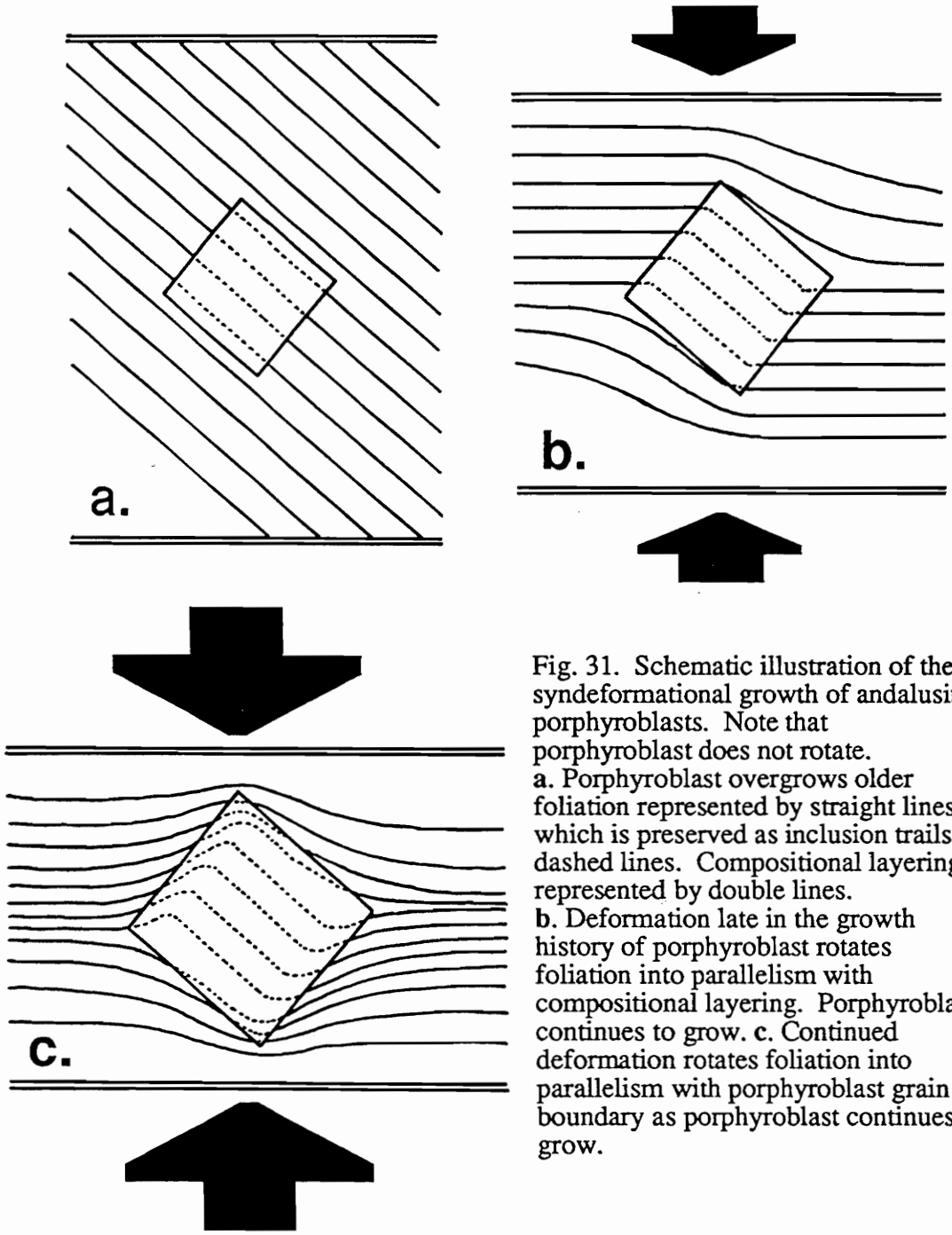

Fig. 31. Schematic illustration of the syndeformational growth of andalusite porphyroblasts. Note that porphyroblast does not rotate. **a.** Porphyroblast overgrows older foliation represented by straight lines, which is preserved as inclusion trails, dashed lines. Compositional layering represented by double lines. **b.** Deformation late in the growth history of porphyroblast rotates foliation into parallelism with compositional layering. Porphyroblast continues to grow. **c.** Continued deformation rotates foliation into parallelism with porphyroblast grain boundary as porphyroblast continues to grow.

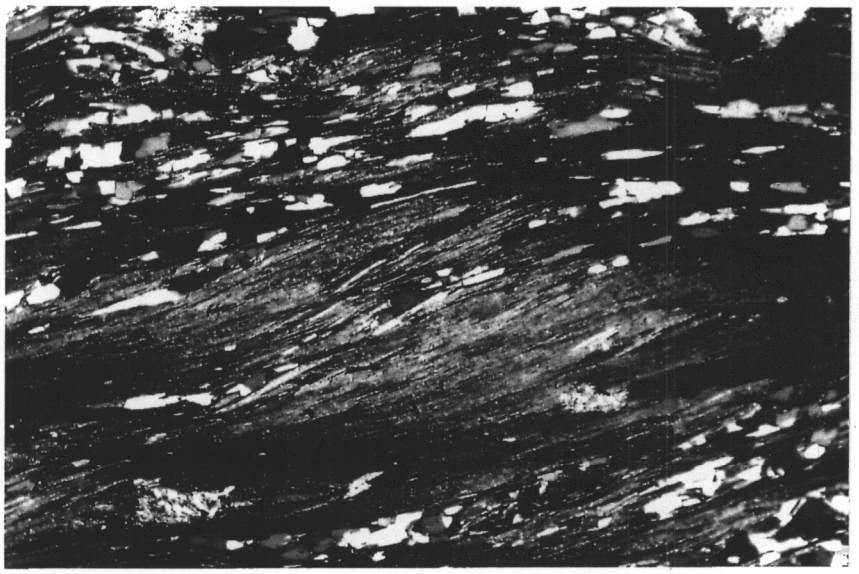

Fig. 32. Photomicrograph of muscovite fish in sample PF 245, collected from the same outcrop as PF 246. Length of rock covered in photo is 3.25 mm. Foliation is parallel to long edge of photograph and view is towards the NE. Asymmetry of 'fish' indicates a top to the SE sense of shear.

has occurred and the amount of rotation is not the same for all porphyroblasts. This argument, in turn, suggests that porphyroblasts in the other eleven samples with more constant orientations of Sic, have not been affected by a component of simple shear deformation.

These observed relationships in sample PF 246b, do not support Bell's (1985) argument for partitioning of coaxial and noncoaxial strain components. Bell (1985) argued that in schistose rocks undergoing a general shear, the micaceous matrix will experience the noncoaxial deformation and the rigid porphyroblasts will only feel the affects of coaxial deformation. The random orientation of Sic in the andalusite porphyroblasts from sample PF 246b suggests that the porphyroblasts did feel the affects of the noncoaxial deformation, and rotated because of it.

3.6.2 *Pure Shear*

The direction the inclusion trails curve from core to rim to become parallel with the matrix foliation varies and depends primarily on the orientation of Sic (porphyroblast core inclusion trails). As shown in Figure 23, most Sic intersect the thin section, viewed to the NE, in a line that plunges approximately 40° to the SE, if Se is rotated into a horizontal reference frame. In this orientation the sense of rotation of the foliation obtained from examining the curvature of inclusion trails from core to rim (Sir) is counterclockwise. In less than 10 % of the porphyroblasts measured, there is an orientation of Sic which dips to the NW, and in these porphyroblasts Sir curves clockwise from core to rim.

Figure 33 represents the schematic sequence of events for syndeformational growth of two andalusite porphyroblasts, viewed to the NE, that have had the foliation rotated clockwise and counterclockwise around them as they grew. The direction of maximum shortening relative to the porphyroblasts does not have to change to produce both

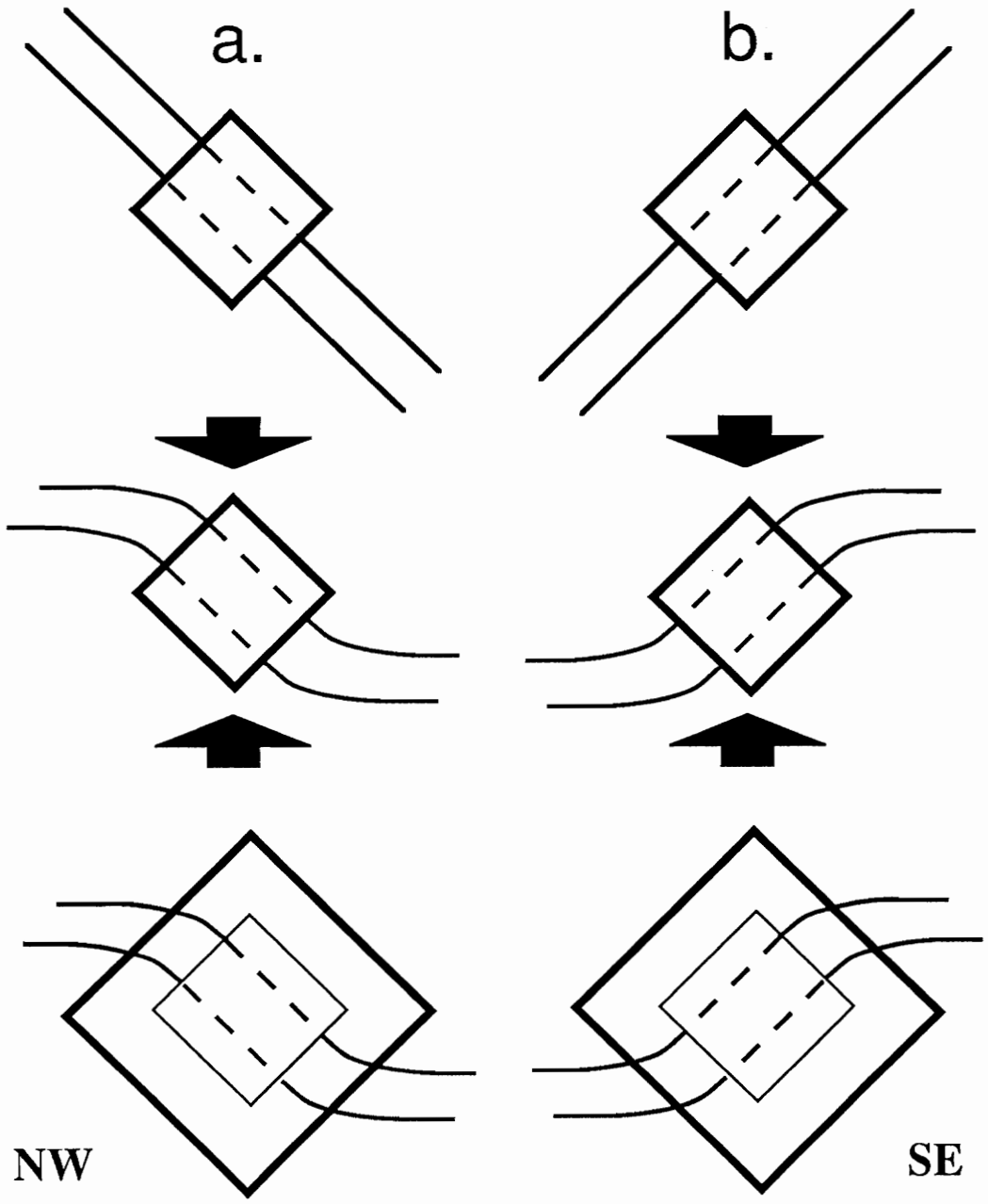

Fig. 33. Rotation of the external foliation into parallelism with compositional layering as andalusite porphyroblasts grow. View to the north and east. **a.** Most porphyroblasts have Si dipping to the SE. **b.** <10% of porphyroblasts have Si dipping to the NW and display a curvature of the foliation around the porphyroblast opposite to the porphyroblasts in **a.**

clockwise and counterclockwise rotations of the foliation. Using the porphyroblast as a stable reference, only the original orientation of dip of Sic must change to produce different senses of rotation. Therefore, the orientation of the maximum principal stress thought to produce the rotation of the foliation is inferred to be at ~90° to the present matrix foliation and the deformation is inferred to have been in part coaxial.

In summary, the matrix foliation was forced to rotate into parallelism with lithologic boundaries (sensu Ramsay 1962, p. 323) as attenuation occurred. Inclusion trails in the rims of porphyroblasts track the matrix foliation as it rotated towards lithologic boundaries and flattened against the porphyroblast grain boundary as the porphyroblast grew (Fig. 31). Deformation took place after andalusite porphyroblasts had grown to a considerable size. Hence, up to this point in time, porphyroblasts had included only planar incusion trails. Subsequent deformation was synchronous with the second period of andalusite growth, which is suggested by the curvature of inclusion trails into parallelism with Se, the coarser inclusion grain size, and the less dense concentration of inclusions.

3.6.3 *Pure Shear in the Low Strain Zone*

At Location 105 (Fig. 22) the Harkless shales exhibit the least deformation and metamorphism. It is the only known exposed location within the aureole, on the western half of the pluton, where the Harkless Formation loses its concordancy with the pluton and strikes north as both strain and metamorphism decrease rapidly with distance from the pluton. The narrowness of the aureole is well illustrated at Location 105 which is situated 250 m from the pluton. Here biotite is not found within the Harkless shales/schists. Biotite is ubiquituous in the Harkless schist where the schist is concordant to the pluton. Andalusite is the only phase larger in diameter than 50 μm and is typically 1000 to 1500 μm in diameter. The Harkless shales at Location 105 are, except for the presence of

andalusite, best classified as a phyllite. The andalusite porphyroblasts do not display the sharp change in orientation between Sic and Sir that is so characteristic of porphyroblasts adjacent to the pluton. There is no distinct rim region, although there is a gradual curvature of inclusion trails towards the edge of porphyroblasts. Inclusion grain size does not coarsen, and the concentration of inclusions does not change towards the edge of porphyroblasts (Fig. 27).

Sample PF 281 was collected at location 105 and is ideal for examining the details of the deformation history because the lack of intense strain and metamorphism has left the porphyroblast-matrix relationships relatively undisrupted. It also, perhaps, offers the chance to view an earlier stage in the development of the more intensely deformed Harkless schist adjacent to the pluton.

The quartz grains in the more quartzose portion of PF 281 are unrecrystallized and display a planar arrangement of serrated grain boundaries indicative of diffusive mass transfer. Interstitial micas are randomly oriented. Andalusite porphyroblasts have the tightest cluster of Sic orientations of all twelve samples measured (PF 281, Figs. 22, 23, & 27), which could be a result of not having undergone the intense strain that the rocks farther to the south and west have undergone.

Sample PF 281 is also unique in that andalusite porphyroblasts with large aspect ratios are usually aligned either parallel or perpendicular to Se (Fig. 34). Elongate porphyroblasts that are aligned perpendicular to Se have an orientation of Sic that is at ~40° to Se, parallel to the general trend of Sic in andalusite porphyroblasts throughout the aureole. The majority of andalusite porphyroblasts are equidimensional and also maintain the consistent 40° angle between Sic and Se. Most elongate porphyroblasts which are aligned parallel to Se have orientations of Sic oblique to the general inclusion trail trend of Sic (Fig. 34). This relationship is interpreted as resulting from a *rotation of elongate porphyroblasts into parallelism with Se if they were not originally oriented parallel or*

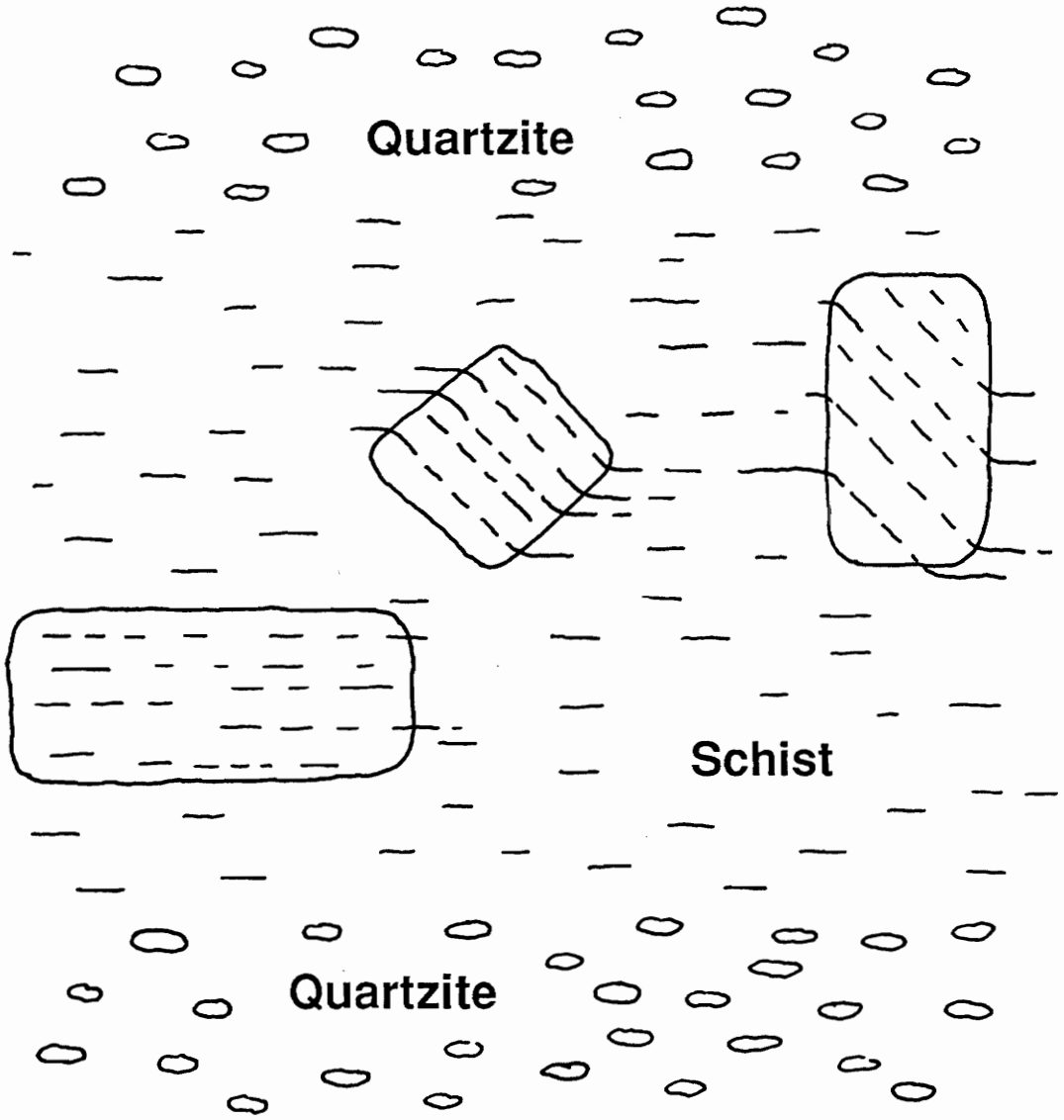

Fig. 34. Drawing of porphyroblast-matrix relationships in sample PF 281. Andalusite porphyroblasts with inclusion trails are outlined. See text for details.

perpendicular to Se.

Porphyroblasts with large aspect ratios which are elongate at 90° to Se, have the same angle between Sic and Se that the equidimensional porphyroblasts maintain (Fig. 34). Although these porphyroblasts have large aspect ratios, it seems that their orthogonal alignment relative to the foliation is responsible their non-rotation.

Whether or not elongate porphyroblasts have rotated seems to be dependent upon their initial orientation relative to the present foliation. Most elongate porphyroblasts with their long dimensions parallel or perpendicular to the foliation have not rotated, whereas other elongate porphyroblasts aligned parallel to the foliation seem to have rotated, as suggested by their oblique orientation of Sic (Fig. 34). It is this obliquity between elongate grain shape and foliation which has caused the porphyroblasts to rotate into parallelism with Se. The deduction that rotation or non-rotation of porphyroblasts was dependent on the original orientation of elongate grain shapes suggests that *the deformation that produced Se was to a large degree coaxial, since strong components of simple shear deformation would have rotated the elongate porphyroblasts that are oriented at 90° to the foliation towards parallelism with the foliation.*

3.6.4 *Noncoaxial Deformation and Pure Shear*

The deformation that produced the intense attenuation of the Harkless shales surrounding the Papoose Flat pluton is interpreted to be noncoaxial, but the component of simple shear is believed to be relatively small in comparison to the pure shear component and heterogeneously developed. It is not known whether the dominant strain path for attenuation is either pure shear plane strain (k=1), flattening (k=0), or some intermediate pure shear strain path. The well developed stretching lineation found throughout the high strain zone is related to the development of the strong preferred crystallographic orientation

in both the quartz veins within the gneiss and also in the overlying Harkless quartzites (Law et al. 1992). The a-axis crystallographic fabric patterns along with the c-axis fabrics indicate that the quartz veins deformed along a strain path close to simple shear (Law et al. 1992). The timing of formation of the lineation in relation to the attenuation of the Harkless schist is not clear. If the lineation is related to the attenuation event and the development of the porphyroblast-matrix relationships, then the deformation in the schist might approximate pure shear plane strain. There is evidence, at least within the granite, that the deformation within the quartz veins might be later than the development of the gneiss (see Chapter One), and then, possibly, the lineation within the Harkless schists might also be a later phenomena. If the development of the lineation within the Harkless schist is later than the development of the porphyroblast-matrix relationships, the deformation in the Harkless schist might be closer to flattening with a late component of simple shear.

The evidence for the pure shear component of the defomation is reviewed below:

1) The constant orientation of Sic, with respect to Se, indicates that andalusite porphyroblasts have not rotated, even though the Harkless schist they are found in has undergone attenuation to less than 10% of its original stratigraphic thickness. This relationship suggests that the foliation has rotated around the porphyroblasts.

2) The only sample location which has a random distribution of Sic orientations, out of twelve locations from the western margin of the pluton, is also the only location with abundant microstructural evidence for a strong component of simple shear deformation. This relationship suggests that where simple shear is localized, it will be recorded in the microstructures and will rotate equidimensional shaped porphyroblasts.

3) The curvature of Sir from Sic to Se mostly indicates a rotation of the external foliation in a counterclockwise fashion, viewed to the NE. The observation that approximately 10% of the porphyroblasts contain a sense of curvature of Sir from Sic to Se that indicates a rotation of the external foliation in a clockwise fashion, viewed to the NE, suggests that flow around individual porphyroblasts was both to the NW and to the SE. This relationship suggests that the orientation of the principal stress direction was approximately perpendicular to Se.

4) In the low strain zone, the orientation and inclusion patterns of andalusite porphyroblasts with large aspect ratios indicates that those porphyroblasts that were originally oriented either parallel or perpendicular to Se have not rotated with respect to Se.

CHAPTER 4

DISCUSSION AND CONCLUSION

4.1 *Intrusion and Emplacement*

Within the Harkless schists, evidence exists for a significant period of andalusite growth prior to the deformation that created the present foliation. It is suggested that the Papoose Flat granitic magma may have ponded, probably as a sill, primarily within the Poleta Formation before any significant deformation occurred. Sills of granite are observed within the Campito Formation and the Poleta Formation at the northern and western margins of the pluton, respectively.

The magma may have initially risen along a pre-existing fault (Nelson 1987), in a manner similar to that previously proposed for the emplacement history of the Birch Creek pluton (Nelson and Sylvester 1971) 30 km to the north of the Papoose Flat pluton (Fig. 1). The Birch Creek pluton, which is of similar age to the Papoose Flat pluton, is situated along and truncates a large fault, and probably folded large faults adjacent to the pluton as the pluton bulged to the NW (Nelson and Sylvester 1971). The Papoose Flat granitic magma is believed to have first risen into the Poleta Formation within the western limb of the Inyo Mountain anticline and then become stationary. The duration of time taken for andalusite porphyroblasts within the Harkless shales to nucleate and grow to the size of their core region is believed to be the duration of time over which the magma ponded. Porphyroblasts overgrew a planar foliation which might represent the regional NW striking axial planar cleavage (axial planar to the Inyo Mountain anticline) (Sylvester and Babcock 1975; Dunne et al. 1978), or possibly a deformation fabric formed during the initial stage of intrusion. Subsequent pulses of magma into the sill caused the outer, more crystallized

rind of the sill to dilate, primarily out to the west, and forced the overlying Poleta, Harkless, Saline Valley, and Mule Spring Formations to bulge out of their position in the SW limb of the Inyo Mountain anticline. Porphyroblasts continued to grow during the dilation event, which is recorded in the rims of andalusite porphyroblasts where inclusion trails curve into parallelism with the present foliation (Figs. 21 & 31). The metasedimentary units maintained their coherent stratigraphy and were thinned uniformly due to the increased ductility of the rocks at higher temperatures and pressures and due to the strong component of pure shear involved in the deformation.

4.2 *Forceful Emplacement*

The evidence for the forceful emplacement of the Papoose Flat pluton is based on interpretation of the strain path. Oblate/flattening strains (k=0) are believed to be the best indication of a ballooning type of forceful emplacement (Ramsay 1989). The only macroscopic evidence for flattening strain within the deformed rocks around the Papoose Flat pluton is the chocolate tablet boudinage recorded in the skarn at the pluton/wall rock contact. The a-axis fabrics from the quartzites at this horizon (Law et al. 1992, figs. 9 & 11) also indicate flattening strains. The gneissic foliation at the border of the pluton may be a result of pure shear flattening (k=0), but pure shear plane strain (k=1) cannot be ruled out. The opposing shear sense indicators within the quartz veins in the gneiss also might indicate that bulk pure shear dominated the deformation within the gneissic border facies. The parallel orientation of inclusion trails in andalusite porphyroblasts and porphyroblast-matrix relationships suggests a significant component of pure shear deformation (?flattening k=0, ?plane strain k=1) recorded in the Harkless schist. Lastly, the symmetrically boudinaged siltstone layers in the Saline Valley Formation are a further indication of pure shear plane strain.

Pure shear plane strain (K=1), is obviously a different type of strain path than flattening (K=0), which is required for strict ballooning. Therefore, strict ballooning cannot be invoked for the mechanism of emplacement of the Papoose Flat pluton. The deformation surrounding the Papoose Flat pluton records components of pure shear plane strain and flattening, suggesting that there was a considerable component of compressive stress oriented perpendicular to the pluton/wall rock contact. The lineation related to the component of simple shear deformation in the quartz tectonites is parallel to the extension direction within the boudinaged (plane strain) Saline Valley Formation, suggesting that a more complex type of forceful 'inflation' was involved in the emplacement. Either a component of 'ballooning' or inflation occured during a regional deformational event (overthrusting to the SE), or the inflation of the pluton was more directed to the NW (parallel to the orientation of the lineation).

The synchroneity of second stage growth (metamorphism) of andalusite with the deformation that created the present foliation also indicates that expansion of the pluton may have caused the deformation. The boundary between the core and rim regions in andalusite porphyroblasts marks the onset of change in the metamorphic environment; inclusion trails in andalusite porphyroblasts begin to coarsen in grain size and the density of inclusions decreases significantly (Fig. 21). The increase in inclusion grain size and the decrease in number of inclusions in the porphyroblast *suggests* that the change in metamorphic conditions is related to an increase in temperature, although other possible interpretations exist (i.e., change in fluid flow, reaction boundary, etc.). The porphyroblast core-rim boundary is also where the inclusion trails change orientation and curve into parallelism with the present foliation. The change in metamorphic environment coincides exactly with the onset of deformation, which is expected in a model of forceful expansion. Intrusion of more magma into the core of the granitic mush/magma would bring an increase in heat and in volume which is accompanied by deformation and change in metamorphic conditions.

This synchroneity of deformation with second stage metamorphism is somewhat coincidental if related to a regional deformational event, although deformation assisted/induced reactions can also be invoked to explain the synchronous nature of events.

Other evidence for forceful expansion of the pluton is the interpretation that the bulging of the pluton overturned the Wyman Formation on the NE margin of the pluton (Nelson 1987). North of Waucoba Mountain, located within the eastern central portion of the Papoose Flat pluton (and also the highest point in the Inyo Mountains), the Wyman Formation is overturned, as well as the SW limb of the Inyo Mountain anticline (Nelson 1987). North of the pluton along the SW limb of the anticline, the Wyman Formation displays the regional NW strike. Approaching the pluton, the rocks steepen and eventually overturn approaching the pluton contact. The gneissic foliation is absent here, but a weak internal foliation exists. No where else on the west limb of the anticline are the strata overturned, suggesting that the pluton also bulged to the NE (Nelson, 1987).

4.3 *Evidence for a thrust model*

When examined by itself, the large component of plane strain (k=1), both simple shear and pure shear deformation, is most easily explained by an overthrusting event to the SE which occurred during or soon after emplacement of the Papoose Flat pluton. The most striking macroscopic structural evidence for plane strain is the well developed stretching lineation observed throughout the western margin of the pluton. The lineation is associated with the strong component of simple shear deformation observed within the quartz veins in the gneiss and within the Harkless quartzites (Law et al. 1990; Law et al. 1992). These observations are difficult to reconcile with a "ballooning" model of forceful emplacement, and therefore add weight to the validity of the overthrust model.

There is also no observed compositional zoning within the pluton, which Paterson

et al. (1991) have used as evidence against the forceful emplacement model. Although, if the pluton is modelled as a sphere, and by calculating the area of the sphere/pluton exposed by examination of the dip angle of the pluton/wall rock contact, less than 10% of the pluton is exposed at the earth's surface. It is possible that the pluton is compositionally zoned, but present levels of exposure have not yet revealed the zoning.

The Birch Creek pluton, located 33 km to the north of the Papoose Flat pluton (Fig. 1), is also reported to have more intense deformation at the NW margin (Nelson and Sylvester 1971). Although the deformation there is much less intense, this localized deformation at the NW margin of two plutons of similar age is more easily explained by a regional deformational event. Paterson et al. (1991) have stated that as many as five other plutons in the White-Inyo Mountains exhibit deformation along their western margins, and suggest that it is unlikely that so many plutons all "ballooned" out to the west or northwest. Nelson (pers. comm.), who has mapped much of the White-Inyo Mountains (Nelson 1966; Nelson 1971; Nelson et al. 1977) and who has published on the stratigraphy of the White-Inyo Range (Nelson and Perry 1955; Nelson 1962) and the granites that intrude the sedimentary sequence (Nelson and Sylvester 1971; Nelson et al. 1972, Sylvester et al. 1978), has reservations about whether other plutons in the White-Inyo Mountains, except for the Papoose Flat and Birch Creek, exhibit deformation along their western margins.

It should be noted though, that the "...kinematic indicators of sinistral shear everywhere within and adjacent to the western half of the pluton...", stated by Paterson et al. (1991, p. 324) have not been observed by the author.

4.4 *Evidence against a thrust model*

Evidence against the thrust model begins with an analysis of the structures formed assuming that they are thrust related. Complications to the thrust model that are difficult to

reconcile with the observed structures are; 1) the amount and direction of translation of rock mass during simple shear deformation, and 2) the variation in strain between quartz veins and quartzites in the low strain zone.

1) The pluton/wall rock contact is probably the zone of highest strain (see Chapter Two) and therefore in the thrusting model must be assumed to be the inner most part of the shear zone, and likewise parallel to the shear zone boundary. The pluton/wall rock contact at the northern margin has an average dip of around 40° to the north and at the southern margin has an average dip of 40° to the south. If thrusting to the SSE attenuated the sedimentary rocks, assuming strict simple shear, 90% of the sedimentary rock surrounding the pluton (the amount of stratigraphic thickness that is missing) has been transported to the SE. There is no evidence for deformed and metamorphosed sedimentary rocks south of the pluton. If the material is being transported parallel to the shear zone boundary, then the lost mass of rock is being transported 40° down from horizontal, parallel to the pluton-wall rock contact.

Obviously the bulk deformation did not approximate strict simple shear, and the shear zone model employed above is simplified, yet the lost mass of rock must be accounted for. The missing mass of rock is more easily accounted for in the forceful 'inflation' model, where the material is not transported away, but simply stretched and thinned across the pluton as the pluton expands. This also helps to explain the uniformity of the deformation, i.e., the sedimentary sequence is intensely attenuated but remains a coherent and identifiable sequence.

2) In the low strain zone at location 26 (Fig. 9), the gneissic quartz veins exhibit a much higher degree of strain than within the Harkless quartzites (Fig. 20). The gneissic foliation at location 26 is also well developed, similar to the gneiss in the high strain zone, although the attenuation of the metasedimentary units is much less extreme than in the high strain zone. Since the strain intensity decreases to the east along the pluton/wall rock

contact (low strain zone), it seems as if thrust related deformation was waning to the east. Here the granitic rocks exhibits much more strain than the metasedimentary units, which is difficult to reconcile in the thrusting model since the metasedimentary units are composed of rheologically weaker marbles, shales, and quartzites. Either the pluton acted as a strain 'sink', or the principal stresses originated from the interior of the pluton and were directed outward.

4.5 *Conclusions*

The intense strain within the metasedimentary and plutonic rocks around the western border of the Papoose Flat pluton is partitioned by rock type. The bulk deformation is noncoaxial. Various amounts of pure and simple shear deformation, depending on rock type, combined to produce the observed structures.

A dominantly pure shear (flattening and/or plane strain) strain path is believed to have resulted in producing the structures observed within: A) the gneissic border facies of the pluton, B) the skarn rocks at the pluton/wall rock contact, C) the Harkless schist and, D) the Saline Valley limestone. A dominantly simple shear strain path is believed to have resulted in producing some of the structures within; A) quartz veins within the gneiss, B) the Harkless quartzite, C) micaceous rich horizons within the Harkless schist, and D) the Poleta Formation (see Law et al. 1992)

Quartz crystallographic fabric patterns suggest that a strain gradient exists across the pluton/wall rock contact. The highest strain is within the quartz tectonites at the contact and decreases to the lowest strain within the quartzites moving away from pluton, indicating that the pluton/wall rock contact is the zone of most intense strain. The c-axis fabric patterns from the quartz veins are dominated by asymmetric single girdles, and locally indicate either top to the SE or top to the NW sense of shear. The fabrics from the

Harkless quartzite are dominated by asymmetric cross girdles and indicate a predominant top to the SE sense of shear. The Harkless quartzite may have accomodated a stronger component of pure shear than the quartz veins within the gneiss, but both quartz rich units deformed approximately under simple shear deformation.

Porphyroblast-matrix relationships within the Harkless schist indicate that andalusite porphyroblasts have not rotated during the intense deformation, and indicate that a dominant component of pure shear was involved in producing the schistose foliation. The orientation of inclusion trails in porphyroblasts suggests that initial metamorphism was static and that significant deformation did not occur until late in the growth history of the porphyroblasts. Porphyroblast rim growth is syndeformational.

Considering the rapid time frame that intrusion and cooling of shallow level plutons are thought to occur in (Paterson et al. 1992), components of pure and simple shear deformation are believed to have developed in the different rock types synchronously with intrusion. There is evidence that at least within the gneiss, simple shear deformation within the quartz veins occurred later than the initial development of the gneissic foliation.

The following lines of evidence indicate that the Papoose Flat pluton was forcefully emplaced: 1) the flattening strains observed at the pluton/wall rock contact, 2) the large component of pure shear deformation observed in many different rock types, 3) the variation in strain in the low strain zone and, 4) the second stage of metamorphism being synchronous with deformation.

The deformation is believed to be a result of a complex path of forceful inflation of the Papoose Flat pluton, where inflation of the pluton is not symmetrical like a balloon, but is heterogeneously developed and possibly directed more to the NW. A regional thrusting event to the SE may have, or may not have, occurred synchronously with forceful emplacement.

References

Bateman, P.C., Clark, L.C., Huber, N.K., Moore, J.G. & Rinehart, C.D. 1963 The Sierra Nevada batholith: a synthesis of recent work across the central part. U.S. Geological Survey Professional Paper 414-D, 46p.

Bell, T.H. 1985 Deformation partitioning and porphyroblast rotation in metamorphic rocks: a radical reinterpretation. J. Metamorphic Geology, 3, 109-118.

Bell, T.H. 1986 Foliation development and refraction in metamorphic rocks: reactivation of earlier foliations and decrenulation due to shifting patterns of deformation partitioning. J. Metamorphic Petrology 4, 421 - 444.

Bell, T.H. & Johnson, S.E. 1989 Porphyroblast inclusion trails: the key to orogenesis. J. Metamorphic Petrology 7, 219 - 310.

Bell, T.H. & Johnson, S.E. 1990 Roation of relatively large rigid objects during ductile deformation: well established fact or intuitive prejudice. Australian Journal of Earth Sciences 37, 441 - 446.

Bell, T.H., Johnson, S.E., Davis, B., Forde, A., Hayward, N. & Wilkins, C. 1992 Pophyroblast rotation: eppur non son girate *! J. Metamorphic Petrology 10, 295 - 307.

Bell, T.H., Rubenach, M.J., and Fleming, P.D. 1986 Porphyroblast nucleation, growth and dissolution in regional metamorphic rocks as a function of deformation partitioning during foliation development. J. Metamorphic Geology, 4, 37-67.

Bouchez, J.L. and Duval, P. 1982 The fabric of polycrystalline ice deformed in simple shear: experiments in torsion, natural deformation and geometrical interpretation. Textures and Microstructures 5, 171 - 190.

Bouchez, J.-L., Lister, G.S., & Nicolas, A. 1983 Fabric asymmetry and shear sense in movement zones. Geol. Rdschg. 72, 401 - 19.

Dell'Angelo, L.N. and Tullis, J. 1989 Fabric development in experimentally sheared quartzites. Tectonophysics 169, 1 - 21.

De Paor, D. G. 1989 An interactive program for doing fry strain analysis on the Macintosh microcomputer. J. of Geololgical Education 37, 171.

den Driessche, J. van and Brun, J.P. 1987 Rolling structures at large shear strain. J. Struct. Geol., 9, 691-704.

Dunne, G.C., Gulliver, R.M. & Sylvester, A.G. 1978 Mesozoic evolution of rocks of the White, Inyo, Argus, and Slate ranges, eastern California. In: Howell, D.G. & McDougall, K.A. (eds.) Mesozoic paleogeography of the western United States. Pacific Section, Society of Economic Paleontologists and Mineralogists, Pacific Coast Paleogeography Symposium 2, 189 - 208.

Etchecopar, A. & Vasseur, G. 1987 A 3-D kinematic model of fabric development in polycrystalline aggregates: comparisons with experimental and natural examples. J. Struct. Geol. 9, 705 - 17.

Frondel, C. 1962 Dana's System of Mineralogy, Vol. 3, Silica Minerals. John Wiley, New York.

Fry, N. 1979 Density distribution techniques and strained length methods for determination of finite strains. J. Struct. Geol. 1, 221 - 230.

Fyson, W.K. 1980 Fold fabrics and emplacement of an Archean granitoid pluton, Cleft Lake, Northwest Territories. Canadian J. Earth Sciences 12, 325 - 332.

Gleason, G.C., Tullis, J. & Heidelbach, F. 1992 The role of dynamic recrystallization in the development of lattice preferred orientations in experimentally deformed quartz aggregates. J. Struct. Geol. in review.

Godin, P.D. & Paterson, S.R. 1991 Re-evaluation of a blistering pluton: post-emplacement regional deformation at the Cretaceous Papoose Flat pluton, White-Inyo Mountains, California. Geol. Soc. Am. Abstracts 23 (2), A29.

Hanmer, S. & Passchier, C. 1991 Shear-sense Indicators: a Review. Geological Survey of Canada. Paper 90-17, 72pp.

Hobbs, B.E. 1985 The geological significance of microfabric analysis. In Wenk, H.-R. (ed.) Preferred orientations in deformed metals and rocks: an introduction to modern texture analysis, pp. 463 - 484. Academic Press, Orlando.

Hobbs, B.E., Means, W.D., and Williams, P.F. 1976 An Outline of Structural Geology. Wiley

Hudleston, P.J. 1977 Progressive deformation and development of fabric across zones of shear in glacial ice. In: Saxena, S.K. & Battacharji, S. (eds) Energetics of Geological Processes. Springer-Verlag, New York, 121 - 150.

Jamieson, R.A. 1988 Textures, sequences of events, and assemblages in metamorphic rocks. In Nisbet, E. G. & Fowler, C.M R. (eds) Heat, Metamorphism, and Tectonics. Mineralogical Association of Canada, Short Course Handbook, Vol. 14.

Jessell, M. 1988a Simulation of fabric development in recrystallizing aggregates - I. Description of the model. J. Struct. Geol. 10, 771 - 778.

Jessell, M. 1988b Simulation of fabric development in recrystallizing aggregates - II. Example model runs. J. Struct. Geol. 10, 779 - 793.

Jessell, M.W. & Lister, G.S. 1990 A simulation of the temperature dependence of quartz fabrics. In: Knipe, R.J. & Rutter, E.H. (editors) Deformation Mechanisms, Rheology and Tectonics. Geol. Soc. of London Special Publication No. 54, 353 - 362.

Johnson, S.E. 1990 Lack of porphyroblast in the Otago schists, New Zealand:

implications for crenulation cleavage development, folding and deformation partitioning. J. Metamorphic Petrology 8, 13 - 30.

Kistler, R.W., Bateman, P.C. & Branock, W.W. 1965 Isotopic ages of minerals from granitic rocks of the central Sierra Nevada and Inyo Mountains. Bull. Geol. Soc. Am. 76, 155 - 64.

Law, R.D. 1986 Relationships between strain and quartz crystallographic fabrics in the Roche Maurice quartzites of Plougastel, western Brittany. J. Struct. Geol. 8, 493 - 515.

Law, R.D. 1990 Crystalographic fabrics: a selective review of their applications to research in structural geology. In: Knipe, R.J. & Rutter, E.H. (eds) Deformation Mechanisms, Rheology and Tectonics. Spec. Publ. Geol. Soc. of London 54, 335 - 52.

Law, R.D., Morgan, S..M., Casey, M., Sylvester, A.G., & Nyman, M. 1992 The Papoose Flat pluton of eastern California: a reassessment of its emplacement history in the light of new microstructural and crystallographic fabric observations. Transactions Royal Society of Edinburgh: Earth Sciences 83, 361 - 375. 2nd Hutton Conference on the Origin of Granites. Conference volume also published as Geol. Soc. Am.- Special Paper 272.

Law, R.D., Morgan, S.S. & Sylvester, A.G. 1990 Evidence for large scale shearing during emplacement of the Papoose Flat pluton, California: a re-examination of the microstructures and crystallographic fabrics. Geol. Soc. Am. Abstracts 22 (7), A183.

Law, R.D., Morgan, S.S. & Sylvester, A.G. 1991 The Papoose Flat Pluton of California: a re-assessment of its emplacement history in the light of new microstructural and crystal fabric evidence. Second Hutton Conference on the Origin of Granites. Australian Academy of Sciences - Australian National University, Canberra, Australia. 23 - 28 September 1991.

Lister, G.S. 1977 Cross-girdle c-axis fabrics in quartzites plastically deformed by plane strain and progressive simple shear. Tectonophysics 39, 51 - 54.

Lister, G.S. & Dornsiepen, U.F. 1982 Fabric transitions in the Saxony granulite terrain. J. Struct. Geol. 4, 81 - 92.

Lister, G.S. & Hobbs, B.E. 1980 The simulation of fabric development during plastic deformation and its application to quartzite: the influence of deformation history. J. Struct. Geol. 2, 355 - 370.

Lister, G.S. & Paterson, M.S. 1979 The simulation of fabric development during plastic deformation and its application to quartzite: fabric transitions. J. Struct. Geol. 1, 99 - 115.

Lister, G.S. & Price, G.P. 1978 Fabric development in a quartz-feldspar mylonite. Tectonophysics 49, 37-78.

Lister, G.S. & Snoke, A. 1984 S-C mylonites. J. Struct. Geol. 6, 617 - 38.

Lister, G.S. & Williams, P.F. 1983 The partitioning of deformation in flowing rock masses. Tectonophysics 92, 1 - 33.

Lister, G.S., Paterson, M.S. & Hobbs, B.E. 1978 The simulation of fabric development in plastic deformation and its application to quartzite: the model. Tectonophysics 45, 107 - 158.

Mancklетow, N.S. 1987 Quartz textures from the Simplon Fault Zone, NW Switzerland and N. Italy. Tectonophysics, 135, 133-153.

Mancktelow, N.S. 1990 The Simplon Fault Zone Materiaux pour la Carte Geologique de la Suisse. Service Hydrologique et Geologique National et la Commission Geologique Suisse. Lieferung 163.

McKee, E.H. & Nash, D.B. 1967 Potassium argon ages of granitic rocks in the Inyo batholith, east-central California. Bull. Geol. Soc. Am. 78, 669 - 680.

Morgan, S.S. Law, R.D. & Sylvester, A.G. 1991 Strain-path partitioning during contact metamorphism and emplacement of the Papoose Flat pluton, eastern California. Geol. Soc. Am. Abstracts with Programs 23 (5), A175.

Nelson, C.A. 1966 Geologic map of the Waucoba Mountain quadrangle, Inyo County, California. U.S. Geological Survey Quadrangle Map GQ-528, scale 1:62,500.

Nelson, C.A. 1971 Geologic map of the Waucoba Spring quadrangle, Inyo County, California. U.S. Geological Survey Quadrangle Map GQ-921, scale 1:62,500.

Nelson, C.A. 1981 Basin and Range Province. In: Ernst, W.G. (editor) The Geotectonic Development of California - Rubey Volume 1. Prentice-Hall, New Jersey, 203 - 216

Nelson, C.A. 1987 Papoose Flat pluton, Inyo Mountains, California. Geol. Soc. Am. Centennial Field Guide - Cordilleran Section 157 - 160.

Nelson, C.A., Oertel, G., Christie, J.M. & Sylvester, A.G. 1972 Structure and emplacement history of Papoose Flat pluton, Inyo Mountains, California. Geol. Soc. Am. Abstract with Programs 4, 208 - 209.

Nelson, C.A., Oertel, G., Christie, J.M. & Sylvester, A.G. 1977 Geologic map, structure sections and palinspastic map of the Papoose Flat pluton, Inyo Mountains, California. Geol. Soc. Am. Map & Chart Series MC-20.

Nelson, C.A. & Sylvester, A.G. 1971 Wall-rock decarbonation and forcible emplacement of Birch Creek pluton, southern White Mountain, California. Geol. Soc. Am. Bull. 82, 2891 - 2904.

Nicolas, A. and Poirier, J.P. 1976 Crystalline plasticity and solid-state flow in metamorphic rocks. Wiley.

Nyman, M.W., Law, R.D. & Morgan, S.S. 1992 Contact metamorphism associated with emplacement of the Papoose Flat Pluton, Inyo Mountains, California. 104th Annual General Meeting, Cincinnati, Ohio, USA. 26 - 26 October 1992. Geol. Soc. Am. Abstracts with Programs 24, No 7.

Oleson, N.O. 1982 Heterogeneous strain of a phyllite as revealled by porphyroblast-matrix relationships. J. Struct. Geol. 4, 481 - 490.

Ord, A. & Christie, J.M. 1984 Flow stresses from microstructures in mylonitic quartzites of the Moine thrust zone, Assynt area, Scotland. J. Struct. Geol. 6, 639 - 654.

Passchier, C.W. & Simpson, C. 1986 Porphyroclast systems as kinematic indicators. J. Struct. Geol. 8, 831 - 844.

Passchier, C.W., Trouw, R.A.J., Zwart, H.J. & Vissers, R.L.M. 1992 Pophyroblast rotation: eppur si muove*? J. Metamorphic Petrology 10, 283 - 294.

Paterson, S.R., Brudos, T., Fowler, K., Carlson, C., Bishop, K & Vernon, R.H. 1991 Papoose Flat pluton: forceful expansion or postemplacement deformation. Geology 19, 324 - 327.

Paterson, S.R. & Tobisch, O.T. 1992 Rates of processes in magmatic arcs: implications for the timing and nature of pluton emplacement and wall rock deformation. J. Struct. Geol. 14, 291 - 300.

Pfiffner, O.A. and Ramsay, J.G. 1982 Constraints on geological strain rates: arguments from finite strain states of naturally deformed rocks. J. Geophys. Res. 87, 311-321.

Ramsay, J.G. 1962 The geometry and mechanics of formation of 'similar' type folds. Geology 70, 309 - 328.

Ramsay, J.G. 1989 Emplacement kinematics of a granite diapir: the Chindamora batholith, Zimbabwe. J. Struct. Geol. 11, 191 - 209.

Rosenfeld, J.L. 1968 Garnet rotations due to major Paleozoic deformations in Southeast Vermont. In Zen, E.A. (ed) Studies of Appalachian Geology,Wiley, N.Y. pp. 185-202.

Rosenfeld, J.L. 1970 Rotated garnets in metamorphic rocks. Geol. Soc. Am. Special Paper 129, 102 p.

Ross, D.C. 1965 Geology of the Independence quadrangle, Inyo County, California. Bull. U.S. Geol. Survey 1181-0, 64.

Schmid, S.M. & Casey, M. 1986 Complete fabric analysis of some commonly observed quartz c-axis patterns. In Heard, H.C & Hobbs, B.E. (eds) Mineral and Rock Deformation: Laboratory Studies, the Paterson Volume. Am. Geophys. Union, Geophys. Monograph 36, 263 - 86.

Schoneveld, C. 1977 A study of some typical inclusion patterns in strongly

paracrystalline- rotated garnets. Tectonophysics 39, 453-471.

Spry, A. 1969 Metamorphic Textures. Pergamon Press

Starkey, J. 1989 Microcomputer Workshop: Quantitative Petrofabric Analysis. 9th Annual Meeting, Structural Geology & Tectonics Division, Geol. Assoc. of Canada, London, Ontario, Canada.

Steinhardt, C.K. 1989 Lack of porphyroblast rotation in non-coaxially deformed schist from Petrel Cove, South Australia, and its implications. Tectonophysics 158, 127 - 1450.

Sylvester, A.G. & Babcock, J.W. 1975 Significance of multiphase folding in the White-Inyo range, eastern california. Geol. Soc. Am. Abstracts with Programs 7, 1289.

Sylvester, A.G. & Christie, J.M. 1968 The origin of crossed-girdle orientations of optic axes in deformed quartzites. Geology 76, 571 - 80.

Sylvester, A.G., Oertel, G., Nelson, C.A. & Christie, J.M. 1978 Papoose Flat pluton: a granitic blister in the Inyo Mountains, California. Bull. Geol. Soc. Am. 89, 1205 - 19.

Turner, F.J. & Weiss, L.E. 1963 Structural Analysis of Metamorphic Tectonites. McGraw Hill, New York.

Vernon, R.H. 1978 Porphyroblast-matrix microstructural relationships in deformed metamorphic rocks. Geol. Rundsch., 67, 288-305.

Vernon, R.H. 1989 Porphyroblast-matrix microstructural relationships: recent approaches and problems. In: Daly, J.S., Cliff, R.A. & Yardley, B.W.D. (eds) Evolution of Metamorphic Belts. Geol. Soc. of London Special Publication No. 43, 83 - 102.

Vissers, R.L.M. 1989 On quartz c-axis fabrics in non-coaxial deformation using rotated skeletal garnets and their included ghost fabrics. J. Struct. Geol. 11, 231 - 244.

White, S.H. 1979 Grain and sub-grain variations across a mylonite zone. Contrib. Mineral. Petrol., 70, 193-202.

Williams, P.R. and Schoneveld, C. 1981 Garnet rotation and the development of axial plane crenulation cleavage. Tectonophysics, 78, 307-334.

Zwart, H.J. 1962 On the deformation of polymetamorphic mineral associations and its application to the Bosost area (Central Pyrenees). Geol. Rundsch., 52, 38 - 65.

VITA

Sven Morgan received his B.S. degree in geology from Allegheny College in Meadville, PA. He traveled and worked for two years before spending two years in the Peace Corps in Mauritania as an Agricultural Extension Agent. Upon returning to the States he returned to school and spent three years at V.P.I. & S.U. working on his master's degree and enjoying Blacksburg. After completion of this degree Sven is entering a Ph.D. program in geology at the U. of Minnesota.